Order Number 1352383

The effects of temperature and motility on the advective transport of a deep subsurface bacteria through saturated sediment

McCaulou, Douglas Ray, M.S.

The University of Arizona, 1993

U·M·I
300 N. Zeeb Rd.
Ann Arbor, MI 48106

THE EFFECTS OF TEMPERATURE AND MOTILITY ON THE ADVECTIVE TRANSPORT OF A DEEP SUBSURFACE BACTERIA THROUGH SATURATED SEDIMENT

by

Douglas Ray McCaulou

A Thesis Submitted to the Faculty of the

DEPARTMENT OF HYDROLOGY AND WATER RESOURCES

In Partial Fulfillment of the Requirements
For the Degree of

MASTER OF SCIENCE
WITH A MAJOR IN HYDROLOGY

In the Graduate College

THE UNIVERSITY OF ARIZONA

1993

STATEMENT BY AUTHOR

This thesis has been submitted in partial fulfillment of requirements for an advanced degree at the University of Arizona and is deposited in the University Library to be made available to borrowers under the rules of the library.

Brief quotations from this thesis are allowable without special permission, provided that accurate acknowledgment of source is made. Requests for permission for extended quotation from or reproduction of this manuscript in whole or in part may be granted by the head of the major department or the Dean of the Graduate College when in his or her judgment the proposed use of the material is in the interests of scholarship. In all other instances, however, permission must be obtained from the author.

SIGNED: Doug McCauley

APPROVAL BY THESIS CO-DIRECTORS

This thesis has been approved on the date shown below:

John C Bales — 4/27/93

R. C. Bales
Associate Professor of Hydrology

Date

R G Arnold — 4/30/93

R. G. Arnold
Associate Professor of Civil Engineering

Date

ACKNOWLEDGMENTS

Most importantly I thank my wife, Teri, and my daughters, Kirsten and Catie, for their support throughout the past few years. Teri, thank you for helping me to stay focused on my goals, for bolstering my confidence, and having faith in me during the difficult moments.

I also wish to thank the co-investigators of this project, Dr. Roger Bales and Dr. Robert Arnold for their time and effort in my educational process. Their regular reviews of my work and insightful suggestions helped me stay on the direct path to complete this thesis research. In addition, I thank Dr. Bruce Logan and the rest of the Environmental Engineering Department for use of their laboratories and for the invaluable research discussions.

Thank you Tim Corley for the generous help in the laboratory and in our discussions. I thank my friends Dave Jewett and Otto Albinger for their advice and support.

Lastly, I wish to thank the DOE Environmental Restoration and Waste Management Fellowship Program and the Oak Ridge Institute for Science and Education for their financial support over the last two years. Research was supported by DOE grant DE-FG02-91ER61200 #A002 to the University of Arizona.

DEDICATION

To Virginia McCaulou

whose inspiration led me to the rewards of higher education

TABLE OF CONTENTS

TABLE OF CONTENTS (continued)

LIST OF FIGURES

LIST OF TABLES

ABSTRACT

Replicate column experiments were done to quantify the effects of temperature and bacterial motility on advective transport through repacked, but otherwise unaltered, natural aquifer sediment. The bacteria used in this study, *A0500*, was a flagellated, spore-forming rod isolated from the deep subsurface at DOE's Savannah River Laboratory. Motility was controlled by turning on flagellar metabolism at 18°C but off at 4°C. Microspheres were used to independently quantify the effects of temperature on the sticking efficiency (α), estimated using a steady-state filtration model. The observed greater microsphere removal at the higher temperature agreed with the physical-chemical model, but bacteria removal at 18°C was only half that at 4°C. The sticking efficiency for non-motile *A0500* (4°C) was over three times that of the motile *A0500* (18°C), 0.073 versus 0.022 respectively.

Analysis of complete breakthrough curves using a non-steady, kinetically limited, transport model to estimate the time scales of attachment and detachment suggested that motile *A0500* bacteria traveled twice as far as non-motile *A0500* bacteria before becoming attached. Once attached, non-motile colloids detached on the time scale of 9 to 17 days. The time scale for detachment of motile *A0500* bacteria was shorter, 4 to 5 days.

Results indicate that bacterial attachment was reversible and detachment was enhanced by bacterial motility. The kinetic energy of bacterial motility changed the attachment-detachment kinetics in favor of the detached state. The chemical factors responsible for the enhanced transport are not known. However, motility may have caused weakly held bacteria to detach from the secondary minimum, and possibly from the primary minimum, as described by DLVO theory .

1.0 INTRODUCTION

Interest in movement of bacteria in groundwater has over the past decade gone beyond the traditional concern of pathogens in pubic water supplies to *in situ* biodegradation of contaminated soils, facilitating transport of radionuclides and other dissolved contaminants, to the study of the origins of deep subsurface prokaryotes. Bacteria have been shown to move through soil columns at pore velocities of 0.3 to 30 m day^{-1} in laboratory experiments [*Wollum and Cassel, 1978; Smith et al., 1985; Fontes et al., 1991*] as well as field studies [*Harvey et al., 1989; Martin et al., 1991; Harvey and Garabedian 1991*]. Chemical and biochemical factors controlling transport and retardation of bacteria generally are neither known nor controlled in natural field experiments. Laboratory column experiments have been used to examine the influence of hydrophobic effects, pH, and ionic strength [*Fontes et al., 1991; Kinoshita et al., 1992*].

Steady-state filtration theory has been applied to interpret laboratory column studies of bacterial transport [*Martin et al., 1991; Kinoshita et al., 1992*] and field studies of bacterial transport [*Harvey et al., 1989; Harvey and Garabedian 1991; Bouwer and Rittmann, 1992*]. *Fontes et al.* [*1991*] applied a non-steady transport model to laboratory column results; but these data were too coarse to interpret rate coefficients using filtration theory. *Bales et al.* [*1991*] illustrated use of filtration theory to interpret virus transport and retardation under kinetically limited, non-steady conditions. They found similar results in steady-state experiments [*Bales et al., 1992*]. *McCaulou et al.* [*1993*] used a non-steady transport model to estimate bacteria retardation under kinetically-limited conditions, time scales for attachment and detachment and used filtration theory to estimate removal rates of bacteria in column experiments.

1.1 Bacteria Attachment and Detachment in Porous Media

Theories that describe initial attachment of bacteria to solid surfaces are based on either surface free energy calculations or colloid stability. The Derjaguin, Landau, Verwey, and Overbeek (DLVO) theory combines the van der Waals forces (attractive) with electrostatic double-layer forces (repulsive) to explain the stability of colloids. The net colloid stability is a sum of the two forces. Attractive forces are independent of temperature, but calculations of repulsive force interactions depend on temperature and should be greater at higher temperature [*Stumm and Morgan, 1981*]. Therefore, colloid stability theory predicts that higher temperatures favors less attachment.

The surface free energy approach assumes that a bacterium is in direct contact with the solid surface and is under the control of short-range interactions (i.e., steric effects, hydrogen bonding) [*Harvey, 1991*]. The net free energy of attachment is a balance of bacteria-liquid, bacteria-solid, and liquid-solid surface tensions when the bacteria-solid phase boundary is created [*Absolom et al., 1983*]. Surface tensions decrease at higher temperatures [*Stumm and Morgan, 1981*] and should favor greater attachment at higher temperatures. Once attached, higher temperatures may allow a bacterium to overcome the weakened short-attractive forces under its own motility. The two theories of colloid sorption are fundamentally different and do not yield a unified prediction of the effects of temperature.

Investigations of chemical factors controlling bacterial transport through porous media have identified ionic strength, pH, and organic carbon content as master variables.

Van Loosdretch et al. [*1989*] found that changes in the attachment of four different bacteria strains to polystyrene due to higher ionic strength of a solvent could be quantitatively predicted by DLVO theory. At a higher ionic strength, the thickness of the repulsive double layer was smaller, allowing a negatively charged colloid to move closer

to a negatively charged solid surface. When the thickness of the double layer was reduced to a distance at which the short-attractive van der Waals forces dominate, greater adhesion of the colloid to the surface was observed. A critical electrolyte concentration of 10^{-2} molar was found to shrink the double layer to ~4 nm and saturate polystyrene with bound bacteria [*van Loosdretch et al., 1989*]. Laboratory column studies of bacterial transport through soils found that high ionic strength solvents increased the amount of attached bacteria due to less electrostatic repulsion [*Sharma et al., 1985; Fontes et al., 1991*].

The control of biocolloid transport in laboratory soil columns by pH is well documented. Bacteria typically have a net negatively charged surface at pH's found in nature and become less negative as pH is reduced [*Richmond and Fisher, 1973; Gerritsen and Bradley, 1987; Bayer and Sloyer, 1990*]. Ionizable functional groups on the surface of a bacteria (i.e., carboxyl, hydroxyl, amino) and oxides in porous media can affect the net surface charge when protonated at lower pH [*Scholl and Harvey, 1992*]. It is reasonable to assume that the magnitude of electrostatic repulsion between a negatively charged bacterium and a negatively charged solid surface is smaller at a lower pH. *Scholl et al.* [*1990*] found that greater attachment of bacteria occurred in support of the concept that oxide surfaces become protonated as pH decreased, which led to a greater number of positively charged surface sites. They concluded that bacteria were likely to encounter more favorable attachment sites on quartz at lower pH. *McEldowney and Fletcher* [*1988*] also observed greater attachment of bacteria at lower pH. *Bales et al* [*1992*] showed that transport of bacteriophage through silica porous media was greater at pH 7.0 than 5.5.

Hydrophobic interactions between biocolloids and organic carbon in porous media have been shown to enhance attachment of biocolloids to solids. *Bales et al.* [*1992*] showed that small amounts of organic carbon immobilized on the surface of silica collectors resulted in greater retention and less transport of bacteriophage in column

experiments. Laboratory experiments have shown that electrostatic and hydrophobic interactions affect transport of both hydrophobic and hydrophilic bacteria. The hydrophobic bacteria had a greater affinity for hydrophobic polymer-coated quartz surfaces than did hydrophilic bacteria [*McCaulou et al., 1993*]. *Van Loosdretch et al.* [*1987a*] showed that hydrophobic bacteria adhere in larger numbers to sulfated polystyrene than do hydrophilic bacteria. Hydrophobic interactions are often difficult to separate from electrostatic interactions at typical ionic strengths of groundwater. It is reasonable to predict that attachment due to hydrophobic interactions is more prominent in low ionic strength solutions where the distance of electrostatic repulsive forces is maximized. Attachment in high ionic strength solutions is dominated by the fact that the distance of electrostatic repulsive forces is minimized.

The effects of temperature and motility on transport of biocolloids have not been quantitatively investigated. *Bales et al.* [*1991*], using batch adsorption experiments found that bacteriophage attached in larger numbers to silica beads at 24°C versus 4°C. *Hendricks et al.* [*1979*] showed that bacteria adsorption on soils in batch experiments could be modeled using Langmuir isotherms and that changes in temperature followed the van't Hoff equation. Their results suggest that adsorption of bacteria was greater at higher temperatures. There was no investigation of bacteria motility in the *Hendricks et al.* study. Studies with a marine *pseudomonad* in batch cultures showed that adhesion to polystyrene was enhanced by higher temperatures [*Fletcher*, 1977]. The marine psychrophilic *pseudomonad* was randomly motile at 3°C and 20°C. In a slow sand filtration study, removal of bacteria was 100 times greater at 17°C versus 2°C [*Bellamy et al., 1988*]. In pilot-scale wastewater treatment study of slow sand filtration, removal of *E. coli* and coliform bacteria was 99% during the summer; removal was reduced to 41% and 88% in the winter, respectively [*Burman, 1962*].

Model predictions of the effects of temperature on filtration indicate that removal rate of colloids should be higher at higher temperatures due to an increased collision efficiency [*Yao et al., 1971*]. To my knowledge, there are no published experimental tests of temperature or bacteria motility effects, quantified by the filtration model. Attachment-detachment processes that control advective transport are not known in sufficient detail to develop a predictive transport model. Therefore, in this study attachment-detachment is discussed as a pseudo-first-order kinetic process that controls retardation and transport of colloids. Processes affecting attachment and detachment will be discussed to assist interpretation of the observed phenomena.

1.2 Bacteria in Deep Subsurface Environments

Microbiology of deep subsurface sediments has recently become the subject of great interest because deep aquifers are a major source of freshwater and are at risk from contamination with toxic compounds from human activities [*Craun, 1984; Keswick, 1984*]. Large diverse populations of microorganisms found in deep subsurface sediments [*Balkwill et al., 1989; Brockman et al., 1992*] may play an important role in the degradation of toxic ground-water compounds by nutrient stimulation [*Hazen, 1989*].

In 1986 the Department of Energy's (DOE) Deep Subsurface Microbiology Program began its investigation of deep aquifer environments at the Savannah River Site. Hundreds of bacteria were isolated and extensively cataloged [*Balkwill, 1989; Sargent and Fliermans, 1989; Sinclair and Ghiorse; Fredrickson et al., 1989*]. Summary of initial findings suggest that; chemoheterotrophic communities found in saturated sediments are capable of degrading a variety of organic compounds [*Hazen, 1989*]; population densities are positively correlated with porosity [*Balkwill et al., 1989*]; the presence of iron and sulfate-reducing bacteria indicate the presence of anaerobic respiration within microsites in

an aerobic aquifer [*Jones et al., 1989*]; and that the highest microbial diversity and *in situ* respiration rates were associated with relatively young groundwater [*Lovley and Chapelle, 1989*].

One of the present objectives of DOE's Deep Subsurface Microbiology Program is to develop a conceptual and mechanistic understanding of microbial transport. Improved understanding of transport mechanisms will permit testing the hypothesis that subsurface bacteria have recently moved into deep sediments from recharge waters. This study addresses the stated objective by identifying random bacterial motility as a process that enhances advective transport.

1.3 Transport and Filtration Models

Advective transport parameters for bacteria and polystyrene microspheres through porous media can be estimated by fitting transport equations to observed breakthrough data. An equilibrium one-dimensional, advection-dispersion model can be used to estimate hydrodynamic dispersion of a salt tracer. Two different one-dimensional, non-steady, advection-dispersion models (first-order kinetic, and two-site kinetic) have been used to estimate the time scales of attachment and detachment of colloids [*Bales et al., 1991*]. In the two-site model one assumes that there are two types of adsorption sites; adsorption on type 1 sites is assumed to be fast relative to flow, while adsorption to type 2 sites is kinetically limited [*van Genuchten, 1981*]. In the first-order model one assumes that only type-2 sites are present and that sorption can be described by first-order kinetics.

Governing equations for one-dimensional colliod transport in a porous media with two types of sites for colliod attachment to and detachment from surfaces, one of which is kinetically limited, have been given by various investigators [*Cameron and Klute, 1977; Rao et al., 1979*].

$$\theta \frac{\partial C}{\partial t} + \rho_b \frac{\partial S_1}{\partial t} + \rho_b \frac{\partial S_2}{\partial t} = \theta D \frac{\partial^2 C}{\partial x^2} - u\theta \frac{\partial C}{\partial x} \quad (1)$$

$$S_1 = K_{p1} C \quad (2)$$

$$\rho_b \frac{\partial S_2}{\partial t} = \theta k_1 C - \rho_b k_2 S_2 \quad (3)$$

where C is the concentration of bacteria or microspheres in the aqueous phase; S_1 and S_2 are the concentrations bound to the surface, for fast and kinetically limited sites, respectively; θ is porosity; ρ_b is the dry bulk density of the solid material; D is the longitudinal dispersion coefficient; u is the average interstitial velocity; k_1 is the pseudo-first-order rate coefficient (s^{-1}) for attachment, which depends on the colloid's molecular diffusion coefficient and the sticking efficiency (i.e., net energy of interaction between colloid and porous media); and k_2 is a pseudo-first-order detachment rate coefficient, which also depends on the energy of colloid-surface interaction. These rate coefficients do not depend on the surface site concentration, as only a very small fraction of the surface was covered by attached colloids in our experiments.

Equation (1) expresses the total change in concentration with time due to advection, dispersion, attachment, and detachment. This equation assumes that flow through a saturated, homogeneous porous media is at steady state and that immobile flow regions do not exist. Equation (2) expresses the linear attachment-detachment equilibrium for the fast (type 1, equilibrium) sites. Type 1 sites could correspond to colloids held near the surface in a secondary minimum of the potential energy of interaction, with little or no energy barrier for detachment. In equation (3), the change in colloid concentration bound to type 2 sites with time is the difference between the attachment and detachment rates.

Total attachment, S, at equilibrium is expressed as;

$$S = S_1 + S_2 = f K_{p1} C + (1 - f) \frac{\theta k_1}{\rho_b k_2} C = K_p C \quad (4)$$

where f is the fraction of type 1 sites; and K_{p1} and $\theta k_1 / \rho_b k_2$ are the equilibrium partition coefficients for the type 1 and type 2 sites, respectively. Letting $K_{p2} = \theta k_1 / \rho_b k_2$, the overall, total equilibrium partition coefficient for $t \rightarrow \infty$ is $K_p = K_{p1} + K_{p2}$.

It is often useful to express the model parameters in dimensionless terms in order to make comparisons between different systems. *Van Genuchten [1981]* has written computer programs that solve dimensionless forms of equations (1), (2), and (3). A non-linear-least-squares curve-fitting algorithm, CFITIM, finds the best fit solution to reported data and an analytical solution to the dimensionless equations provides visual curve fits from estimated model parameters. In order to transform equations (1), (2) and (3) into dimensionless equations the following variables are substituted:

$$T = \frac{v t}{L} \quad (5)$$

$$Z = \frac{x}{L} \quad (6)$$

$$C_1 = \frac{C}{C_o} \quad (7)$$

$$C_2 = \frac{S_2}{(1 - f) K_p C_o} \quad (8)$$

The substitution results in the following dimensionless equations and model parameters:

$$\beta R\frac{\partial C_1}{\partial T} + (1-\beta)R\frac{\partial C_2}{\partial T} = \frac{1}{P}\frac{\partial^2 C_1}{\partial Z^2} - \frac{\partial C_1}{\partial Z} \tag{9}$$

$$(1-\beta)\mathrm{R}\frac{\partial C_2}{\partial T} = \omega(C_1 - \mathrm{C}_2) \tag{10}$$

The total partition coefficient, $K_p = K_{p1} + K_{p2}$ is related to the retardation factor:

$$R = 1 + \frac{\rho_b\,(K_{p1} + K_{p2})}{\theta} = 1 + \frac{\rho_b\,K_{p1}}{\theta} + \frac{k_1}{k_2} \tag{11}$$

The Peclet number is P: $P = \dfrac{L\,u}{D} = \dfrac{\textit{Time scale for dispersion}}{\textit{Residence time}}$ (12)

The dimensionless mass-transfer coefficient is a Damkohler number [*Valocchi, 1985; Bahr and Rubin, 1987*]:

$$\omega = \frac{L/u}{1/k_1} = \frac{k_1 L}{u} = \frac{\textit{Residence time}}{\textit{Chemical time scale}} \tag{13}$$

where L is the length of the column. When $\omega > 100$, local equilibrium applies, and as ω drops below about 0.1-0.5, adsorption is too slow to observe and the solute appears to be conservative. A fourth parameter, β, related to the ratio of equilibrium to total adsorption, can be defined by

$$\beta = \frac{\theta + \rho_b\,K_{p1}}{\theta + \rho_b\,K_{p1} + \theta k_1/k_2} = 1 - \frac{k_1}{k_2 R} = 1 - \frac{\omega u}{k_2 L R} \tag{14}$$

For no type 1 sites, a three-parameter ($K_{p1} = 0$; $\beta = 1/R$ and $R = 1 + (k_1/k_2)$) first-order model can be used. For no type 2 sites ($\beta = 1/R$ and $\omega > 100$; $\mathrm{R} = 1 + (\rho_b K_p/\theta)$), a two-parameter equilibrium model can be used.

The *van Genuchten [1981]* computer programs were used to fit observed breakthrough data. The reported model solutions used the following initial conditions;

$$C_1(Z,0) = C_2(Z,0) = 0$$

$$S_1(Z,0) = S_2(Z,0) = 0$$

and boundary conditions for a step injection:

$$\left\{ -\frac{1}{P}\frac{\partial C_1}{\partial Z} + C_1 \right\}_{(0,T)} = \left\{ \begin{array}{l} 1 \; ; \; 0 < t < t_1 \\ 0 \; ; \; t > t_1 \end{array} \right\}$$

$$\left.\frac{\partial C_1}{\partial Z}\right|_{(\infty,T)} = 0$$

Physical and chemical factors influencing the magnitude of k_1 can be described separately following the single-collector model used to describe particle removal in water filtration [*O'Melia, 1980*]. The single-collector removal efficiency, η, is defined as

$$\eta = \frac{\textit{rate at which particles strike a collector}}{\textit{rate at which particles approach collector}} \tag{15}$$

and the sticking efficiency, α, is defined as

$$\alpha = \frac{\textit{rate at which particles stick to a collector}}{\textit{rate at which particles strike a collector}} \tag{16}$$

Particles are removed from a unit volume of fluid at the rate $k_1 C$ and thus are removed by (stick to) a single collector at the rate $k_1 C (\pi \theta d^3 / 6 (1-\theta))$, where the quantity in parentheses is the volume of fluid associated with a single, spherical collector of diameter d. The rate at which particles approach this volume is $\theta u C (\pi d^2 / 4)$, giving

$$\eta \alpha = \frac{2}{3} \frac{k_1 d}{u} \frac{1}{(1-\theta)} \tag{17}$$

If close-approach effects are neglected, removal efficiency can be estimated by the following [*O'Melia, 1985*]:

$$\eta = \eta_D + \eta_I + \eta_G$$

$$\eta = 0.9\, A_s^{1/3} \left[\frac{\bar{k}\,T}{\mu\, d_p\, d\, u}\right]^{2/3} + \frac{3}{2} A_s \left[\frac{d_p}{d}\right]^2 + \frac{(\rho_p - \rho) g\, d_p^{\,2}}{18\, \mu\, u} \qquad (18)$$

where η_D is for collection by Brownian diffusion, η_I collection by interception, η_G collection by settling, A_s is a parameter that accounts for the effects of adjacent media grains on the flow about a collector, $\bar{k}$ the Boltzman constant, T the solute temperature, μ the water viscosity, d_p the colloid diameter, ρ the water density, ρ_p the colloid density, and g the gravitational constant. Equivalent expressions derived for non-spherical particles differ only slightly [*Bales, 1984*]. For a spherical collector, A_s has been given as:

$$A_s = \frac{1 - \varepsilon^5}{1 - 1.5\,\varepsilon + 1.5\,\varepsilon^5 - \varepsilon^6} \qquad (19)$$

where $\varepsilon = (1 - \theta)^{1/3}$ [*O'Melia, 1985*].

For bacteria and microsphere colloids, Brownian diffusion is the primary mechanism for particle transport to a collector. In the steady-state case, neglecting dispersion, detachment, and weak (equilibrium) binding sites, equations (1), (3) and (17) become:

$$\frac{\partial C}{\partial z} = -\frac{k_1 C}{u} = -\frac{3}{2}\,\frac{1-\theta}{d}\,\eta\,\alpha\, C \qquad (20)$$

Integrating equation (20), given C is the colloid concentration in the influent (C_o) at $z = 0$, and C is the colloid concentration at the column outlet ($z = L$), yields:

$$\alpha = -\frac{2}{3}\,\frac{\ln (C / C_o)\, d}{(1-\theta)\,\eta\, L} \qquad (21)$$

Using equation (18) to estimate collision efficiency, η is substituted into equation (21) with observed effluent colloid concentration at steady state (C_s / C_o) data to estimate the

sticking efficiency, α. Sticking efficiency and η are substituted into equation (17) to solve for k_1 . Equation (13) uses k_1 to calculate ω for use in both the non-steady transport models. Using the steady-state model to estimate the attachment rate constant (k_1) and ω for the non-steady models, eliminates one of the fitting parameters.

1.4 Research Objectives

Previous laboratory investigations of bacteria transport have used strict experimental controls in order to quantify transport parameters. Many investigators sterilized porous media or used genetically altered bacteria to remove indigenous microorganisms from assay counts, and most investigators controlled growth during transport experiments by cooling to ~4°C. The first objective of this study was to investigate the effects of bacterial motility on advective transport through natural aquifer sediments at typical groundwater temperatures without altering the sediment or bacteria surface chemistry. The motile *A0500* bacteria was selected from the Deep Subsurface Savannah River Collection because it displayed excellent transport characteristics in screening experiments [*Gross et al., in preparation*]. Microsphere transport experiments were used to quantify temperature effects on advective transport of non-motile colloids. As a secondary objective, data were used to test the validity of existing mathematical models for bacteria and colloid transport.

2.0 MATERIALS AND METHODS

Replicate sediment column experiments were run to estimate the effects of bacterial motility and temperature on colloid transport; three experiments with *A0500* bacteria at 4°C, two with *A0500* at 18°C, two with microspheres at 4°C, and two with microspheres at 18°C . A sodium chloride breakthrough experiment was run after eight of the nine colloid transport experiments. Five bacteria survival experiments were run at the same time as the bacteria transport experiments. In addition, two *A0500* transport experiments were run through sediment acquired from Georgetown, South Carolina (Appendix D).

2.1 Porous Media and Groundwater

2.1.1 Ringold Sediment

Porous media used were obtained from the Pacific Northwest Laboratories at Hanford, Washington. Samples were collected from near-surface sediments of the Ringold Formation (BB-91-1). The age of these sediments is greater than 4 million years [*Brockman et al., 1992*]. Sieve analysis of the Ringold sediment indicates it was a medium sand with a weighted average grain diameter of 224 μm, 1% silt and clay, and had a dry bulk density (ρ_b) of 2.37 g cm^{-3}. Moisture content was 1.5% on a dry weight basis. Desert Analytics determined the fraction organic carbon to be 0.011 on a dry weight basis using the elemental pyrolysis method. BET surface area was estimated at 0.83 m^2 g^{-1} using mono-layer coverage of N_2 gas. This material was selected for transport experiments because it was readily available at the surface and representative of the type of aquifer material at depth. The sediment was washed with 0.1% sodium pyrophosphate and the liquid was plated on peptone, tryptone, yeast extract, and glucose (PTYG) agar to enumerate indigenous microorganisms (1.5 x 10^4 cells g^{-1} dry sediment). Approximately

48 hours were required for indigenous microorganisms to grow on PTYG agar at room temperature. There was no visible growth of indigenous organisms after 24 hours of incubation. *A0500* colonies were counted within 24 hours after plating. The Ringold sediment was used in its natural condition, without sterilization, for all experiments.

2.1.2 Artificial Groundwater

Artificial groundwater was used in all experiments. Water chemistry analyses from three wells (699-43-88, 699-50-85, 699-53-103) in an unconfined aquifer near the Yakima Barricade, Hanford Site, Washington, were used as the basis for the groundwater recipe (1 L deionized water, 69 mg $MgSO_4$-$7H_2O$, 50 mg $NaHCO_3$, 14.5 mg $CaCl_2$-$2H_2O$, 64 mg $CaNO_3$-$4H_2O$, 2 mg KF, and ~700 μL 0.01 N HCl for pH = 8.0 adjustment). The artificial groundwater had the same ionic composition and ionic strength ($I = 2.8 \times 10^{-3}$ M) as the average well water. Water from these wells had a pH range of 7.8 - 8.0 and an average temperature of 21°C. Using a water similar to that found in the Ringold Formation minimized surface chemistry changes on the sediment when it was saturated. Artificial groundwater was sterilized by autoclaving for > 40 minutes at 121°C and 15 psi, then adjusted to pH = 8.0.

2.2 Bacteria and Microspheres

2.2.1 *A0500* Bacteria

Twelve strains of bacteria were acquired from the Savannah River Deep Subsurface Collection (David L. Balkwill, Florida State University) and screened for transport experiments. A single strain, *A0500*, was used for sediment column transport experiments because its sticking coefficient, α, was very small (0.007) in short-column glass bead experiments [*Gross et al., in preparation*]. *A0500* is a flagellated spore-

forming rod, isolated from well P28 at the Savannah River Site in June-July 1986 at a depth of 180 m, which was in the Middendorf geologic formation. *A0500* originally isolated on PTYG at 23°C, formed characteristic colonies (flat, lobate, creamy colored with transparent edges) when incubated 18 to 24 hours at room temperature. The *A0500* colonies received were immediately grown in PTYG broth and frozen in a mixture of 50% glycerol. Bacteria used in all experiments were first isolated on PTYG plates from frozen stock cultures. The size of the average bacterium at stationary phase was 1.7 x 0.8 μm. *A0500* did not form aggregates during log or stationary phases and had a 1.2 hour doubling time (Fig. 1). Motility was determined by diluting stationary phase bacteria with artificial groundwater to a concentration of ~10^6 cells mL^{-1} and observing movement under a light microscope (1000X). *A0500* swam smoothly in random directions, as opposed to tumbling, at 18°C. There was no movement of *A0500* at 4°C.

2.2.2 Microspheres

Polystyrene, carboxylated, yellow-green microspheres (Polysciences, Inc., Warrington, PA) with a diameter of 1.54 μm were diluted into artificial groundwater to form a stock solution of 1.85 x 10^8 spheres mL^{-1}. Density of the microspheres was reported as 1.055 g cm^{-3}.

2.2.3 *A0500* Density Measurements

Density of the *A0500* bacteria at stationary phase was determined by the Percoll method [*Pertoft, 1980*]. Standardized density marker beads were suspended and centrifuged (30,000 x g) for 15 minutes in Percoll-NaCl solution. *A0500* cells were harvested at stationary phase and stained with acridine orange, suspended in the Percoll-NaCl solution and centrifuged (400 x g) for 20 minutes. The density of *A0500* was

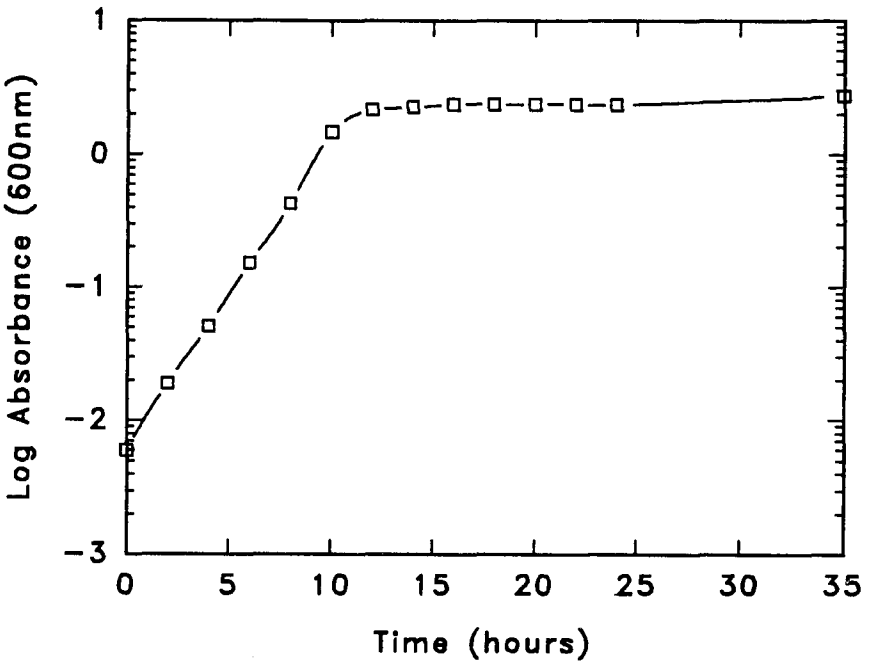

Figure 1. Growth curve of *A0500* in PTYG broth at room temperature.

determined to be 1.082 g cm^{-3} by comparing the resting level of *A0500* cells in the centrifuge tube to the resting level of various density marker beads.

2.2.4 Microelectrophoresis

Net surface charge of *A0500* and microspheres in groundwater were estimated by electrophoretic-mobility. Rank Brothers Mark II particle-electrophoresis apparatus (Rank Brothers, Ltd., Cambridge, England) was used to determine mobility. A cylindrical cell was used with a He-Ar laser (Scientifica-Cook, Ltd, London, England) for both microspheres and *A0500* bacteria.

For each value, 20 particles were timed for each polarity under constant voltage. Mean mobility (u_m) was calculated by (particle velocity)/(gradient of potential) using the average travel time of particles:

$$u_m = \frac{X / t}{V / l} \tag{22}$$

where X is the travel distance (μm), t is the travel time (sec), l is the cell length (cm), and V is the applied voltage (v). Electrophoretic mobility of the microspheres in groundwater (pH =7.7) was measured at -1.35 μm cm s^{-1} v^{-1}. Electrophoretic mobility of *A0500* in groundwater (pH= 7.8) was measured at -0.73 μm cm s^{-1} v^{-1}.

2.2.5 *A0500* Preparation

Bacteria were cultured in the same manner for each experiment (Fig. 2). Single colonies were taken from PTYG plates to inoculate 6 mL PTYG broth in culture tubes. Test tube cultures were grown overnight for 15 hours at room temperature on a culture tube rotator. Two, 1-L Erlenmeyer flasks with 500 mL PTYG broth and cotton stoppers were inoculated with 5 mL of the overnight culture. Cultures were grown to stationary

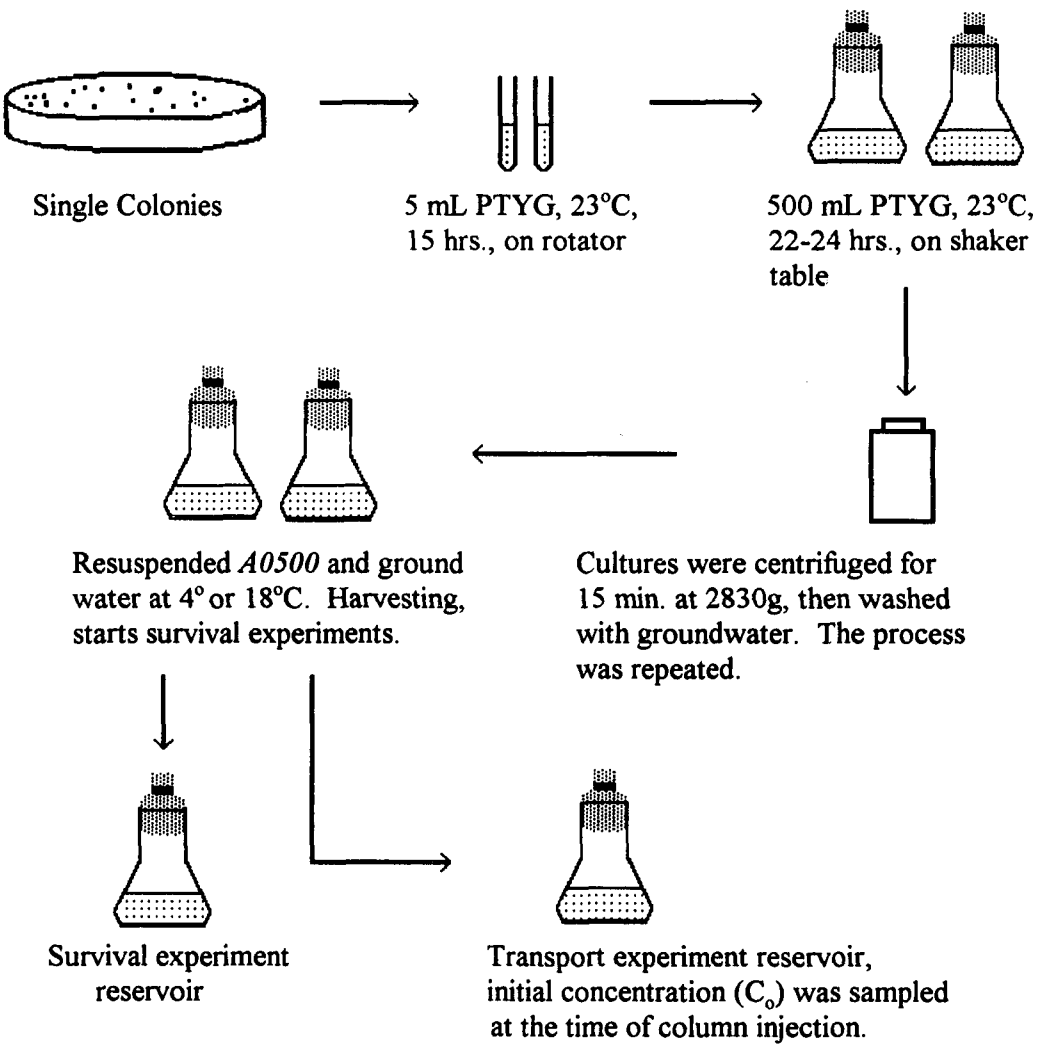

Figure 2. Schematic of *A0500* preparation procedures.

phase (22 -24 hours) on a shaker table at room temperature. The corresponding optical density (Shimadzu UV-160A spectrophotometer, $\lambda = 600$ nm) was 2.2. Cultures were centrifuged three times (15 min. at 2830 g) and washed with groundwater at either 4° or 18°C between centrifuge cycles. In the final step bacteria were resuspended in groundwater. The time at which cultures were resuspended in groundwater (harvested) marked the beginning of each survival experiment ($t = 0$). The concentration of viable *A0500* cells in the groundwater resuspension was 1.1 - 3.0 x10^9 CFU mL^{-1}, at pH of 7.8 to 7.9.

2.2.6 Microsphere Preparation

Prior to each microsphere transport experiment, aliquots of stock solution were diluted with groundwater to approximately 5 x 10^7 spheres mL^{-1}. The stock microsphere solution and the input reservoir of microspheres were sonicated for 10 minutes to assure a homogeneous, mono-particulate size distribution. The final pH of the mixture was 7.7 to 7.9.

2.3 Assay Procedures

Bacteria were enumerated by counting colonies grown on PTYG agar. The spread-plate method was adapted from that outlined in Standard Methods for the Examination of Water and Wastewater [*American Public Health Association, 1992*].

2.3.1 Media

Liquid growth media (PTYG) consisted of 5 g peptone, 5 g tryptone, 10 g glucose, 10 g yeast extract, 0.6 g $MgSO_4$-$7H_2O$, 0.07 g $CaCl_2$-$2H_2O$ dissolved in 1000 mL deionized water and autoclaved at 121°C, 15 psi for 30 minutes. For PTYG agar plates,

15 g Bacto-agar (Difco Laboratories, Detroit, MI) was added to liquid PTYG prior to autoclaving.

2.3.2 Bacteria Enumeration

Bacteria counts were done by serial dilution with sterile 4°C, 0.001 M NaCl and spread-plating on PTYG agar. Assuming that a single bacterium grows into a single colony on a agar plate, bacterial counts were reported as colony forming units (CFU). After harvesting, two independent samples of resuspended bacteria in groundwater (C_o) were diluted separately, and three of the dilution tubes were plated in triplicate. Therefore, each C_o reported was an average of 6 to 18 individual plate counts with a standard deviation of 30%. C_o samples contained approximately 10^9 CFU mL^{-1}. The error associated with measuring 1-mL samples transferred sequentially to each dilution tube was included in the 30% standard deviation. Each reported bacterial count for the survival experiments was an average of 3 to 9 plate counts. The transport experiment data points represented an average of 1 to 3 plate counts.

2.3.3 Microsphere Enumeration

Microspheres were counted via epifluorescent microscopy. Column effluent samples were filtered through 0.2 μm black filters (Poretics, polycarbonate membrane) and mounted on microscope slides for viewing with immersion oil. Between 20 and 200 microspheres were counted on a field or grid. Twenty fields or grids were counted for each sample slide, reporting the average. The concentration of microspheres (C_o) in the input reservoir was sampled twice, filtered on two filters and counted. Replicate counts had a standard deviation of 6%. A minimum of 10^6 microspheres per filter were necessary to get reproducible counts. Early in the breakthrough experiments, several milliliters of

effluent were filtered to reach the 10^6 minimum. Therefore, the rising limb of the microsphere breakthrough experiments did not have as many data points as the bacteria experiments. Microsphere concentrations in 1-mL effluent samples were sufficient for counting after 0.7 pore volumes of injectate.

2.4 Survival Experiment Procedures

Samples were periodically taken from the 1/2-L stock *A0500* groundwater suspension to determine the concentration of viable cells over time. For each column experiment, a survival experiment was run in parallel at the same temperature. Samples from the survival reservoir were handled similarly to the column effluent samples. All bacteria samples were diluted in sterile 4°C, 0.001 M NaCl water and 50 μL were plated within one hour. Initial experiments, not reported, showed the time between taking a sample and plating was critical to getting reproducible numbers. Plating both survival and column experiment samples within one hour yielded reproducible colony counts. The column experiment injection pulse started approximately one hour after harvesting ($t = 1$) and ended no later than 5 hours after harvesting ($t = 5$). Survival experiment reservoirs were sampled for more than 9 hours.

2.5 Column Experiment Procedures

2.5.1 Apparatus

The column-experiment apparatus is illustrated in Fig. 3. The entire apparatus was enclosed in a constant-temperature refrigerator box (Fisher Scientific Co.). For the experiments at 18°C, a constant-temperature water bath (Haake GH-4962) was used for the influent reservoirs and all tubing, fittings and the column were insulated. Colloid solutions and sterile groundwater were sent to the column through independent channels

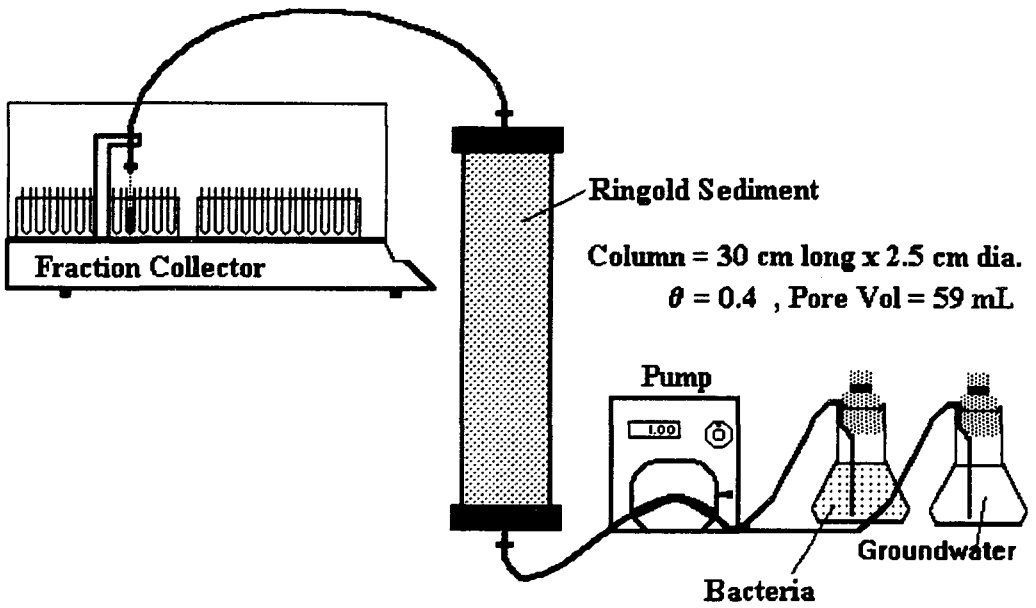

Figure 3. Sediment column experiment apparatus.

of a peristaltic pump (Masterflex model 7523-01). Silicone tubing (Masterflex, #16, 3.1 mm I.D.) was used to supply groundwater and colloid solutions to the column. The inlet to the column and the outlet to the fraction collector were plumbed with silicone tubing (1/16" I.D.) to reduce the volume between the column and collector. Porous Teflon frits (20 μm) were used in the bacterial experiment columns to disperse the inlet solutions across the 5.0 cm^2 cross-sectional area. There was no measurable removal of bacteria by the Teflon frits. The microsphere experiment columns were constructed with 500-μm frits because some of the microspheres were removed on the 20-μm frits. The fraction collector (Isco, Inc., model Foxy-2000, Lincoln, NE) was covered throughout the experiments to reduce the possibility of contaminating collection tubes by airborne microorganisms. A PTYG agar plate was opened in the refrigerator for the duration of each experiment to assure that circulating air would not contaminate collection tubes. No colonies grew on the refrigerator PTYG plate within the 24 hour-incubation period of *A0500*. Prior to packing each column, the tubing, fittings and glass column were sterilized with 5% NaClO and rinsed with sterile groundwater. Ringold sediment was dry-packed into 30 x 2.5 cm glass chromatography columns (Kontes, Inc.) by the tap and fill method of *Snyder and Kirkland [1979]*. Approximately 3-ml fractions were collected in sterile tubes.

2.5.2 Elution Experiment Procedure

Effluent samples were collected from two columns immediately after saturation and were plated on PTYG plates to estimate the number of mobile indigenous microorganisms. Incubation of indigenous microorganisms at room temperature took approximately 48 hours. *A0500* colonies could be counted without having to sterilize the sediment because *A0500* colonies grew in less than 24 hours. Effluent samples were

analyzed for organic matter using a UV-spectrophotometer (Beckman DU-40, $\lambda = 254$ nm). No measurable organic matter was rinsed out of the column after passing one pore volume of sterile groundwater through the column..

2.5.3 Transport Experiment Procedure

Standardized time, or pore volume (*PV*), was used for the breakthrough curves. Pore volume was calculated in terms of residence time of water in the column. The *PV* at a time *t* is;

$$PV = \frac{t}{\bar{t}} = \frac{t}{L / u}$$

where $\bar{t}$ is the hydraulic residence time, L is the column length, and u is the interstitial velocity. This leads to

$$PV = \frac{t}{L / u} = \frac{t}{\frac{L}{Q / A\theta}} = \frac{tQ}{LA\theta} = \frac{Volume\ of\ water\ that\ passed\ through\ a\ column}{Volume\ of\ pore - space\ in\ a\ column}$$

where Q is the volumetric flow rate, A is the cross-sectional area of the column and θ is porosity. Hence, "one pore volume" means the time it takes the average water molecule to travel the length of the column or the time it takes to replace the water in the column. The pore volume of a column was determined by difference of saturated and unsaturated column weight (~59 mL).

The columns were flooded from the bottom to minimize air entrapment. Ten pore volumes of sterile groundwater were pumped through the column at 0.5 mL min^{-1} to thoroughly saturate the sand. This procedure assured that indigenous bacteria removed from the Ringold sediment during the transport experiment were below the detection limit of the spread plate method. Immediately prior to the beginning of a transport experiment

the groundwater flow rate was increased to the experimental setting of 1.0 mL min^{-1} for one pore volume.

A pump rate of approximately 1.0 mL min^{-1} was maintained for groundwater and bacteria/microsphere solutions. The actual flow rate was determined by measuring effluent volume, by weight, periodically throughout the experiments. The measured flow rates of all experiments were between 1.09 and 1.00 mL min^{-1}. The beginning of each transport experiment was established by the start of the bacteria/microsphere injection pulse.

Sample collection tubes were removed from the fraction collector and samples were plated within one hour of elution.

2.5.4 Conservative Tracer Experiment Procedure

Sodium chloride tracer experiments, which consisted of measuring the time for a chloride solution to pass through the column at a known flow rate, were run on each column, except column 3. Salt tracer experiments were run after the bacteria/microsphere transport experiment to estimate the pore volume and hydrodynamic dispersion in the packed column. Salt solution (0.1 M NaCl) was injected at 1.0 mL min^{-1} for approximately two pore volumes and conductivity measurements were taken every three seconds using a Wescan model 213a conductivity detector (Wescan Instruments Inc., Santa Clara, CA) with a flow-through cell. Time and conductivity data were collected with an automatic data logger (Campbell Scientific, Inc., Logan, UT, model CR10). Desorption curves could not be accurately measured because pulses of low ionic strength water after the salt tracer caused significant mobilization of sediment particles. Dispersion was calculated from conservative-tracer breakthrough curves by fitting equilibrium model parameters using a non-linear-least-squares algorithm [*van Genuchten, 1981*].

3. RESULTS

3.1 Elution Experiments

Fig. 4 shows the results of flushing two separate Ringold sediment columns with sterile groundwater. The pore velocity of the flushing water was similar to that in the transport experiments, 9.0×10^{-3} cm s^{-1}. Of the 1.4×10^{4} microorganisms g^{-1} dry sediment or approximately 3.3×10^{6} microorganisms per column, fewer than 6×10^{3} could be mobilized by flushing the column under experimental conditions. The majority of indigenous microorganisms that were mobilized moved out of the column with the first pore volume of effluent. Therefore, all newly packed columns were flushed for more than 10 pore volumes prior to introduction of *A0500* bacteria or microspheres.

3.2 Survival Experiments

Three *A0500*, 4°C survival experiments were run in parallel with the *A0500*, 4°C transport experiments (Fig. 5). Death or decay of viable *A0500* bacteria during the transport experiments was not significant. Therefore, it is reasonable to assume that the influent concentration of viable bacteria into the Ringold sediment columns was constant. To determine the maximum time the constant concentration assumption was valid, one survival experiment at 4°C was allowed to run for 5 days (Fig. 5b). Thirty-six hours after harvesting was the maximum time *A0500*, at concentrations of $\sim 10^{9}$ cells mL^{-1}, could be maintained at 4°C before measurable death or decay of viable cells occurred.

Survival experiments at 18°C were run at the same time as the *A0500*, 18°C column experiments (Fig. 6). Results were more variable than the 4°C survival experiments. One of the survival cultures experienced growth after six hours followed by death at nine to ten hours. The concentration of viable *A0500* cells in the survival flask was constant during

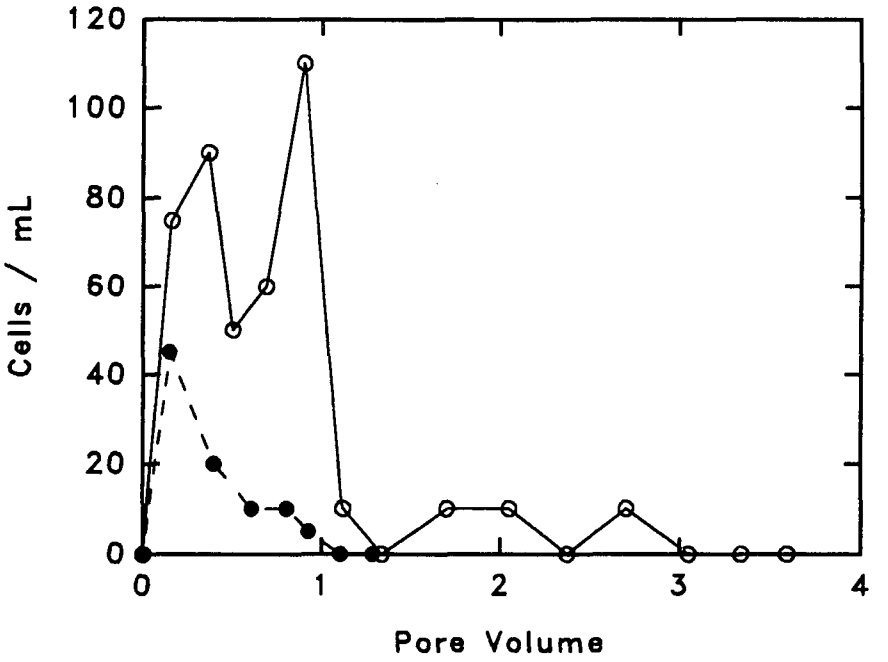

Figure 4. Results of flushing Ringold sediment columns with sterile groundwater. Most of the viable bacteria were eluted, from columns 1 (o) and 2 (●), in the first pore volume of flushing water. Assays were made by directly plating 100 μL of effluent.

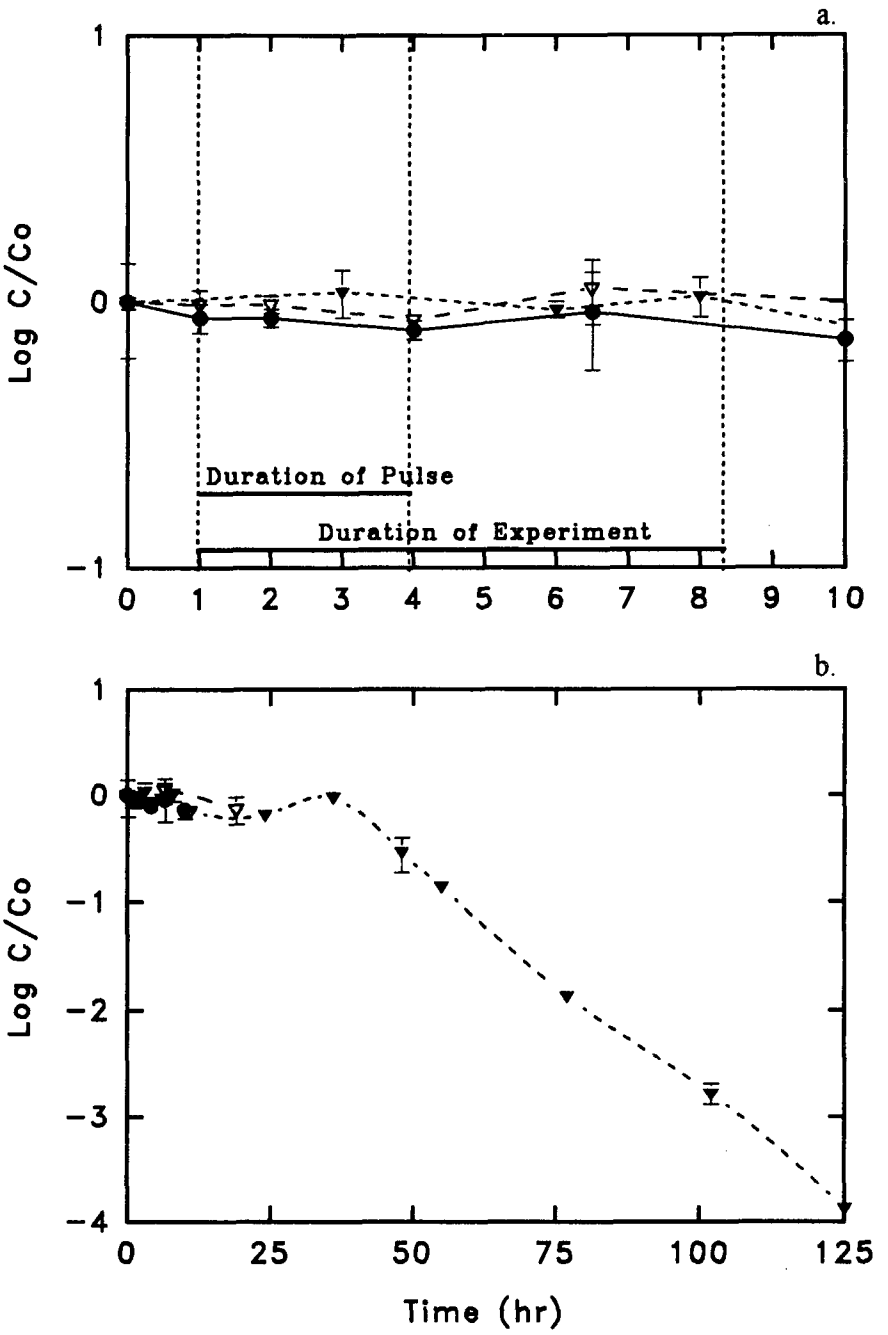

Figure 5. Results of three *A0500* survival experiments at 4° C. a.) Normalized concentrations of bacteria were constant throughout the duration of the transport experiments. b.) Significant death occured after 36 hours.

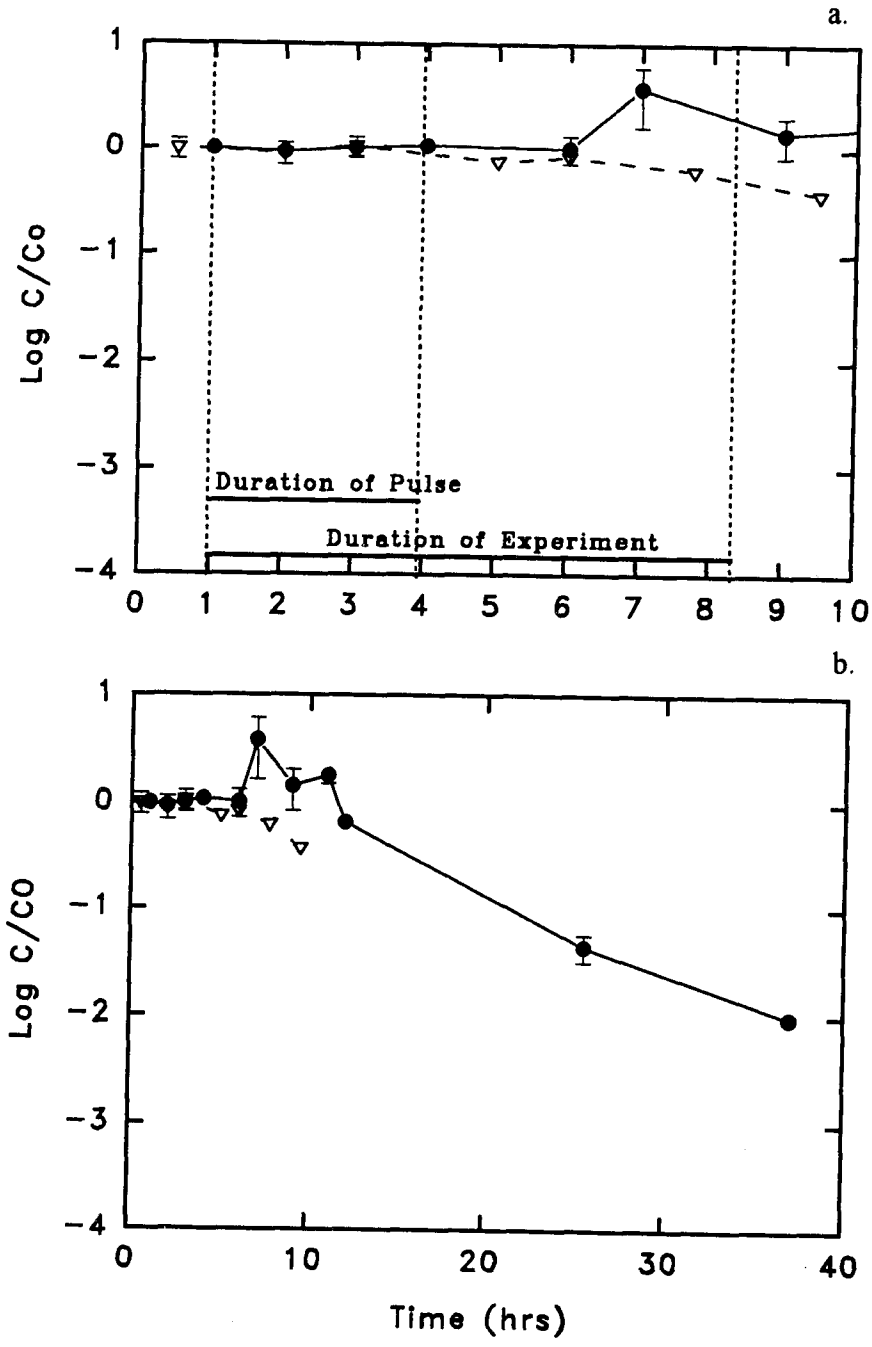

Figure 6. Results of two *A0500* survival experiments at 18° C. a.) Normalized concentrations of influent bacteria were constant during the input pulse of the transport experiments. b.) Significant death occured after 9-10 hours.

the time in which *A0500* was pumped into the sediment columns. Therefore, it was assumed that the concentration of influent bacteria during the injection pulse was constant. Because the growth measured in one survival flask was not reproducible, a mathematical term to account for growth in the transport model was not needed.

3.3 Breakthrough Experiments

Conditions of each column experiment are listed in Table 1. Data collected in each transport experiment are listed in Appendix A.

The breakthrough curves of the NaCl tracer, bacteria, microspheres, and the best fit model solutions are shown in Fig. 7 through 11. The detection limits for the NaCl tracer and bacteria were approximately log C/C_o of -4 and -8, respectively. The vertical dashed line represents the time (pore volumes) of the constant injection pulse of bacteria or microspheres (C_o). Each data point (C/C_o) is an average of 1 to 3 plate counts for the bacteria and 20 grid counts for the microspheres, normalized by the constant injection concentration. The error bars show the standard deviation of the averaged samples for a given data point. The model fit line represents the visual best fit of the first-order kinetic transport model.

A0500 bacteria transport experiments through Ringold sediment at 4°C were replicated in columns 1, 2, and 3. The breakthrough curves show a slow rise to a steady-state C/C_o value at about 2 to 2.5 pore volumes. The average steady-state C/C_o value for the three experiments was 0.28 with a standard deviation of 21%, between experiments. Approximately one pore volume after the injection pulse was replaced with bacteria-free groundwater, the descending limb of the breakthrough curve reached a constant C/C_o between 10^{-3} and 10^{-2}. Replicate measurements of any single effluent concentration sample were within 75% of the average.

Table 1. Conditions of column experiments and filtration model results.

	L (cm)	θ	t_h (min.)	u (cm/s)	C_o	Pulse (PV)	Mean C_s/C_o ±Std.Dev	η	α
Bacteria									
Exp 1- 4°	30	0.390	53.7	9.28×10^{-3}	3.0×10^{9}	3.4	0.217 ± 0.060	0.0136	0.093
Exp 2- 4°	30	0.381	56.2	8.89×10^{-3}	2.5×10^{9}	4.2	0.291 ± 0.087	0.0144	0.070
Exp 3- 4°	30	0.390	56.7	8.55×10^{-3}	3.4×10^{9}	3.9	0.334 ± 0.086	0.0141	0.065
Exp 4-18°	29.8	0.385	54.6	9.13×10^{-3}	2.0×10^{9}	4.0	0.593 ± 0.275	0.0177	0.029
Exp 5-18°	29.9	0.397	57.7	8.63×10^{-3}	1.1×10^{9}	3.9	0.580 ± 0.138	0.0173	0.028
Spheres									
Exp 6- 4°	30.4	0.385	58.4	8.70×10^{-3}	5.4×10^{7}	3.9	0.046 ± 0.004	0.0144	0.168
Exp 7- 4°	30.5	0.387	58.7	8.65×10^{-3}	5.4×10^{7}	3.9	0.093 ± 0.011	0.0143	0.130
Exp 8-18°	30.2	0.380	54.5	9.23×10^{-3}	4.5×10^{7}	3.9	0.0113 ± 0.0007	0.0183	0.192
Exp 9-18°	30.2	0.385	55.2	9.11×10^{-3}	4.5×10^{7}	3.9	0.0037 ± 0.0009	0.0180	0.247

L is the column length, θ is the porosity, t_h is the hydraulic detention time, u is the interstitial velocity, C_o is the colloid concentration of injection solutions, pulse is the number of pore volumes of colloid injection, C_s/C_o is the normalized colloid concentration of effluent at steady-state, η is the collision efficiency and α is the sticking efficiency.

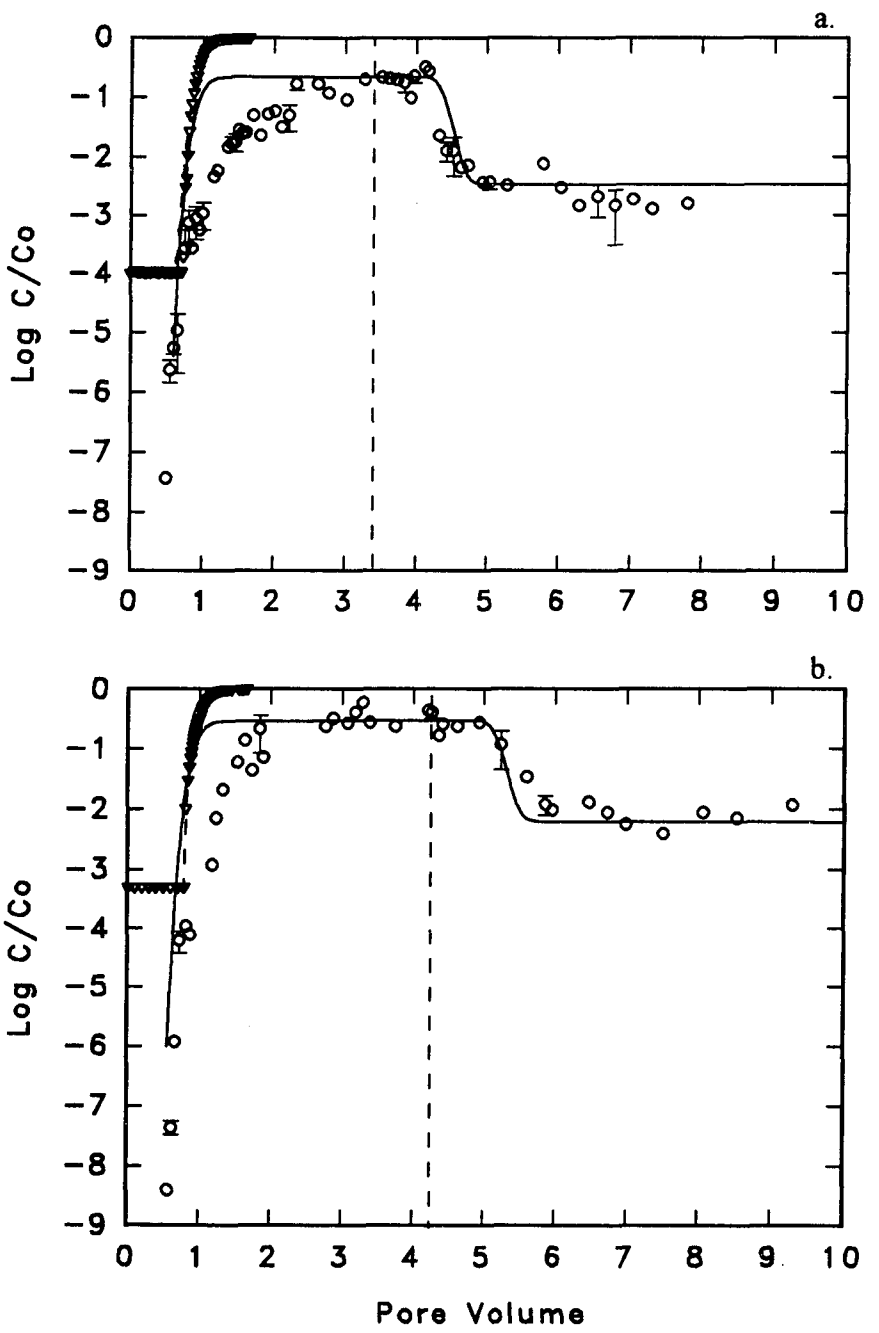

Figure 7. Breakthrough curves of *A0500* bacteria (○) and NaCl tracer (▽) at 4° C with the best fit line of the first-order kinetic transport model. a.) Experiment 1. b.) Experiment 2.

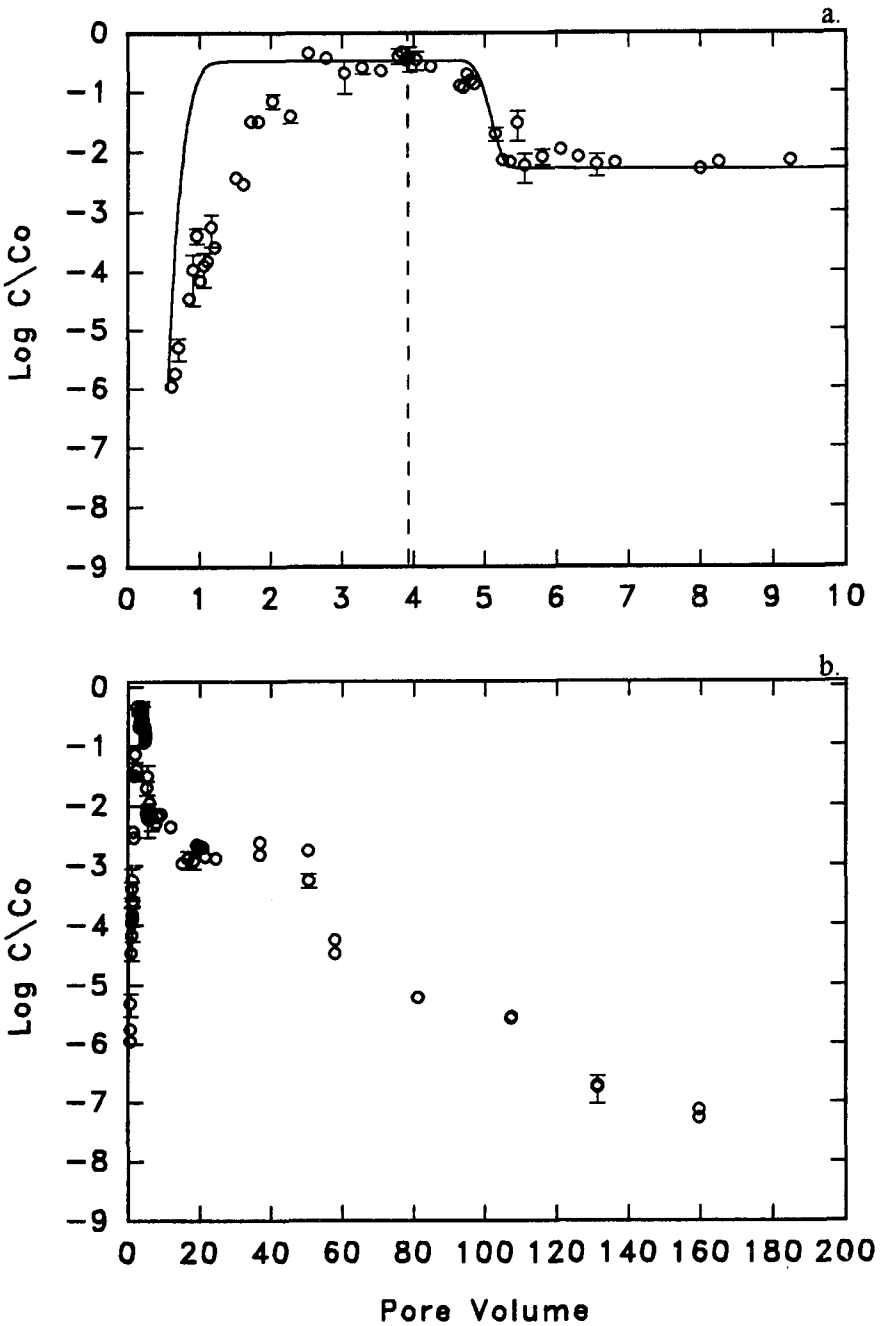

Figure 8. Experiment 3 breakthrough curve of A0500 bacteria (o) at 4° C. a.) with the best fit line of the first-order kinetic transport model. b.) Detachment curve of *A0500* bacteria at 4° C for approximately eight days.

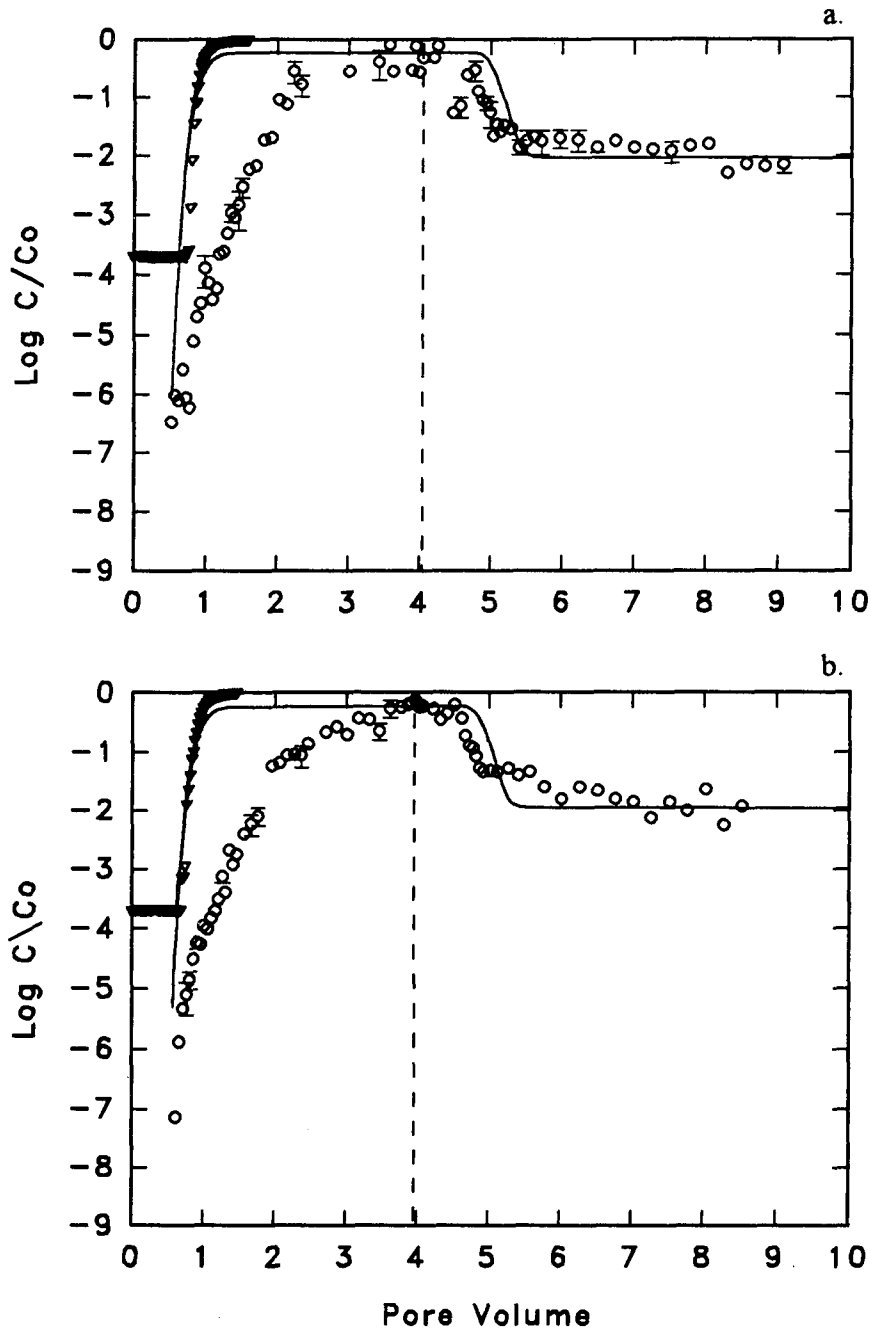

Figure 9. Breakthrough curves of *A0500* bacteria (○) and NaCl tracer (▽) at 18° C with the best fit line of the first-order kinetic transport model. a.) Experiment 4. b.) Experiment 5.

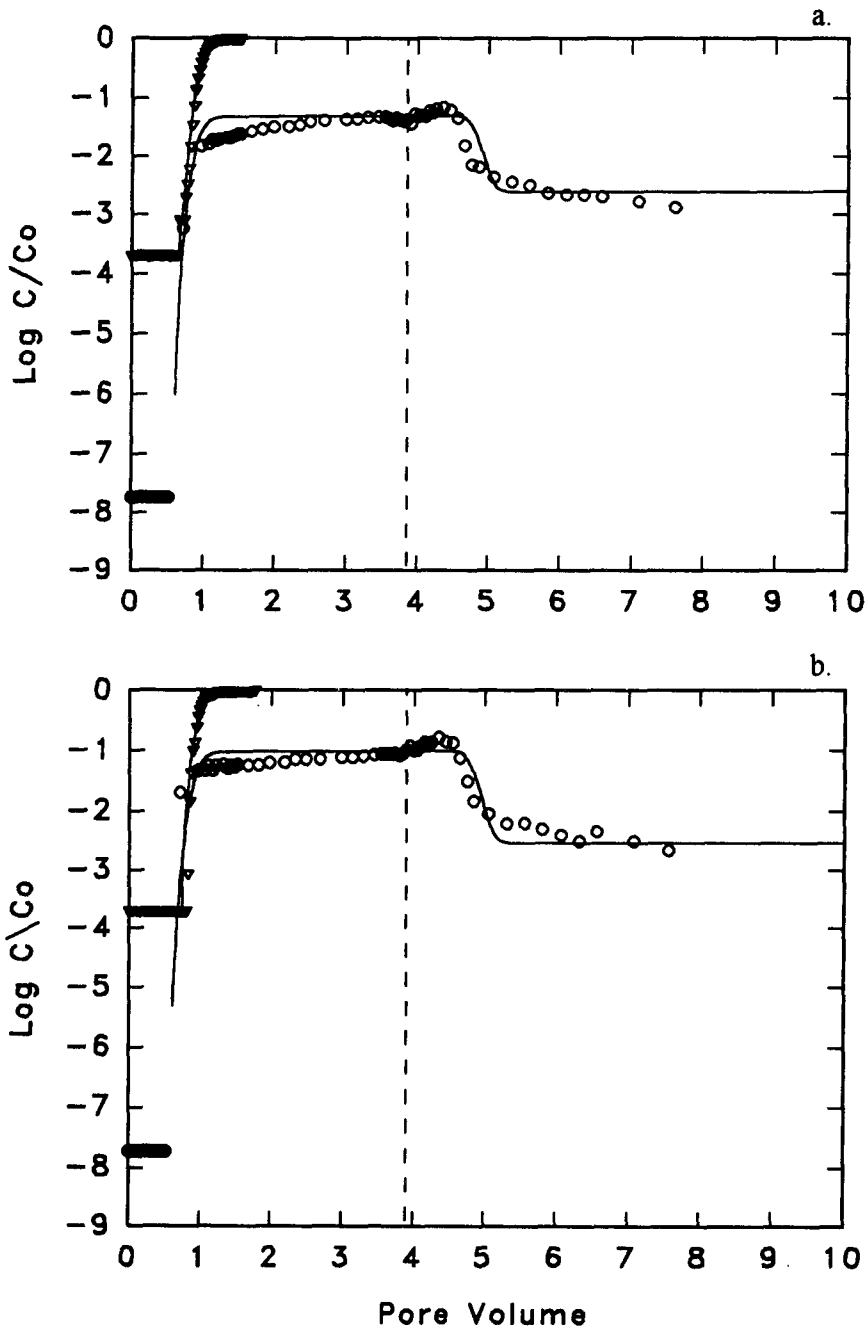

Figure 10. Breakthrough curves of microspheres (o) and NaCl tracer (▽) at 4° C with the best fit line of the first-order kinetic transport model. a.) Experiment 6. b.) Experiment 7.

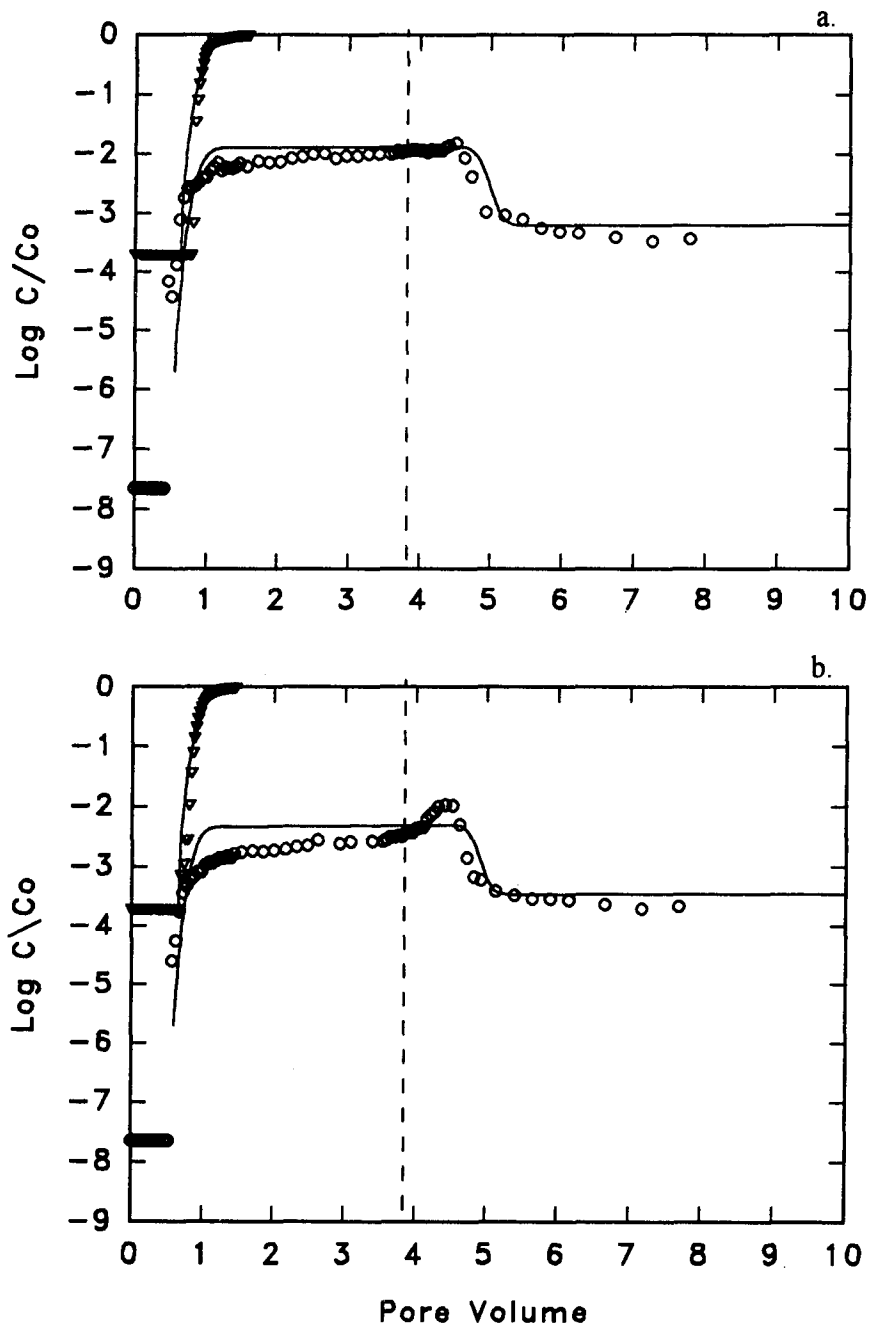

Figure 11. Breakthrough curves of microspheres (○) and NaCl tracer (▽) at 18° C with the best fit line of the first-order kinetic transport model. a.) Experiment 8. b.) Experiment 9.

Experiment 3 ran for approximately eight days (Fig.8b). The injection pulse of 4 pore volumes of *A0500* was similar to experiments 1 and 2, however, detachment was followed until the concentration of bacteria in the effluent was below detection limits. The data shown in Fig. 8b are only *A0500* bacteria. A parallel survival experiment (Fig. 6b) during column experiment 3 showed that significant death or decay of viable cells occurred after 36 hours. It is unknown if the bacteria in the column experienced the same death rate as the bacteria in the survival flask without sediment. The detachment rate could be estimated for the entire eight days if one assumes a similar death rate occurred in the column as in the survival flask. The slope of the breakthrough curve may combine the effects of detachment and death.

On the eighth day, blue-green colonies formed on the assay plates. The bacteria responsible for the blue-green color may have been a spore forming organism native to the Ringold sediment, which grew in response to the previous eight days of saturation. The blue-green bacterium was similar to *A0500* under the microscope. It was a flagellated motile rod approximately the same size as *A0500*. Column 3 was dissected and sediment samples at different lengths of the column were washed with sterile groundwater. The liquid was plated on PTYG for enumeration. The blue-green colonies overwhelmed the *A0500* colonies on the assay plates and were evenly distributed throughout the column at $\sim 2.2 \times 10^5$ CFU g^{-1} of wet sediment. Both the sterile groundwater reservoir and the *A0500* injection reservoir were assayed for contamination. The groundwater reservoir assay plates were negative for any organisms and the *A0500* injection reservoir assay plates only had *A0500* colonies. There were no further investigations of the blue-green organism. A salt tracer experiment on column 3 was not possible because the column was dissected for bacterial assay.

A0500 bacteria through Ringold sediment at 18°C were experiments 4 and 5. The breakthrough curves rose slowly to steady-state and required over 3 pore volumes of injection to reach a steady-state C/C_o. The average steady-state C/C_o was 0.59 with a standard deviation of 2% between experiments. The descending limb of the breakthrough curve became constant at 10^{-2} approximately one pore volume after the injection pulse was replaced with bacteria-free groundwater.

Replicate columns of microspheres through Ringold sediment at 4°C were experiments 6 and 7, and microspheres through Ringold sediment at 18°C were experiments 8 and 9. The breakthrough curves for all the microsphere experiments had very similar shapes. A fast rise to a steady-state C/C_o after about one pore volume. There were few data points between the detection limit and the steady-state values because large effluent samples were needed for accurate counts. Immediately after the injection pulse was replaced with microsphere-free groundwater, a slight rise in C/C_o was observed in all microsphere experiments. An increase in detachment may have occurred due to a pH change between the microsphere solution (pH = 7.7) and the groundwater pulse (pH = 8.0). All the descending limbs of the breakthrough curves reached a constant C/C_o approximately one pore volume after the injection pulse was replaced with microsphere-free groundwater.

3.4 Filtration Model Results

A steady-state filtration model was used to estimate the sticking efficiency (α) for each experiment (Table 1). Eight or nine values of C/C_o during the steady-state region of each breakthrough curve, near the end of the pulse, were averaged. C_s/C_o is defined as the concentration of bacteria or microspheres normalized by the constant input concentration at steady-state. The average C_s/C_o of bacteria in the 18°C experiments,

0.585, was approximately twice the average C_s/C_o of the 4°C experiments, 0.280. Microsphere experiments showed an opposite trend in C_s/C_o with temperature; the average C_s/C_o of the 18°C experiments, 0.0075, was only 11 percent of the average C_s/C_o in the 4°C experiments, 0.067.

Single-collector collision efficiency (η) values were nearly the same for experiments done at the same temperature (Table 1). The collision efficiency is a term related to the column geometry and physical parameters (velocity, porosity, viscosity) of the experiment. Column construction was designed to limit the variation in η. The major difference in the collision efficiency between experiments was changes in the viscosity of water due to temperature. Collision efficiencies for the 4°C and 18°C experiments were approximately 0.0142 and 0.177 respectively.

The approach velocity (flow rate / cross-sectional area) of each experiment was slightly different. Collision efficiencies depend on velocity and are higher for lower approach velocities. In order to compare the results of all experiments, η and C_s/C_o values were adjusted to the values expected at a common approach velocity of 8.9×10^{-3} cm s^{-1}, prior to statistical analyses. Adjustments were made by first calculating a new η for each experiment with the common velocity. Using equation (21) and assuming α to be independent of velocity, C_s/C_o values were calculated based on the velocity-adjusted η. A list of observed C_s/C_o values, velocity adjusted C_s/C_o values, and the percentage change of the velocity adjustments (less than 2.6%) is in Appendix B.

Statistical analyses were done to determine the level of significance of comparing the mean behavior between the two temperature experiment sets (Table 2). Documentation of the statistical analyses is in Appendix B. Differences between the mean C_s/C_o values were analyzed using the Wilcoxon rank sum test and the t-test.

Table 2. Results of t-test analysis.

	A0500 4°C	A0500 18°C	Microspheres 4°C	Microspheres 18°C
Experiments	1 , 2, 3	4 , 5	6 , 7	8 , 9
Number of C_s/C_o samples	44	27	27	29
Mean of C_s/C_o (velocity adjusted)	0.280	0.627	0.0682	0.0077
95% confidence limits (C_s/C_o)	0.315 0.245	0.724 0.530	0.0782 0.0582	0.0092 0.0062
Mean η (velocity adjusted)	0.0141	0.0177	0.0143	0.0185
Mean α	0.073	0.022	0.149	0.209
95% confidence limits (α)	0.080 0.066	0.029 0.015	0.157 0.141	0.218 0.201

Each bacteria sample point represents a single plate count. Each microsphere sample point represents an average of 20 field counts under 1000X microscope. The combined samples of each experiment set are approximately normally distributed, as estimated by the Chi-square test. (Appendix B). All observed C_s/C_o values were adjusted to a common approach velocity of 8.9×10^{-3} cm s^{-1} (Appendix B).

The mean velocity-adjusted C_s/C_o values of each experiment set were compared using the Wilcoxon rank sum non-parametric test, which is valid regardless of population distribution type. The individual values of C_s/C_o for experiments 1, 2, and 3 (*A0500*, 4°C experiments) were compared to experiments 4 and 5 (*A0500*, 18°C experiments). The null hypothesis of the one-sided test was that the means of the two experimental sets were equal. The null hypothesis was rejected at the 0.025 level of significance, indicating the mean C_s/C_o of the *A0500*, 4°C experiments were significantly different than the *A0500*, 18°C experiments. The mean C_s/C_o of the microsphere experimental sets (4°C vs. 18°C) were also significantly different.

The t-test assumes a normal distribution. The eight or nine C_s/C_o values used in the reported mean C_s/C_o for each experiment did not plot as a straight line on probability paper and were not normally distributed. In addition, each C_s/C_o value reported was an average of several plate counts or microscope field counts. Therefore, all the individual plate and microscope counts in the steady-state region of each experimental setup (i.e., all the *A0500*, 4°C data) were combined and tested using the Chi-squared test. The Chi-squared test was used to determine if a normal distribution could accurately describe the raw data. The combinations of three *A0500*, 4°C experiments, two *A0500*, 18°C experiments, and two microsphere, 4°C experiments were found to be adequately represented by a normal distribution at the 0.05 level of significance. The combined microsphere, 18°C experiments were adequately represented by the normal distribution at the 0.02 level of significance.

The t-test comparisons of the mean C_s/C_o values were made using the normally distributed combined raw data. Comparing the mean C_s/C_o of the *A0500*, 4°C experiments to the *A0500*, 18°C experiments, 0.280 and 0.627 respectively, the null hypothesis that there was no difference between the means was rejected. The probability

of a type I error (rejecting the hypothesis even though it is true) was 1.8×10^{-11}. Comparing the mean C_s/C_o values of the microsphere, 4°C experiments to the microsphere, 18°C experiments, 0.0682 and 0.0077 respectively, the null hypothesis was also rejected. The probability of a type I error was 2.2×10^{-16}.

The combination of the Wilcoxon rank sum non-parametric test and t-test indicates the mean C_s/C_o values for each experimental set reported in Table 2 were significantly different. A mean α for each experimental condition was calculated using the average (velocity adjusted) C_s/C_o, the average η (velocity adjusted) (Table 2), and equation (21). The upper and lower 95% confidence limits on C_s/C_o and α, calculated within the t-test (Table 2), do not overlap confidence limits of other experiments. Similar results were found when C_s/C_o and η values were not adjusted to a common velocity because the velocity adjustment was very small.

Estimates of the sticking efficiency (α) for *A0500* bacteria show the average value at the higher temperature (0.022 at 18°C) was 30% of the value at 4°C (0.073). The average microsphere sticking efficiencies, 0.15 at 4°C and 0.21 at 18°C, show an opposite trend, with a 40% higher value at the higher temperature. Larger C_s/C_o values at higher temperatures were predicted by the filtration model because of higher collision efficiencies (η). Higher temperatures mean lower fluid viscosity and greater Brownian motion of a particle. The number of collisions in the system was greater at 18°C than 4°C because collisions due to diffusion (η_D) and collisions due to sedimentation (η_G) were 36% and 3% more frequent, respectively.

Greater collision efficiencies at 18°C was not sufficient to explain the observed microsphere behavior. Using the calculated η at 18°C and assuming the same α at 18°C as estimated for 4°C, the C_s/C_o for microspheres at 18°C should be only 50% of that at 4°C. However, the observed 18°C microsphere C_s/C_o value was only 11% of the 4°C value

(Appendix B). The mean C_s/C_o for bacteria at 18°C was 120% higher than the mean C_s/C_o for bacteria at 4°C. The model for η suggests that the opposite should be true; thus α for non-motile bacteria at 4°C are statistically different than motile bacteria at 18°C.

An additional t-test was done in order to determine if the difference between the observed C_s/C_o value versus the model predicted value of the microspheres at 18°C was significant. Comparing the observed mean C_s/C_o of the microsphere, 18°C experiments to the microsphere, 18°C model prediction, 0.0077 and 0.034 respectively, the null hypothesis of no difference between the means was rejected. The probability of a type I error was 7.8×10^{-12}. Therefore, the difference between the observed and predicted C_s/C_o values indicate that physical or chemical processes other than greater collision efficiency were responsible for the larger removal of microspheres.

3.5 Transport Model Results

Table 1 lists the conditions and physical parameters of each column transport experiment. A one-dimensional equilibrium transport model with a non-linear-least-squares curve fitting algorithm was used to estimate hydrodynamic dispersion by fitting the NaCl breakthrough curves (Fig. 12-15). The estimated Peclet numbers from the equilibrium model solutions were used in the first-order kinetic model (Table 3). Note the Peclet number for experiment 3 was the average of the Peclet numbers for experiments 1 and 2 because column 3 was dissected for bacteria assay. The estimated dispersion, by equation (12), for the salt tracer was approximately 2.0×10^{-3} cm^2 s^{-1} for the 4°C experiments and 2.6×10^{-3} cm^2 s^{-1} for the 18°C experiments (Table 3). Greater dispersion at higher temperature was expected because of lower viscosity of water and greater Brownian motion of the salt ions.

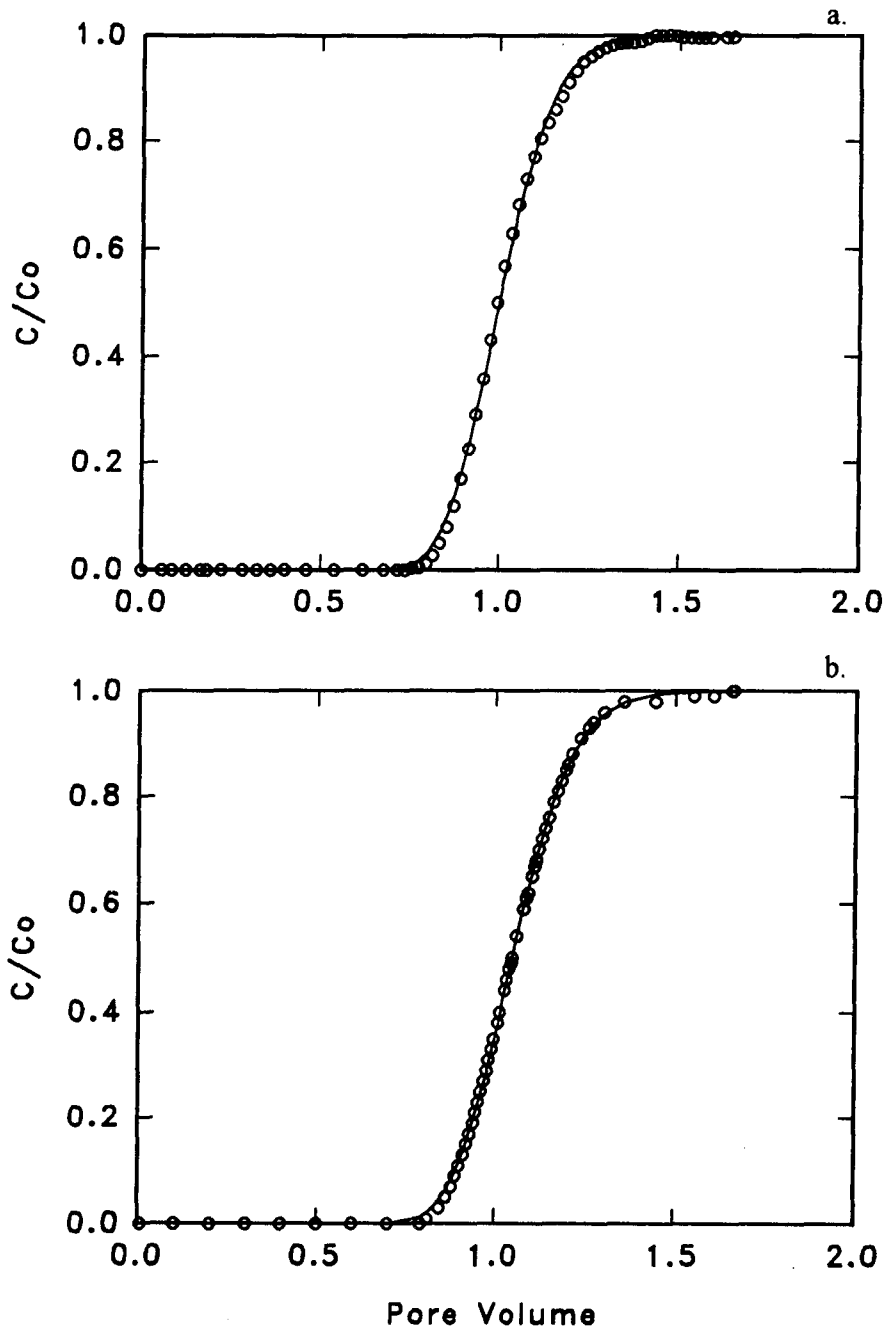

Figure 12. Breakthrough curves of NaCl tracer (o) at 4° C with the best fit line of the equilibrium transport model. a.) Experiment 1. b.) Experiment 2.

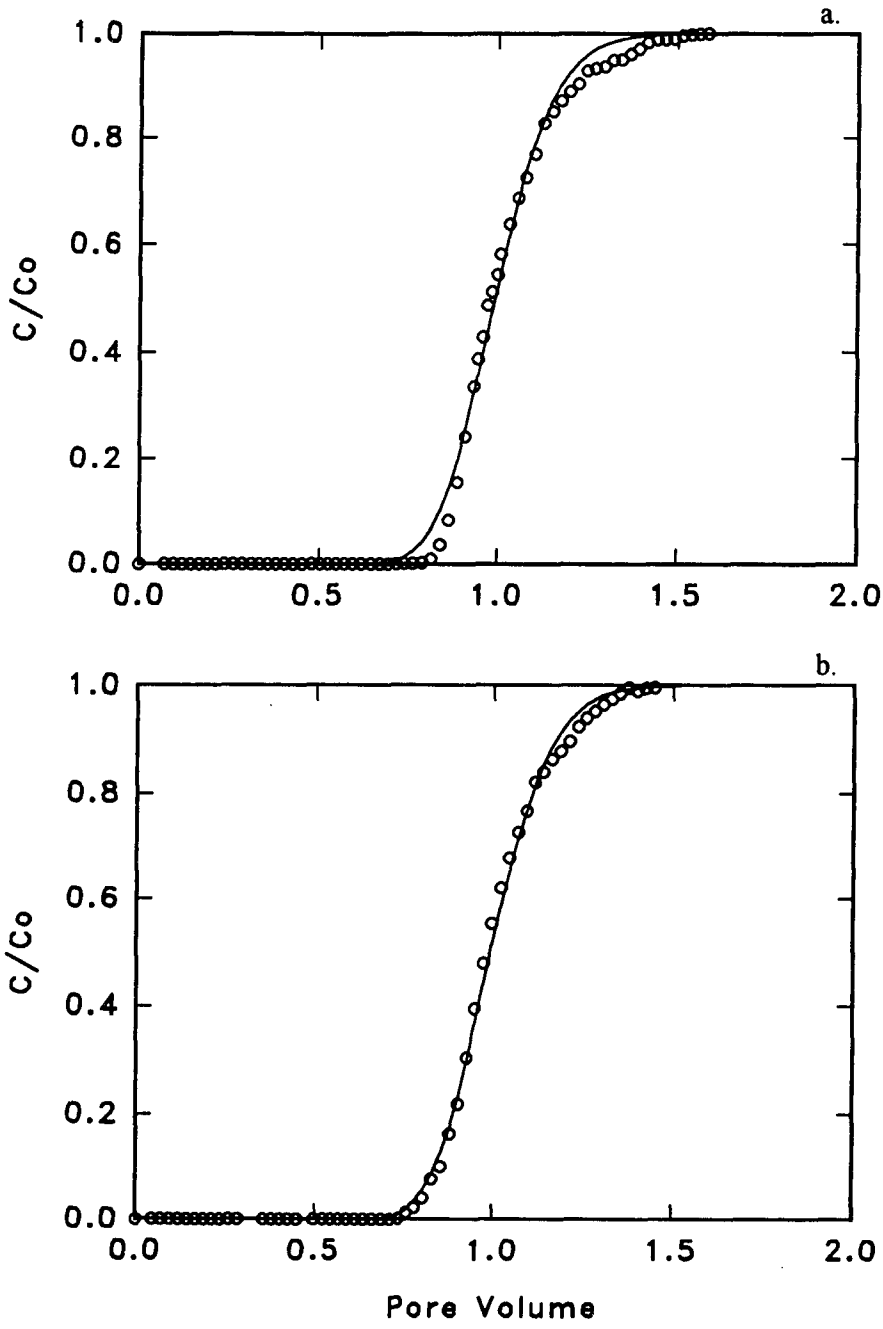

Figure 13. Breakthrough curves of NaCl tracer (o) at 4° C with the best fit line of the equilibrium transport model. a.) Experiment 4. b.) Experiment 5.

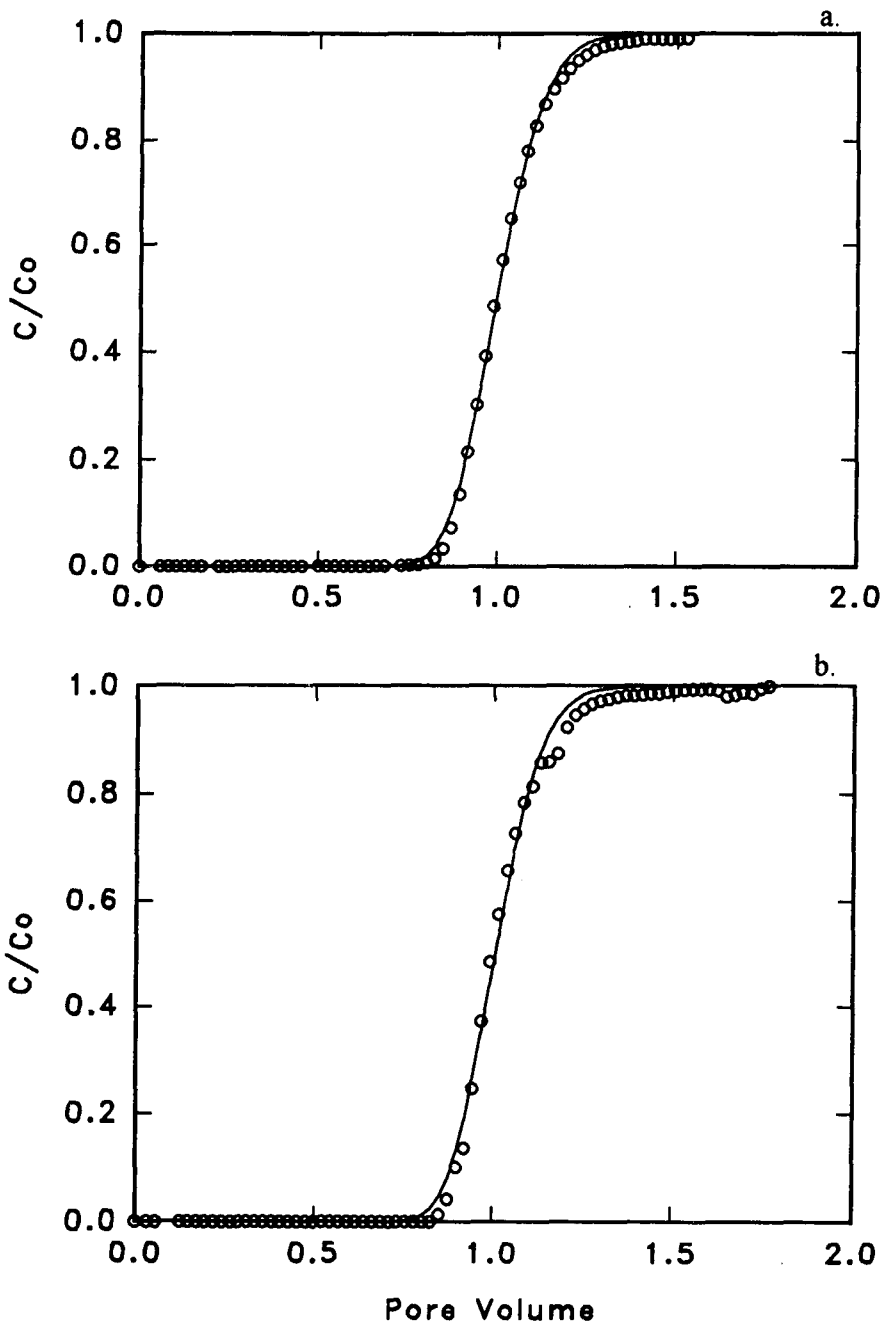

Figure 15. Breakthrough curves of NaCl tracer (o) at 18° C with the best fit line of the equilibrium transport model. a.) Experiment 8. b.) Experiment 9.

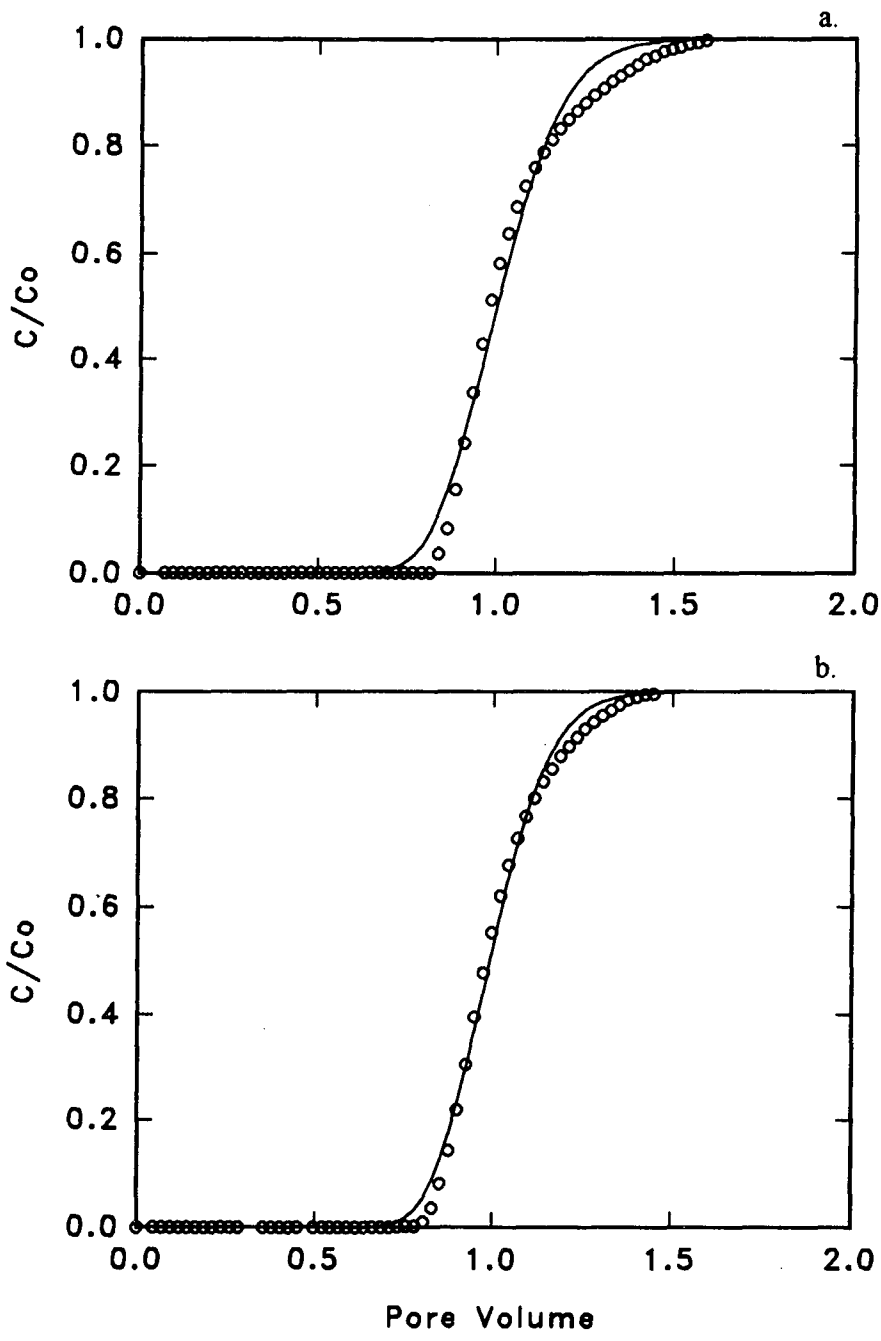

Figure 15. Breakthrough curves of NaCl tracer (o) at 18° C with the best fit line of the equilibrium transport model. a.) Experiment 8. b.) Experiment 9.

Table 3. Results from the first-order, kinetically limited, non-steady transport model fits.

	Model	Pe	R	β	ω	k_1 (10^{-3} s^{-1})	k_2 (10^{-6} s^{-1})	dispersion (10^{-2} cm^2 s^{-1})
Bacteria								
Exp 1 - 4°	F-O	136	700		1.528	0.473	0.676	0.205
	2-S	11.5	1000	0.0023	1.528	0.473	0.474	2.421
Exp 2 - 4°	F-O	124	300		1.234	0.366	1.223	0.215
	2-S	10.7	500	0.0035	1.234	0.366	0.734	2.493
Exp 3 - 4°	F-O	130	300		1.097	0.317	1.046	0.197
	2-S	10.6	500	0.0036	1.097	0.317	0.628	2.420
Exp 4 -18°	F-O	104	70		0.523	0.160	2.322	0.262
	2-S	5.3	70	0.0238	0.523	0.160	2.345	5.133
Exp 5 -18°	F-O	108	60		0.545	0.176	2.975	0.267
	2-S	5.2	60	0.0260	0.545	0.176	3.004	5.537
Spheres								
Exp 6 - 4°	F-O	138	700		3.079	0.881	1.261	0.192
	2-S	35	700	0.0020	3.079	0.881	1.261	0.756
Exp 7 - 4°	F-O	125	700		2.375	0.674	0.924	0.211
	2-S	35	600	0.0022	2.375	0.674	1.125	0.754
Exp 8 -18°	F-O	95	1500		4.510	1.378	0.920	0.293
	2-S	55	1800	0.0005	4.510	1.378	0.766	0.507
Exp 9 -18°	F-O	115	1500		5.600	1.689	1.127	0.239
	2-S	55	1900	0.0006	5.600	1.689	0.890	0.500

First-order model (F-O) had ω fixed to the steady-state filtration model solution and fixed Pe to the salt tracer equilibrium transport model solution. Results from the two-site non-steady transport model (2-S) had ω fixed to the steady-state filtration model solution.

The bacteria and microsphere breakthrough curves were fit by the first-order, kinetically limited, non-steady transport model (Fig.7-11). Only one model parameter was fit by the data, retardation factor (R). Peclet number for each model solution was set to the predetermined Peclet number of the salt tracer. This assumes that the bacteria and microspheres experienced the same hydrodynamic dispersion as the salt ions. The attachment rate coefficient k_1 was estimated using the steady-state filtration model, equation (17). The model parameter ω was calculated from k_1 using equation (13). Retardation factors were determined by visually fitting the height of the tailing descending limb of the breakthrough data.

The best model fit was determined by visual inspection of plotted model solutions and the observed data. The model fit to the observed data was very good for the top of the breakthrough curve, steady-state region, and for the descending limb. The model solution did not fit the rising limb of the breakthrough curve because the attachment rate (k_1) was probably not constant at early times. A non-linear-least-squares curve fitting algorithm was not used. Accurate data span multiple log units; least-squares fitting sums squared errors, and would essentially ignore low C/C_o points in favor of higher C/C_o points.

Attachment (k_1) and detachment (k_2) rate coefficients (Table 3) were estimated from model parameters (P, R and ω), and physical column parameters (Table 1) using equations (13) and (11). The time scales of attachment and detachment are indicated by $1/k_1$ and $1/k_2$. Bacteria in the 4°C experiment took less than 1 hour to become attached, where as the bacteria took more than 1.5 hours to become attached in the 18°C experiments. Therefore, *A0500* bacteria moved almost twice as far in 18°C columns before attaching to the sediment. Once attached, bacteria took 10-17 days to detach at 4°C and only 4-5 days to detach at 18°C.

An alternative transport modeling approach was taken to find a better fit to the rising limb of the breakthrough data and to evaluate model fit without assuming that hydrodynamic dispersion of salt tracer was equal to the dispersion of bacteria or microspheres. Using the two-site transport model, Peclet number, R and β were fitted and ω was held constant at the value previously determined from the filtration model. The non-linear-least-squares algorithm was used to simultaneously fit the three parameters to the rising limb of breakthrough. R and β were then fit to the complete breakthrough curves, while keeping Peclet number and ω constant (Appendix C) (Table 3). Model solutions fit the shape of the rising limb very well. However, the model underestimated detachment immediately after the pulse of colliod-free water was applied . The curve fits for the entire breakthrough curve did not converge on a single set of parameters in 40 iterations; estimations of R were increasing systematically on the 40th iteration. Additional model runs that had larger initial guesses of R did not solve the convergence problem. R continued to increase on the 40th iteration, and the visual fits of the model solutions were degrading. The reported two-site model solutions come from using the first-order model solutions as initial values for fitted parameters. The sum of standard errors of parameter estimations were; Peclet 10-50, retardation factor >5,000, and β 0.02-0.05. Standard error is simply the standard deviation of the estimator or a measure of precision, where a small standard error represents a precise estimate. Therefore, the non-linear-least-squares curve fitting algorithm estimated β very well but, did not estimate the retardation factor or Peclet number very well.

Solutions for Peclet numbers suggest that the dispersion of bacteria and microspheres was 10 times that of the salt tracer, 2.4×10^{-2} cm^2 s^{-1}. Independent estimates of colliod diffusion using the Stokes-Einstein equation combined with empirical estimates of eddy dispersion [*Horvath and Lin, 1976*] were approximately 10^{-4} cm^2 s^{-1}.

Therefore, the apparent dispersion of the observed breakthrough data was not simply an affect of hydrodynamic dispersion. Apparent dispersion, slow rising limb, included the effects of variable attachment-detachment rate coefficients.

The two-site model did improve the shape of the slow rising breakthrough limb but, failed to fit the descending limb or the time of initial colloid breakthrough. By keeping ω constant in both transport modeling efforts, estimates of k_1 are the same. The first-order and the two-site model solutions, as applied to these experiments, yield very similar detachment rate coefficients. Using the filtration model to fix the attachment (k_1) rate coefficient, and fixing the dispersion estimate to the salt tracer solution, gave model parameter solutions with the best visual fits by fitting only one parameter, R. Consequently, the first-order kinetic model solutions provided the best parameter estimates of the observed transport of bacteria and microspheres.

4.0 DISCUSSION

4.1 Experimental Protocol

Bacteria isolated from deep subsurface sediments were pumped through columns packed with unsterilized sediments. In other laboratory studies, porous media were either sterilized by heat [*Fontes et al., 1991*], poisons [*Scholl et al., 1990*], irradiation [*Gannon et al., 1991*] or they used genetically altered antibiotic-resistance bacteria [*Smith et al., 1985*] to distinguish between and accurately count bacteria of interest among many different strains. Experimental procedures that significantly change porous media reduce the applicability of measured transport behavior to a natural material. Autoclaving may break down the internal structure of a sediment and chemical sterilization can alter the surface chemistry of a sediment. I was able to quantify transport of bacteria through Ringold sediment under similar chemical conditions found in the field because *A0500* overwhelmed indigenous bacteria on PTYG plates in 24 hours and were accurately counted against a very low background. One possible improvement to this method would be if columns were made from cored sediment samples because packing sediment mixtures into columns changes the macropore structure and reduces permeability [*Smith et al., 1985*].

The spread-plate counting method was used to distinguish between viable and non-viable bacteria and to selectively remove non-viable cells from the breakthrough counts. The bacteria counted in column effluent were metabolically able to reproduce after traveling through the sediment column. Using this counting method, estimates of transported bacteria reflect the number of bacteria that could participate in biofilm development. Viable bacteria were counted in this study because only viable organisms

can participate in the inoculation of deep aquifers from recharge waters, *in situ* bioremediation, and pathogen transport.

Quantifying the effects of bacteria motility during advective transport was done by running replicate columns at different temperatures. Laboratory conditions (4°C) designed to inhibit growth during a transport experiment also inhibited motility. At temperatures typically found in groundwater (18°C), *A0500* swam in random directions. With all other physical and chemical variables constant, temperature was used to switch on and off bacterial motility. Results of this study suggest that bacteria motility significantly changed the kinetics of attachment and detachment during advective transport. Other published motility studies through porous media focused on chemotaxis and random motility under hydrostatic conditions [*Jang et al., 1983; Jenneman et al., 1985; Reynolds et al., 1989*].

4.2 Conservative Tracers and Dispersion

Apparent dispersion illustrated by slow rising limbs of the bacteria breakthrough curves was caused by a combination of greater dispersion over that of the salt tracer and non-steady attachment-detachment kinetics. Extrapolating hydrodynamic dispersion of a Cl^- ion to a bacteria that is several orders of magnitude larger was a uncertain process because the difference between bacteria and salt tracer breakthrough curves could not be totally attributed to greater dispersion. Using the equilibrium model and known parameters (pore volume, column length, constant pore velocity, and mass flux), observed salt tracer conductivity data were fit very well with only minor variations in retardation factors (<1%, not reported). The model estimates for hydrodynamic dispersion of the salt tracer (Table 3) were interpreted as a sum of eddy diffusion and molecular diffusion. Empirical equations suggest that hydrodynamic dispersion of the larger bacterium should be larger than a salt ion because of greater eddy diffusion [*Horvath and Lin, 1976*] and

molecular diffusion of a bacterium should be smaller according to the Stokes-Einstein equation. Hydrodynamic dispersion, at pore velocities used in this study, was caused mostly by mechanical mixing (eddy diffusion) in the pores and not molecular diffusion. Calculated estimates for eddy dispersion and molecular diffusion of *A0500* bacteria were in the range of 10^{-4} and 10^{-9} cm^2 s^{-1}, respectively. The eddy diffusion and molecular diffusion equations or the salt tracers were not useful in predicting the magnitude of increased apparent dispersion, as shown by a very slow rising bacteria breakthrough. Apparent dispersion in the 2 x 10^{-2} cm^2 s^{-1} range was necessary for the two-site model to fit the shape of the bacteria breakthrough curves' rising limbs.

Modeling results, using the two-site model to fit the slow rising limb of the bacteria breakthrough curves, suggest an apparent dispersion 10 times that found with the salt tracer. The two-site model with increased dispersion could not fit the breakthrough descending limb immediately after the bacteria injection pulse was replaced with colloid-free ground water. This finding suggests there are factors other than dispersion controlling the behavior of the bacteria at early times in the column experiments.

Terms that control effluent concentration in equation (1) are dispersion, advection, attachment and detachment. At early times during a column experiment, dispersion and advection can be assumed constant but, attachment and detachment rates may not be constant. Clean bed sand filters that remove colloids are known to "ripen" to a steady-state removal rate [*Amirthalajah, 1988*]. Assuming that 100% of the injected colloid mass was attached to the sediment, less than 1% of the sediment surface, as estimated by nitrogen gas adsorption, could be covered by colloids . A slow rise of C/C_o to steady-state may be caused by a filter ripening effect, where attachment of colloids is very fast initially and slows to a steady-state with constant kinetic rates. Therefore, fitting the descending limb of the breakthrough curve would provide a more accurate estimate of

hydrodynamic dispersion because attachment and detachment rates are at steady-state. Salt tracer experiment estimates of dispersion with the first-order transport model provided good visual fits of the bacteria and microsphere breakthrough data descending limbs, suggesting that the dispersion difference between the salt tracer and colloids was small. An optimal curve fit of the breakthrough descending limb data using steady-state attachment-detachment rates as initial conditions should give the best estimate of hydrodynamic dispersion for a colloid.

4.3 Microsphere Transport

Microspheres were used as a non-motile colloid to estimate the effects of temperature on the transport models. Temperature influences on microsphere transport were used to separate the effects of temperature and the effects of motility on the observed motile (18°C) and non-motile (4°C) bacteria experiments.

Smaller steady-state breakthrough values, C_s/C_o, of microspheres at 18°C versus 4°C were predicted based on larger collision efficiencies (η) at higher temperatures. Assuming no change in chemical effects on sticking efficiency, constant α and larger collision efficiency predicts a smaller C_s/C_o. The observed microsphere data showed a larger decrease in C_s/C_o at 18°C than predicted by the model, 88% versus 50%. This suggests that either chemical effects increased the sticking efficiency or the model prediction was in error. Deviations from the model predictions could in part be due to errors in the model assumptions. The filtration model uses a single collector diameter and assumes that all collectors are the same size and are spherical in shape. Ringold sediment grains are not spherical or uniform in size. A smaller average collector diameter, similar to many particles in Ringold sediment (20% < 150 μm) would also yield smaller C_s/C_o

values. Therefore, the model correctly predicted the trend but, underestimated the magnitude.

Observed microsphere breakthrough data were much more precise than the bacteria data. Microsphere effluent concentration measurements were very reproducible (standard deviation = 6%) allowing observation of a slight positive slope to the microsphere breakthrough curve in the steady-state region. This phenomenon was not observed in the bacteria breakthrough curves because the measured C/C_o values were too variable (standard deviation = 75%). Steady-state removal refers to the situation where the attachment and detachment rates are constant over time. A slight positive slope to the breakthrough curve indicates small changes in the attachment and detachment rates. This could have been caused by heterogeneous attachment sites on the sediment. But could also just be a slow approach to steady state, where the mass ratio of colloids attaching versus detaching is constant with time. The maximum concentration of attached microspheres (S_2) covered less than 1% of the sediment surface area and therefore, detachment did not contribute significant numbers of microspheres reentering the groundwater. Microsphere surface chemistry was reasonably homogenous in a given experiment. Variation in attachment and detachment rate could be a function of the affinity of a colloid to specific surface sites on the sediment. Different sediment surface sites (negatively charged silica, positively charged iron oxides, and hydrophobic organic carbon) probably have different affinities for microspheres and, thus, would have different attachment and detachment rate coefficients. On a microscale, attachment may have occurred preferentially at high affinity sites first, filling sites with continually lower affinities over time. Again, this is consistent with sand filtration observations, where a clean sand bed ripens with time. Ripening is this case would mean filling those sites with the greatest affinity for a colloid first, resulting in a constant removal rate or a steady-state

attachment-detachment sometime after the high affinity sites were filled. Variable attachment rates could also explain the slow rising limb of the bacteria breakthrough curves to a steady state after more than two pore volumes of colloids were pumped through the column.

4.4 Bacteria Transport

If a non-motile bacterium had been used to investigate temperature effects on colloid transport, interpretation of the data would have been complicated by heterogeneity associated with bacterial cultures at stationary phase. At stationary phase net growth is zero, but some cells are dying and some cells have just replicated. Investigators have shown: *i*) that bacterial cell adhesion to polystyrene decreased with age [*Fletcher, 1977*]; *ii*) that five different bacteria strains had increased surface hydrophobicity with increased age [*van Loosdretch et al, 1987b*]; and *iii*) that adhesion to solids and cell surface hydrophobicity increased when bacteria were starved [*Kjelleburg et al., 1983*]. Therefore, heterogeneity of the bacteria surface within a stationary population may have affected the results. The non-motile temperature effect tests were made with microspheres with relatively homogeneous surface chemistry to avoid complications associated with bacteria.

Hydrodynamic dispersion was expected to increase at 18°C due to the random swimming of *A0500* bacteria. However, the precision of the estimated dispersion in this study was not sufficient to measure differences caused by bacteria motility.

The bacteria experimental findings contradict predictions that higher temperatures favor chemisorption and some types of physical adsorption of solutes from solution [*Shaw, 1976*]. Microsphere removal was enhanced by higher temperatures, but *A0500* bacteria removal was diminished.

Penetration of bacteria at 18°C versus 4°C was significantly greater, with C_s/C_o equal to 0.63 and 0.28 respectively. The steady-state filtration model predicted less penetration at a higher temperature due to a larger collision efficiency, and the non-motile microspheres behaved as predicted. Therefore, bacteria motility, which was the only difference between experiment sets, was thought to be the causative variable to the enhanced transport through the sediment.

A possible mechanism causing greater penetration could be that motile bacteria have the ability to detach from a surface under their own locomotive power. In many bacteria adhesion studies, summarized by *van Loosdrecht et al., 1989*, a relatively low Gibbs free energy of adhesion was found and interpreted as adhesion in the secondary minimum of the DLVO interaction curve. They concluded that the initial step in bacterial adhesion is often a reversible process, which in terms of DLVO theory can be described as secondary minimum adhesion. Motile *A0500* bacteria in this study may have been able to escape the weak attractive forces of the secondary minimum by their only kinetic energy. This would act to decrease the residence time of attachment. A shorter residence time reduces the probability that bacteria become irreversibly attached [*van Loostretch et al., 1989*]. A non-motile colloid would only be able to escape the secondary minimum by Brownian motion and would more likely be irreversibly removed because of a longer residence time of attachment. Support of this transport mechanism is illustrated by the estimates of the time scale for detachment ($1/k_2$). In all non-motile colloid transport experiments, microspheres at 4°C and 18°C and *A0500* at 4°C, a detachment time scale was estimated to be between 9 and 17 days. In the motile transport experiments, *A0500* at 18°C, a detachment time scale was estimated to be between 4 and 5 days.

Other investigators have hypothesized that bacterial motility would increase the likelihood of a bacteria becoming irreversibly attached to a soil because their kinetic

energy would overcome electrostatic repulsive forces and become attached in the primary minimum as described by DLVO theory [*van Loosdrecht et al., 1989; Fletcher, 1977; Marshall et al., 1971*] . Results of this study suggest that bacterial motility more importantly acts to detach weakly held bacteria from the secondary minimum and may detach bacteria from the primary minimum at a slower rate.

Additional research is needed to more accurately predict advective transport of bacteria in the subsurface. Laboratory studies are needed to determine if bacterial attachment and detachment can be accurately described by rate constants or if time-dependent rate functions are needed. Adjustments to the advection-dispersion transport model would be necessary to incorporate time dependent attachment-detachment rate functions. Experimental protocols need to be developed for similar transport experiments as this study, but using truly oligotrophic bacteria. The findings in this study are biased by the fact that bacteria from deep oligotrophic sediments were isolated and grown on concentrated media. One would have to overcome the difficulties in isolating and preparing sufficient concentrations of oligotrophs for an experiment as well as be able to accurately enumerate target oligotrophs among a mixture of indigenous sediment bacteria.

There were limitations to both modeling tools used in this study. Application of the filtration model was limited by the assumptions that collectors in porous media are spherical and are of uniform size. An empirical correction factor applied to ideal conditions maybe developed to overcome the inherent problems with the spherical-uniform assumptions.

In addition, the steady-state filtration model cannot be used to fit a complete breakthrough curve because of the steady-state requirement. A transport model derived using similar principles as the steady-state filtration model but with time-dependent solutions could be developed.

The advection-dispersion transport model used to estimate kinetic coefficients could be improved by using time-dependent attachment and detachment rate functions. Although the changes to the advection-dispersion equation would prohibit an analytical solution, numerical approximations could be used to improve breakthrough curve fitting algorithms.

5.0 CONCLUSIONS

Results indicate that bacterial motility facilitates advective transport through natural aquifer sediments by changing the attachment-detachment kinetics to reduce retardation.. The time scale of attachment was twice as long for bacteria at 18°C, a temperature at which they were motile, than for the same bacteria at 4°C, a temperature at which they were not motile. Attachment was reversible at both temperatures. Bacterial motility is thought to be important in near-surface soil systems where detachment time scales were long relative to grow rate. In deeper, oligotrophic environments, detachment time scales may be small relative to growth rate, suggesting that advective transport controlled by the rate of detachment may be the most important transport process. Detachment time scale for the motile *A0500* bacteria was one-third that of its non-motile relative. Consequently, estimation of travel times to deep aquifers from recharge waters could be significantly affected by bacterial motility.

Calculated arrival times of bacteria from recharge waters, pathogen transport, and *in situ* pumping of bacteria may be in error if investigations ignore motility. This is especially true if transport parameter estimates used in calculating arrival times were taken from laboratory studies that inadvertently restrict motility in order to provide growth controls on the experiments.

Non-motile polystyrene microspheres were found to behave as predicted by the steady-state filtration model, with smaller penetration at higher temperatures. Motile *A0500* bacteria did not behave as predicted by the filtration model, having greater penetration at higher temperatures. These findings indicate that even though the collision efficiency is greater at a higher temperature, motility acts to change attachment-detachment kinetics in favor of the detached state.

Non-steady transport models using attachment and detachment rate constants could not fit the rising limbs of bacteria breakthrough curves. One possible cause of the slow rising curves may have been that the attachment rate coefficient was initially very large and diminished in time. Support of variable attachment and detachment rate coefficients at early times was found in descriptions of clean sand filter ripening.

APPENDIX A

Results of Bacteria and Microsphere Column Experiments

Experiment 1

A0500
Temperature = 4 C
Ringold Sediment
Column Length = 30 cm
Avg. Interstitial Velocity = 9.28 E-3 cm/s
Flow rate = 1.094 mL/min.
Pore Vol. = 58.7 mL

Porosity = 0.39
Hydraulic Detention = 53.7 min.
Bacteria solution pH = 7.8
Final effluent pH = 7.6
Co = 3.00E+09 CFU/mL
Pulse = 3.368

Sample	Effluent Volume (mL)	Pore Volume	C/Co (low)	C/Co (high)	C/Co (avg)	STD. DEV
0	0.00	0.000	3.3E-10	3.3E-10	3.3E-10	0
1	2.95	0.050	3.3E-10	3.3E-10	3.3E-10	0
2	5.90	0.101	3.3E-10	3.3E-10	3.3E-10	0
3	8.85	0.151	3.3E-10	3.3E-10	3.3E-10	0
4	11.80	0.201	3.3E-10	3.3E-10	3.3E-10	0
5	14.76	0.251	3.3E-10	3.3E-10	3.3E-10	0
6	17.71	0.302	3.3E-10	3.3E-10	3.3E-10	0
7	20.66	0.352	3.3E-10	3.3E-10	3.3E-10	0
8	23.61	0.402	3.3E-10	3.3E-10	3.3E-10	0
9	26.56	0.452	3.3E-10	3.3E-10	3.3E-10	0
10	29.51	0.503	3.7E-08	3.7E-08	3.7E-08	0
11	32.46	0.553	1.7E-06	3.1E-06	2.4E-06	4.95E-07
12	35.41	0.603	4.7E-06	6.3E-06	5.5E-06	5.89E-07
13	38.36	0.654	4.3E-06	1.7E-05	1.1E-05	4.48E-06
15	44.27	0.754	6.7E-05	4.7E-04	2.7E-04	0.000141
16	47.22	0.804	4.3E-04	1.1E-03	7.5E-04	0.000224
17	50.17	0.855	2.7E-04	2.7E-04	2.7E-04	0
18	53.12	0.905	5.3E-04	1.2E-03	8.8E-04	0.000247
19	56.07	0.955	5.0E-04	6.3E-04	5.7E-04	4.71E-05
20	59.02	1.005	7.0E-04	1.5E-03	1.1E-03	0.000271
23	67.87	1.156	4.7E-03	4.7E-03	4.7E-03	0
24	70.82	1.207	5.3E-03	6.7E-03	6.0E-03	0.000471
27	79.68	1.357	1.4E-02	1.7E-02	1.5E-02	0.001061
28	82.63	1.408	1.3E-02	2.0E-02	1.7E-02	0.002357
29	85.58	1.458	1.3E-02	2.2E-02	1.8E-02	0.003064
30	88.53	1.508	2.5E-02	3.3E-02	2.9E-02	0.002946

31	91.48	1.558	2.3E-02	2.7E-02	2.5E-02	0.001179
32	94.43	1.609	2.3E-02	3.0E-02	2.6E-02	0.002593
34	100.33	1.709	4.3E-02	5.7E-02	5.0E-02	0.004714
36	106.24	1.810	2.3E-02	2.3E-02	2.3E-02	0
38	112.14	1.910	5.3E-02	5.3E-02	5.3E-02	0
40	118.04	2.011	6.0E-02	6.0E-02	6.0E-02	0
42	123.94	2.111	3.0E-02	3.3E-02	3.2E-02	0.001179
44	129.84	2.212	3.3E-02	6.7E-02	5.0E-02	0.011785
46	135.75	2.313	1.5E-01	2.0E-01	1.7E-01	0.018856
52	153.45	2.614	1.7E-01	1.7E-01	1.7E-01	0
55	162.31	2.765	1.0E-01	1.3E-01	1.2E-01	0.010607
60	177.06	3.016	9.3E-02	9.3E-02	9.3E-02	0
65	191.82	3.268	2.0E-01	2.0E-01	2.0E-01	0
70	206.57	3.519	2.2E-01	2.2E-01	2.2E-01	0
72	212.47	3.620	2.1E-01	2.1E-01	2.1E-01	0
74	218.37	3.720	1.9E-01	2.0E-01	2.0E-01	0.002357
76	224.28	3.821	1.3E-01	2.2E-01	1.8E-01	0.029463
78	230.18	3.921	1.0E-01	1.0E-01	1.0E-01	0
79	233.13	3.972	1.9E-01	2.7E-01	2.3E-01	0.028284
82	241.98	4.122	3.3E-01	3.3E-01	3.3E-01	0
83	244.93	4.173	2.8E-01	2.7E-01	2.8E-01	0.001179
86	253.79	4.323	2.3E-02	2.3E-02	2.3E-02	0
88	259.69	4.424	1.0E-02	1.7E-02	1.3E-02	0.002357
90	265.59	4.525	6.7E-03	1.8E-02	1.3E-02	0.004125
92	271.49	4.625	6.7E-03	6.7E-03	6.7E-03	0
94	277.39	4.726	7.3E-03	7.3E-03	7.3E-03	0
98	289.20	4.927	3.7E-03	3.7E-03	3.7E-03	0
100	295.10	5.027	3.0E-03	4.3E-03	3.7E-03	0.000471
105	309.86	5.279	3.3E-03	3.3E-03	3.3E-03	0
115	339.37	5.781	7.7E-03	7.7E-03	7.7E-03	0
120	354.12	6.033	3.0E-03	3.0E-03	3.0E-03	0
125	368.88	6.284	1.5E-03	1.5E-03	1.5E-03	0
130	383.63	6.535	1.3E-03	3.0E-03	2.1E-03	0.000601
135	398.39	6.787	1.3E-03	2.4E-03	1.9E-03	0.000365
140	413.14	7.038	1.5E-03	1.5E-03	1.5E-03	0
145	427.90	7.290	1.3E-03	1.3E-03	1.3E-03	0
155	457.41	7.792	1.6E-03	1.6E-03	1.6E-03	0

Experiment 2

A0500
Ringold Sediment
Temperature = 4 C
Column Length = 30 cm
Avg. Interstitial Velocity = 8.89 E-3 cm/s
Flow rate = 1.024 mL/min.
Pore Vol. = 57.5 mL

Porosity = 0.381
Hydraulic Detention = 56.2 min.
Bacteria solution pH =7.9
Final Effluent pH = 7.7
Co = 2.50E+09 CFU/mL
Pulse = 4.213

Sample	Effluent Volume (mL)	Pore Volume	C/Co (low)	C/Co (high)	C/Co (avg)	STD.DEV.
0	0.00	0.000	4.0E-10	4.0E-10	4.0E-10	0
1	2.95	0.051	4.0E-10	4.0E-10	4.0E-10	0
2	5.90	0.103	4.0E-10	4.0E-10	4.0E-10	0
3	8.85	0.154	4.0E-10	4.0E-10	4.0E-10	0
4	11.80	0.205	4.0E-10	4.0E-10	4.0E-10	0
5	14.76	0.257	4.0E-10	4.0E-10	4.0E-10	0
6	17.71	0.308	4.0E-10	4.0E-10	4.0E-10	0
7	20.66	0.359	4.0E-10	4.0E-10	4.0E-10	0
8	23.61	0.411	4.0E-10	4.0E-10	4.0E-10	0
9	26.56	0.462	4.0E-10	4.0E-10	4.0E-10	0
10	29.51	0.513	4.0E-10	4.0E-10	4.0E-10	0
11	32.46	0.565	4.0E-09	4.0E-09	4.0E-09	0
12	35.41	0.616	3.3E-08	5.6E-08	4.4E-08	1.16E-08
13	38.36	0.667	1.2E-06	1.2E-06	1.2E-06	0
14	41.31	0.719	3.8E-05	8.8E-05	6.3E-05	2.5E-05
16	47.22	0.821	1.1E-04	1.1E-04	1.1E-04	0
17	50.17	0.872	8.0E-05	8.0E-05	8.0E-05	0
23	67.87	1.180	1.2E-03	1.2E-03	1.2E-03	0
24	70.82	1.232	7.2E-03	7.2E-03	7.2E-03	0
26	76.73	1.334	2.1E-02	2.1E-02	2.1E-02	0
30	88.53	1.540	6.0E-02	6.0E-02	6.0E-02	0
32	94.43	1.642	1.4E-01	1.4E-01	1.4E-01	0
34	100.33	1.745	4.4E-02	4.4E-02	4.4E-02	0
36	106.24	1.848	8.0E-02	3.5E-01	2.2E-01	0.136
37	109.19	1.899	3.2E-01	3.2E-01	3.2E-01	0
53	159.40	2.772	2.4E-01	2.4E-01	2.4E-01	0

55	165.31	2.875	2.6E-01	4.4E-01	3.5E-01	0.088
59	177.11	3.080	2.2E-01	3.2E-01	2.7E-01	0.05
61	183.01	3.183	4.0E-01	4.4E-01	4.2E-01	0.02
63	188.91	3.285	6.0E-01	6.0E-01	6.0E-01	0
65	194.82	3.388	2.8E-01	2.8E-01	2.8E-01	0
72	215.47	3.747	2.4E-01	2.4E-01	2.4E-01	0
76	242.28	4.213	4.0E-01	4.8E-01	4.4E-01	0.04
77	245.23	4.265	3.2E-01	5.2E-01	4.2E-01	0.1
79	251.13	4.367	1.7E-01	1.7E-01	1.7E-01	0
80	254.08	4.419	2.6E-01	2.6E-01	2.6E-01	0
84	265.88	4.624	2.4E-01	2.4E-01	2.4E-01	0
90	283.59	4.932	2.8E-01	2.8E-01	2.8E-01	0
96	301.30	5.240	4.0E-02	1.9E-01	1.2E-01	0.076
103	321.95	5.599	3.4E-02	3.4E-02	3.4E-02	0
108	336.71	5.856	8.0E-03	1.6E-02	1.2E-02	0.0042
110	342.61	5.958	9.6E-03	9.6E-03	9.6E-03	0
120	372.12	6.472	1.3E-02	1.3E-02	1.3E-02	0
125	386.88	6.728	8.8E-03	8.8E-03	8.8E-03	0
130	401.63	6.985	5.6E-03	5.6E-03	5.6E-03	0
140	431.14	7.498	4.0E-03	4.0E-03	4.0E-03	0
151	463.60	8.063	8.8E-03	8.8E-03	8.8E-03	0
160	490.16	8.525	7.2E-03	7.2E-03	7.2E-03	0
175	534.43	9.294	1.2E-02	1.2E-02	1.2E-02	0

Experiment 3

A0500
Ringold Sediment
Temperature = 4 C
Column Length = 30 cm
Avg. Interstitial Velocity = 8.55 E-3 cm/s
Flow rate = 1.008 mL/min.
Pore Volume = 58.9 mL

Porosity = 0.390
Hydraulic Detention = 56.7 min.
Bacteria solution pH = 7.8
Final effluent pH = 7.7
Co = 3.40E+09
Pulse = 3.933

Sample	Effluent Volume (mL)	Pore Volume	C/Co (low)	C/Co (high)	C/Co (avg)	STD.DEV.
0	0.00	0.000	2.9E-10	2.9E-10	2.9E-10	0
1	2.97	0.050	2.9E-10	2.9E-10	2.9E-10	0
2	5.94	0.101	2.9E-10	2.9E-10	2.9E-10	0
3	8.91	0.151	2.9E-10	2.9E-10	2.9E-10	0
4	11.88	0.202	2.9E-10	2.9E-10	2.9E-10	0
5	14.85	0.252	2.9E-10	2.9E-10	2.9E-10	0
6	17.82	0.303	2.9E-10	2.9E-10	2.9E-10	0
7	20.79	0.353	2.9E-10	2.9E-10	2.9E-10	0
8	23.76	0.403	2.9E-10	2.9E-10	2.9E-10	0
9	26.73	0.454	2.9E-10	2.9E-10	2.9E-10	0
10	29.70	0.504	2.9E-10	2.9E-10	2.9E-10	0
11	32.67	0.555	2.9E-10	2.9E-10	2.9E-10	0
12	35.64	0.605	1.1E-06	1.1E-06	1.1E-06	0
13	38.61	0.656	1.8E-06	1.9E-06	1.8E-06	5.88E-08
14	41.58	0.706	2.9E-06	7.1E-06	5.0E-06	2.06E-06
17	50.49	0.857	3.5E-05	3.5E-05	3.5E-05	0
18	53.46	0.908	2.9E-05	2.0E-04	1.1E-04	8.38E-05
19	56.43	0.958	2.9E-04	5.3E-04	4.1E-04	0.000118
20	59.40	1.008	5.9E-05	7.9E-05	6.9E-05	1.03E-05
21	62.37	1.059	5.3E-05	2.1E-04	1.3E-04	7.65E-05
22	65.34	1.109	1.2E-04	1.8E-04	1.5E-04	2.65E-05
23	68.31	1.160	2.6E-04	8.8E-04	5.7E-04	0.000309
24	71.28	1.210	2.4E-04	2.9E-04	2.6E-04	2.94E-05
30	89.10	1.513	2.9E-03	4.4E-03	3.7E-03	0.000735
32	95.04	1.614	2.9E-03	2.9E-03	2.9E-03	0
34	100.98	1.714	2.6E-02	3.8E-02	3.2E-02	0.005882

36	106.92	1.815	2.9E-02	3.5E-02	3.2E-02	0.003382
40	118.80	2.017	5.3E-02	9.1E-02	7.2E-02	0.019118
45	133.65	2.269	2.9E-02	5.0E-02	4.0E-02	0.010294
50	148.50	2.521	4.4E-01	4.7E-01	4.6E-01	0.014706
55	163.35	2.773	3.8E-01	3.8E-01	3.8E-01	0
60	178.20	3.025	8.8E-02	3.2E-01	2.1E-01	0.117647
65	193.05	3.278	2.1E-01	3.2E-01	2.6E-01	0.058824
70	207.90	3.530	2.1E-01	2.5E-01	2.3E-01	0.020588
75	222.75	3.782	2.9E-01	5.3E-01	4.1E-01	0.117647
76	225.72	3.832	4.1E-01	5.3E-01	4.7E-01	0.058824
77	228.69	3.883	3.2E-01	3.8E-01	3.5E-01	0.029412
78	231.66	3.933	2.1E-01	5.6E-01	3.9E-01	0.172059
80	237.60	4.034	2.4E-01	4.7E-01	3.5E-01	0.117647
84	249.48	4.236	2.6E-01	2.8E-01	2.7E-01	0.008824
92	273.24	4.639	1.2E-01	1.4E-01	1.3E-01	0.008824
93	276.21	4.689	1.2E-01	1.2E-01	1.2E-01	0
94	279.18	4.740	2.0E-01	2.0E-01	2.0E-01	0
95	282.15	4.790	1.6E-01	1.6E-01	1.6E-01	0
96	285.12	4.841	1.4E-01	1.4E-01	1.4E-01	0
102	302.94	5.143	2.5E-02	1.5E-02	2.0E-02	0.005147
104	308.88	5.244	7.4E-03	7.4E-03	7.4E-03	0
106	314.82	5.345	6.8E-03	6.8E-03	6.8E-03	0
108	320.76	5.446	4.7E-02	1.5E-02	3.1E-02	0.016176
110	326.70	5.547	9.1E-03	2.9E-03	6.0E-03	0.003088
115	341.55	5.799	5.9E-03	1.1E-02	8.2E-03	0.002353
120	356.40	6.051	9.7E-03	1.2E-02	1.1E-02	0.001029
125	371.25	6.303	8.2E-03	8.2E-03	8.2E-03	0
130	386.10	6.555	3.8E-03	8.8E-03	6.3E-03	0.0025
135	400.95	6.807	5.9E-03	7.1E-03	6.5E-03	0.000588
140	470.80	7.993	4.4E-03	5.9E-03	5.1E-03	0.000735
145	485.65	8.245	5.9E-03	7.4E-03	6.6E-03	0.000735
164	543.76	9.232	7.1E-03	7.1E-03	7.1E-03	0
200	711.16	12.074	4.4E-03	4.4E-03	4.4E-03	0
240	897.16	15.232	1.1E-03	1.1E-03	1.1E-03	0
260	990.16	16.811	8.8E-04	1.7E-03	1.3E-03	0.000397
280	1083.16	18.390	8.8E-04	1.6E-03	1.2E-03	0.000338
290	1129.66	19.179	2.2E-03	2.2E-03	2.2E-03	0
300	1176.16	19.969	2.1E-03	2.1E-03	2.1E-03	0
310	1222.66	20.758	2.0E-03	2.0E-03	2.0E-03	0

320	1269.16	21.548	1.4E-03	1.4E-03	1.4E-03	0
360	1455.16	24.706	1.3E-03	1.3E-03	1.3E-03	0
A	2171.81	36.873	1.5E-03	1.5E-03	1.5E-03	0
B	2176.46	36.952	2.4E-03	2.4E-03	2.4E-03	0
C	2970.41	50.431	1.8E-03	1.8E-03	1.8E-03	0
D	2975.06	50.510	4.1E-04	7.1E-04	5.6E-04	0.000147
E	3398.01	57.691	5.9E-05	5.6E-05	5.7E-05	1.47E-06
F	3402.66	57.770	2.9E-05	3.8E-05	3.4E-05	4.41E-06
G	4777.91	81.119	5.9E-06	6.5E-06	6.2E-06	2.94E-07
H	4782.56	81.198	5.9E-06	6.5E-06	6.2E-06	2.94E-07
I	6320.21	107.304	2.7E-06	2.7E-06	2.7E-06	0
J	6324.86	107.383	2.9E-06	2.9E-06	2.9E-06	0
K	7738.71	131.387	1.8E-07	2.1E-07	1.9E-07	1.47E-08
L	7743.36	131.466	8.8E-08	2.6E-07	1.8E-07	8.82E-08
M	9400.21	159.596	5.9E-08	8.8E-08	7.4E-08	1.47E-08
N	9404.86	159.675	5.0E-08	5.6E-08	5.3E-08	2.94E-09

Experiment 4

A0500
Ringold Sediment
Temperature = 18 C
Column Length = 29.8 cm
Avg. Interstitial Velocity = 9.13 E-3 cm/s
Flow rate = 1.062 mL/min.
Pore Volume = 58.0 mL

Porosity = 0.385
Hydraulic Detention = 54.6 min.
Bacteria solution pH = 7.9
Final effluent pH = 7.7
Co = 2.04E+09
Pulse = 4.045

Sample	Effluent Volume (mL)	Pore Volume	C/Co (low)	C/Co (high)	C/Co (avg)	STD.DEV.
0	0.00	0.000	4.9E-10	4.9E-10	4.9E-10	0
1	3.01	0.052	4.9E-10	4.9E-10	4.9E-10	0
2	6.02	0.104	4.9E-10	4.9E-10	4.9E-10	0
3	9.02	0.156	4.9E-10	4.9E-10	4.9E-10	0
4	12.03	0.207	4.9E-10	4.9E-10	4.9E-10	0
5	15.04	0.259	4.9E-10	4.9E-10	4.9E-10	0
6	18.05	0.311	4.9E-10	4.9E-10	4.9E-10	0
7	21.05	0.363	4.9E-10	4.9E-10	4.9E-10	0
8	24.06	0.415	4.9E-10	4.9E-10	4.9E-10	0
9	27.07	0.467	4.9E-10	4.9E-10	4.9E-10	0
10	30.08	0.519	3.4E-07	3.4E-07	3.4E-07	0
11	33.08	0.570	9.8E-07	9.8E-07	9.8E-07	0
12	36.09	0.622	7.8E-07	7.8E-07	7.8E-07	0
13	39.10	0.674	2.7E-06	2.7E-06	2.7E-06	0
14	42.11	0.726	8.8E-07	8.8E-07	8.8E-07	0
15	45.11	0.778	5.9E-07	5.9E-07	5.9E-07	0
16	48.12	0.830	7.8E-06	7.8E-06	7.8E-06	0
17	51.13	0.882	2.0E-05	2.0E-05	2.0E-05	0
18	54.14	0.933	3.4E-05	3.4E-05	3.4E-05	0
19	57.14	0.985	5.4E-05	2.0E-04	1.3E-04	7.11E-05
20	60.15	1.037	7.4E-05	7.4E-05	7.4E-05	0
21	63.16	1.089	3.9E-05	3.9E-05	3.9E-05	0
22	66.17	1.141	5.9E-05	5.9E-05	5.9E-05	0
23	69.17	1.193	2.2E-04	2.2E-04	2.2E-04	0
24	72.18	1.244	2.4E-04	2.4E-04	2.4E-04	0
25	75.19	1.296	4.9E-04	4.9E-04	4.9E-04	0

26	78.20	1.348	7.8E-04	1.5E-03	1.1E-03	0.000343
27	81.20	1.400	8.8E-04	9.3E-04	9.1E-04	2.45E-05
28	84.21	1.452	5.4E-04	2.5E-03	1.5E-03	0.000956
29	87.22	1.504	2.0E-03	4.1E-03	3.0E-03	0.001078
31	93.23	1.607	5.9E-03	5.9E-03	5.9E-03	0
33	99.25	1.711	6.9E-03	6.9E-03	6.9E-03	0
35	105.26	1.815	1.9E-02	1.9E-02	1.9E-02	0
37	111.28	1.919	2.0E-02	2.0E-02	2.0E-02	0
39	117.29	2.022	8.3E-02	9.8E-02	9.1E-02	0.007353
41	123.31	2.126	6.9E-02	8.3E-02	7.6E-02	0.007353
43	129.32	2.230	1.8E-01	4.1E-01	2.9E-01	0.117647
45	135.34	2.333	9.8E-02	2.4E-01	1.7E-01	0.068627
47	141.35	2.437	6.9E-01	1.7E+00	1.2E+00	0.490196
58	174.44	3.008	2.9E-01	2.9E-01	2.9E-01	0
66	198.50	3.422	2.0E-01	6.4E-01	4.2E-01	0.220588
69	207.52	3.578	8.3E-01	8.3E-01	8.3E-01	0
70	210.53	3.630	2.9E-01	2.9E-01	2.9E-01	0
75	225.56	3.889	3.0E-01	3.0E-01	3.0E-01	0
76	228.57	3.941	7.8E-01	7.8E-01	7.8E-01	0
77	231.58	3.993	2.8E-01	2.8E-01	2.8E-01	0
78	234.59	4.045	4.9E-01	4.9E-01	4.9E-01	0
80	240.60	4.148	1.1E+00	1.1E+00	1.1E+00	0
81	243.61	4.200	4.9E-01	4.9E-01	4.9E-01	0
82	246.62	4.252	7.8E-01	7.8E-01	7.8E-01	0
86	258.65	4.459	4.9E-02	5.9E-02	5.4E-02	0.004902
88	264.66	4.563	4.3E-02	9.8E-02	7.1E-02	0.027451
90	270.68	4.667	2.3E-01	2.8E-01	2.5E-01	0.026961
92	276.69	4.771	1.9E-01	4.1E-01	3.0E-01	0.112745
93	279.70	4.822	1.1E-01	1.5E-01	1.3E-01	0.019608
94	282.71	4.874	7.4E-02	1.1E-01	9.1E-02	0.017157
95	285.71	4.926	5.9E-02	1.0E-01	8.1E-02	0.022059
96	288.72	4.978	2.9E-02	8.3E-02	5.6E-02	0.026961
97	291.73	5.030	2.0E-02	2.5E-02	2.2E-02	0.002451
98	294.74	5.082	3.0E-02	3.9E-02	3.5E-02	0.004412
99	297.74	5.133	2.6E-02	2.6E-02	2.6E-02	0
100	300.75	5.185	2.9E-02	3.6E-02	3.3E-02	0.003431
102	306.77	5.289	2.9E-02	2.9E-02	2.9E-02	0
104	312.78	5.393	9.8E-03	1.8E-02	1.4E-02	0.003922
106	318.80	5.496	9.8E-03	2.5E-02	1.8E-02	0.007843

108	324.81	5.600	1.8E-02	2.5E-02	2.1E-02	0.003431
110	330.83	5.704	9.8E-03	2.5E-02	1.8E-02	0.007843
115	345.86	5.963	1.3E-02	2.6E-02	2.0E-02	0.006863
120	360.90	6.222	1.1E-02	2.6E-02	1.9E-02	0.007598
125	375.94	6.482	1.1E-02	1.7E-02	1.4E-02	0.002941
130	390.98	6.741	1.7E-02	2.0E-02	1.8E-02	0.001471
135	406.01	7.000	1.3E-02	1.6E-02	1.4E-02	0.001471
140	421.05	7.259	1.1E-02	1.4E-02	1.3E-02	0.001225
145	436.09	7.519	7.4E-03	1.7E-02	1.2E-02	0.004657
150	451.13	7.778	1.4E-02	1.6E-02	1.5E-02	0.00098
155	466.16	8.037	1.5E-02	1.7E-02	1.6E-02	0.00098
160	481.20	8.297	4.9E-03	5.4E-03	5.1E-03	0.000245
165	496.24	8.556	5.9E-03	8.8E-03	7.4E-03	0.001471
170	511.28	8.815	5.4E-03	7.8E-03	6.6E-03	0.001225
175	526.31	9.074	4.9E-03	9.3E-03	7.1E-03	0.002206

Experiment 5

A0500
Ringold Sediment
Temperature = 18 C
Column Length = 29.9 cm
Avg. Interstitial Velocity = 8.63 E-3 cm/s
Flow rate = 1.036 mL/min.
Pore Volume = 59.8 mL

Porosity = 0.397
Hydraulic Detention = 57.7 min.
Bacteria solution pH = 7.8
Final effluent pH = 7.7
Co = 1.11E+09
Pulse = 3.912

Sample	Effluent Volume (mL)	Pore Volume	C/Co (low)	C/Co (high)	C/Co (avg)	STD.DEV.
0	0.00	0.000	9.0E-10	9.0E-10	9.0E-10	0
1	3.00	0.050	9.0E-10	9.0E-10	9.0E-10	0
2	6.00	0.100	9.0E-10	9.0E-10	9.0E-10	0
3	9.00	0.150	9.0E-10	9.0E-10	9.0E-10	0
4	12.00	0.201	9.0E-10	9.0E-10	9.0E-10	0
5	15.00	0.251	9.0E-10	9.0E-10	9.0E-10	0
6	17.99	0.301	9.0E-10	9.0E-10	9.0E-10	0
7	20.99	0.351	9.0E-10	9.0E-10	9.0E-10	0
8	23.99	0.401	9.0E-10	9.0E-10	9.0E-10	0
9	26.99	0.451	9.0E-10	9.0E-10	9.0E-10	0
10	29.99	0.502	9.0E-10	9.0E-10	9.0E-10	0
11	32.99	0.552	9.0E-10	9.0E-10	9.0E-10	0
12	35.99	0.602	7.2E-08	7.2E-08	7.2E-08	0
13	38.99	0.652	1.3E-06	1.3E-06	1.3E-06	0
14	41.99	0.702	4.7E-06	4.7E-06	4.7E-06	0
15	44.99	0.752	3.6E-06	1.3E-05	8.1E-06	4.5E-06
16	47.98	0.802	9.0E-06	1.8E-05	1.4E-05	4.5E-06
17	50.98	0.853	3.1E-05	3.1E-05	3.1E-05	0
18	53.98	0.903	4.5E-05	7.2E-05	5.9E-05	1.35E-05
19	56.98	0.953	5.4E-05	5.6E-05	5.5E-05	9.01E-07
20	59.98	1.003	9.0E-05	1.3E-04	1.1E-04	1.8E-05
21	62.98	1.053	9.0E-05	1.1E-04	9.9E-05	9.01E-06
22	65.98	1.103	1.3E-04	1.8E-04	1.5E-04	2.7E-05
23	68.98	1.153	1.8E-04	2.2E-04	2.0E-04	1.8E-05
24	71.98	1.204	3.1E-04	3.2E-04	3.1E-04	4.5E-06
25	74.98	1.254	5.8E-04	9.0E-04	7.4E-04	0.000162

26	77.97	1.304	4.0E-04	4.0E-04	4.0E-04	0
27	80.97	1.354	1.8E-03	2.4E-03	2.1E-03	0.000315
28	83.97	1.404	1.1E-03	1.3E-03	1.2E-03	9.01E-05
29	86.97	1.454	1.5E-03	2.2E-03	1.8E-03	0.000315
31	92.97	1.555	4.0E-03	4.0E-03	4.0E-03	0
33	98.97	1.655	3.6E-03	8.1E-03	5.9E-03	0.002252
35	104.97	1.755	5.4E-03	1.1E-02	8.1E-03	0.002703
39	116.96	1.956	5.4E-02	6.3E-02	5.9E-02	0.004505
41	122.96	2.056	5.4E-02	7.9E-02	6.7E-02	0.012613
43	128.96	2.156	9.0E-02	9.0E-02	9.0E-02	0
45	134.96	2.257	7.6E-02	1.1E-01	9.2E-02	0.016216
47	140.95	2.357	5.4E-01	1.3E+00	9.0E-01	0.36036
49	146.95	2.457	1.4E-01	1.4E-01	1.4E-01	0
54	161.95	2.708	2.2E-01	2.2E-01	2.2E-01	0
57	170.94	2.859	2.7E-01	2.7E-01	2.7E-01	0
60	179.94	3.009	2.0E-01	2.0E-01	2.0E-01	0
63	188.94	3.159	3.6E-01	4.0E-01	3.8E-01	0.018018
66	197.93	3.310	3.6E-01	3.6E-01	3.6E-01	0
69	206.93	3.460	1.6E-01	3.1E-01	2.3E-01	0.072072
72	215.93	3.611	3.8E-01	7.2E-01	5.5E-01	0.171171
75	224.93	3.761	5.4E-01	6.1E-01	5.8E-01	0.036036
77	230.92	3.862	6.5E-01	6.5E-01	6.5E-01	0
78	233.92	3.912	6.8E-01	6.8E-01	6.8E-01	0
79	236.92	3.962	7.7E-01	7.7E-01	7.7E-01	0
80	239.92	4.012	5.9E-01	5.9E-01	5.9E-01	0
81	242.92	4.062	6.1E-01	6.1E-01	6.1E-01	0
84	251.92	4.213	5.4E-01	5.4E-01	5.4E-01	0
86	257.91	4.313	3.6E-01	3.6E-01	3.6E-01	0
88	263.91	4.413	4.5E-01	4.5E-01	4.5E-01	0
90	269.91	4.514	6.3E-01	6.3E-01	6.3E-01	0
92	275.91	4.614	3.8E-01	3.8E-01	3.8E-01	0
93	278.91	4.664	1.8E-01	2.0E-01	1.9E-01	0.009009
94	281.91	4.714	1.3E-01	1.4E-01	1.3E-01	0.004505
95	284.91	4.764	1.2E-01	1.3E-01	1.2E-01	0.004505
96	287.90	4.814	8.5E-02	8.5E-02	8.5E-02	0
97	290.90	4.865	5.4E-02	5.4E-02	5.4E-02	0
98	293.90	4.915	4.7E-02	4.7E-02	4.7E-02	0
100	299.90	5.015	4.9E-02	4.9E-02	4.9E-02	0
102	305.90	5.115	4.7E-02	4.7E-02	4.7E-02	0

105	314.90	5.266	5.4E-02	5.4E-02	5.4E-02	0
108	323.89	5.416	4.0E-02	4.0E-02	4.0E-02	0
111	332.89	5.567	4.7E-02	4.7E-02	4.7E-02	0
115	344.89	5.767	2.5E-02	2.5E-02	2.5E-02	0
120	359.88	6.018	1.6E-02	1.6E-02	1.6E-02	0
125	374.88	6.269	2.5E-02	2.5E-02	2.5E-02	0
130	389.87	6.520	2.2E-02	2.2E-02	2.2E-02	0
135	404.87	6.770	1.6E-02	1.6E-02	1.6E-02	0
140	419.86	7.021	1.4E-02	1.4E-02	1.4E-02	0
145	434.86	7.272	7.4E-03	7.4E-03	7.4E-03	0
150	449.85	7.523	1.4E-02	1.4E-02	1.4E-02	0
155	464.85	7.773	9.9E-03	9.9E-03	9.9E-03	0
160	479.84	8.024	2.3E-02	2.3E-02	2.3E-02	0
165	494.84	8.275	5.6E-03	5.6E-03	5.6E-03	0
170	509.83	8.526	1.2E-02	1.2E-02	1.2E-02	0

Experiment 6

Latex Microspheres
Ringold Sediment
Temperature = 4 C
Colunmn Length = 30.4 cm
Avg. Interstitial Velocity = 8.70 E-3 cm/s
Flow rate = 1.012 mL/min.
Pore Volume = 59.1 mL

Porosity = 0.385
Hydraulic Detention = 58.4 min.
Microsphere solution pH = 7.9
Final effluent pH = 7.8
Co = 5.40E+07
Pulse = 3.858

Sample	Effluent Volume (mL)	Pore Volume	C/Co
0	0.00	0.000	1.85E-08
1	3.00	0.051	1.85E-08
2	6.00	0.102	1.85E-08
3	9.00	0.152	1.85E-08
4	12.00	0.203	1.85E-08
5	15.00	0.254	1.85E-08
6	18.00	0.305	1.85E-08
7	21.00	0.355	1.85E-08
8	24.00	0.406	1.85E-08
9	27.00	0.457	1.85E-08
10	30.00	0.508	1.85E-08
11-17	42.00	0.711	5.78E-03
18-20	57.00	0.964	1.48E-02
21	63.00	1.066	1.64E-02
22	66.00	1.117	1.94E-02
23	69.00	1.168	1.87E-02
24	72.00	1.218	1.98E-02
26	78.00	1.320	2.09E-02
27	81.00	1.371	2.11E-02
28	84.00	1.421	2.26E-02
29	87.00	1.472	2.46E-02
30	90.00	1.523	2.43E-02
33	99.00	1.675	2.65E-02
36	108.00	1.827	2.96E-02
39	117.00	1.980	3.26E-02
43	129.00	2.183	3.33E-02

46	138.00	2.335	3.54E-02
49	147.00	2.487	4.02E-02
53	159.00	2.690	4.15E-02
59	177.00	2.995	4.43E-02
62	186.00	3.147	4.46E-02
65	195.00	3.299	4.69E-02
68	204.00	3.452	4.80E-02
70	210.00	3.553	4.81E-02
71	213.00	3.604	4.48E-02
72	216.00	3.655	4.20E-02
73	219.00	3.706	4.54E-02
74	222.00	3.756	4.31E-02
75	225.00	3.807	4.07E-02
76	228.00	3.858	4.35E-02
77	231.00	3.909	3.74E-02
78	234.00	3.959	5.35E-02
79	237.00	4.010	4.98E-02
80	240.00	4.061	5.04E-02
81	243.00	4.112	4.98E-02
82	246.00	4.162	6.04E-02
83	249.00	4.213	5.67E-02
84	252.00	4.264	6.50E-02
86	258.00	4.365	6.94E-02
88	264.00	4.467	6.28E-02
90	270.00	4.569	4.59E-02
92	276.00	4.670	1.55E-02
94	282.00	4.772	7.22E-03
96	288.00	4.873	6.56E-03
100	300.00	5.076	4.39E-03
105	315.00	5.330	3.59E-03
110	330.00	5.584	3.13E-03
115	345.00	5.838	2.33E-03
120	360.00	6.091	2.19E-03
125	375.00	6.345	2.15E-03
130	390.00	6.599	2.00E-03
140	420.00	7.107	1.68E-03
150	450.00	7.614	1.32E-03

Experiment 7

Latex Microshperes
Ringold Sediment
Temperature = 4 C
Column Length = 30.5 cm
Avg. Interstitial Velocity = 8.65 E-3 cm/s
Flow rate = 1.012 mL/min.
Pore Volume = 59.4 mL

Porosity = 0.387
Hydraulic Detention = 58.7 min.
Microsphere solution pH = 7.9
Final Effluent pH = 7.7
Co = 5.40E+07
Pulse = 3.838

Sample	Effluent Volume (mL)	Pore Volume	C/Co
0	0.00	0.000	1.85E-08
1	3.00	0.051	1.85E-08
2	6.00	0.101	1.85E-08
3	9.00	0.152	1.85E-08
4	12.00	0.202	1.85E-08
5	15.00	0.253	1.85E-08
6	18.00	0.303	1.85E-08
7	21.00	0.354	1.85E-08
8	24.00	0.404	1.85E-08
9	27.00	0.455	1.85E-08
10	30.00	0.505	1.85E-08
11-17	42.00	0.707	2.04E-02
18-20	57.00	0.960	4.70E-02
21	63.00	1.061	4.74E-02
22	66.00	1.111	5.59E-02
23	69.00	1.162	4.78E-02
24	72.00	1.212	5.57E-02
26	78.00	1.313	5.91E-02
27	81.00	1.364	5.15E-02
28	84.00	1.414	5.65E-02
29	87.00	1.465	5.48E-02
30	90.00	1.515	5.87E-02
33	99.00	1.667	5.70E-02
36	108.00	1.818	5.83E-02
39	117.00	1.970	6.30E-02
43	129.00	2.172	6.46E-02

46	138.00	2.323	7.20E-02
49	147.00	2.475	7.33E-02
53	159.00	2.677	7.31E-02
59	177.00	2.980	7.74E-02
62	186.00	3.131	7.85E-02
65	195.00	3.283	8.11E-02
68	204.00	3.434	8.52E-02
70	210.00	3.535	8.81E-02
71	213.00	3.586	8.70E-02
72	216.00	3.636	8.69E-02
73	219.00	3.687	8.87E-02
74	222.00	3.737	8.96E-02
75	225.00	3.788	8.43E-02
76	228.00	3.838	9.07E-02
77	231.00	3.889	1.04E-01
78	234.00	3.939	1.19E-01
79	237.00	3.990	1.02E-01
80	240.00	4.040	1.05E-01
81	243.00	4.091	1.21E-01
82	246.00	4.141	1.36E-01
83	249.00	4.192	1.30E-01
84	252.00	4.242	1.37E-01
86	258.00	4.343	1.67E-01
88	264.00	4.444	1.42E-01
90	270.00	4.545	1.34E-01
92	276.00	4.646	7.67E-02
94	282.00	4.747	3.13E-02
96	288.00	4.848	1.49E-02
100	300.00	5.051	8.93E-03
105	315.00	5.303	6.22E-03
110	330.00	5.556	6.37E-03
115	345.00	5.808	4.98E-03
120	360.00	6.061	3.91E-03
125	375.00	6.313	3.13E-03
130	390.00	6.566	4.57E-03
140	420.00	7.071	3.11E-03
150	450.00	7.576	2.20E-03

Experiment 8

Latex Microspheres
Ringold Sediment
Temperature = 18 C
Column Length = 30.2 cm
Avg. Interstitial Velocity = 9.23 E-3 cm/s
Flow rate = 1.060 mL/min.
Pore Volume = 57.8 mL

Porosity = 0.380
Hydraulic Detention = 54.5 min.
Microsphere solution pH = 7.8
Final effluent pH = 7.7
Co = 4.47E+07
Pulse = 3.945

Sample	Effluent Volume (mL)	Pore Volume	C/Co
0	0.00	0.000	2.24E-08
1	3.00	0.052	2.24E-08
2	6.00	0.104	2.24E-08
3	9.00	0.156	2.24E-08
4	12.00	0.208	2.24E-08
5	15.00	0.260	2.24E-08
6	18.00	0.311	2.24E-08
7	21.00	0.363	2.24E-08
8	24.00	0.415	2.24E-08
9	27.00	0.467	6.80E-05
10	30.00	0.519	3.71E-05
11	33.00	0.571	1.33E-04
12	36.00	0.623	7.92E-04
13	39.00	0.675	1.84E-03
14	42.00	0.727	2.77E-03
15	45.00	0.779	2.77E-03
16	48.00	0.830	2.95E-03
17	51.00	0.882	3.36E-03
18	54.00	0.934	3.96E-03
19	57.00	0.986	4.09E-03
20	60.00	1.038	5.26E-03
21	63.00	1.090	6.06E-03
22	66.00	1.142	7.23E-03
23	69.00	1.194	5.28E-03
24	72.00	1.246	5.95E-03
25	75.00	1.298	5.84E-03

26	78.00	1.349	5.79E-03
27	81.00	1.401	6.29E-03
28	84.00	1.453	7.05E-03
30	90.00	1.557	6.24E-03
33	99.00	1.713	7.74E-03
36	108.00	1.869	7.29E-03
39	117.00	2.024	7.45E-03
42	126.00	2.180	8.64E-03
45	135.00	2.336	9.26E-03
48	144.00	2.491	1.02E-02
51	153.00	2.647	1.05E-02
54	162.00	2.803	8.64E-03
57	171.00	2.958	9.44E-03
60	180.00	3.114	9.44E-03
63	189.00	3.270	1.02E-02
66	198.00	3.426	1.01E-02
69	207.00	3.581	1.02E-02
70	210.00	3.633	1.06E-02
71	213.00	3.685	1.16E-02
72	216.00	3.737	1.09E-02
73	219.00	3.789	1.15E-02
74	222.00	3.841	1.17E-02
75	225.00	3.893	1.19E-02
76	228.00	3.945	1.21E-02
77	231.00	3.997	1.18E-02
78	234.00	4.048	1.16E-02
79	237.00	4.100	1.10E-02
80	240.00	4.152	1.19E-02
81	243.00	4.204	1.18E-02
82	246.00	4.256	1.16E-02
83	249.00	4.308	1.18E-02
84	252.00	4.360	1.33E-02
85	255.00	4.412	1.42E-02
87	261.00	4.516	1.55E-02
89	267.00	4.619	8.93E-03
91	273.00	4.723	4.25E-03
95	285.00	4.931	1.07E-03
100	300.00	5.190	9.57E-04
105	315.00	5.450	8.01E-04

110	330.00	5.709	5.75E-04
115	345.00	5.969	4.94E-04
120	360.00	6.228	4.74E-04
130	390.00	6.747	3.94E-04
140	420.00	7.266	3.38E-04
150	450.00	7.785	3.71E-04

Experiment 9

Latex Microshperes
Ringold Sediment
Temperature = 18 C
Column Length = 30.2 cm
Avg. Interstitial Velocity = 9.11 E-3 cm/s
Flow rate = 1.060 mL/min.
Pore Volume = 58.5 mL

Porosity = 0.385
Hydraulic Detention = 55.2 min.
Microsphere solution pH = 7.8
Final effluent pH = 7.7
Co = 4.47E+07
Pulse = 3.897

Sample	Effluent Volume (mL)	Pore Volume	C/Co
0	0.00	0.000	2.24E-08
1	3.00	0.051	2.24E-08
2	6.00	0.103	2.24E-08
3	9.00	0.154	2.24E-08
4	12.00	0.205	2.24E-08
5	15.00	0.256	2.24E-08
6	18.00	0.308	2.24E-08
7	21.00	0.359	2.24E-08
8	24.00	0.410	2.24E-08
9	27.00	0.462	2.24E-08
10	30.00	0.513	2.24E-08
11	33.00	0.564	2.51E-05
12	36.00	0.615	5.59E-05
13	39.00	0.667	1.79E-04
14	42.00	0.718	3.71E-04
15	45.00	0.769	4.72E-04
16	48.00	0.821	6.00E-04
17	51.00	0.872	7.02E-04
18	54.00	0.923	8.14E-04
19	57.00	0.974	8.23E-04
20	60.00	1.026	1.05E-03
21	63.00	1.077	1.17E-03
22	66.00	1.128	1.14E-03
23	69.00	1.179	1.26E-03
24	72.00	1.231	1.36E-03
25	75.00	1.282	1.39E-03

26	78.00	1.333	1.48E-03
27	81.00	1.385	1.40E-03
28	84.00	1.436	1.63E-03
30	90.00	1.538	1.72E-03
33	99.00	1.692	1.82E-03
36	108.00	1.846	1.77E-03
39	117.00	2.000	1.87E-03
42	126.00	2.154	1.97E-03
45	135.00	2.308	2.15E-03
48	144.00	2.462	2.26E-03
51	153.00	2.615	2.75E-03
57	171.00	2.923	2.39E-03
60	180.00	3.077	2.62E-03
66	198.00	3.385	2.64E-03
69	207.00	3.538	2.64E-03
70	210.00	3.590	2.86E-03
71	213.00	3.641	3.09E-03
72	216.00	3.692	3.11E-03
73	219.00	3.744	3.27E-03
74	222.00	3.795	3.24E-03
75	225.00	3.846	3.62E-03
76	228.00	3.897	3.87E-03
77	231.00	3.949	3.67E-03
78	234.00	4.000	4.27E-03
79	237.00	4.051	4.47E-03
80	240.00	4.103	4.56E-03
81	243.00	4.154	6.22E-03
82	246.00	4.205	7.38E-03
83	249.00	4.256	8.12E-03
84	252.00	4.308	9.80E-03
86	258.00	4.410	1.05E-02
88	264.00	4.513	1.03E-02
90	270.00	4.615	4.94E-03
92	276.00	4.718	1.40E-03
94	282.00	4.821	6.80E-04
96	288.00	4.923	6.00E-04
100	300.00	5.128	3.94E-04
105	315.00	5.385	3.38E-04
110	330.00	5.641	2.91E-04

115	345.00	5.897	2.89E-04
120	360.00	6.154	2.79E-04
130	390.00	6.667	2.33E-04
140	420.00	7.179	1.99E-04
150	450.00	7.692	2.18E-04

APPENDIX B

Results of Statistical Analyses

Effect of Velocity Adjustment on Average Cs/Co

		Observed Cs/Co	Velocity Adjusted	% Change
	A0500-4C			
Mean		0.2791	0.2799	0.3
Std.Dev.		0.1189	0.1174	-1.3
	A0500-18C			
Mean		0.6196	0.6268	1.2
Std.Dev.		0.2420	0.2457	1.5
	Spheres-4C			
Mean		0.0687	0.0682	-0.7
Std.Dev.		0.0254	0.0252	-0.8
	Spheres-18C			
Mean		0.0076	0.0077	1.3
Std.Dev.		0.0039	0.0040	2.6

Steady-State A0500 Cs/Co - Raw data

Observed Cs/Co	Velocity Corrected Cs/Co	Observed Cs/Co	Velocity Corrected Cs/Co	Observed Cs/Co	Velocity Corrected Cs/Co
Exp 1		**Exp3**		**Exp 4**	
0.2000	0.2059	0.3235	0.3212	0.6373	0.6461
0.2200	0.2265	0.0882	0.0876	0.8333	0.8474
0.2067	0.2127	0.3235	0.3212	0.8824	0.8973
0.2000	0.2059	0.2059	0.2044	0.2941	0.2991
0.1933	0.1990	0.2059	0.2044	0.3039	0.3091
0.2167	0.2231	0.2471	0.2453	1.1765	1.1964
0.1333	0.1372	0.5294	0.5257	0.7843	0.7976
0.1000	0.1029	0.2971	0.2949	0.2843	0.2891
0.1867	0.1922	0.5294	0.5256	0.4902	0.4985
0.2667	0.2745	0.4235	0.4205	1.1275	1.1465
0.3333	0.3431	0.3235	0.3212	0.4902	0.4985
0.2733	0.2814	0.3824	0.3797	0.4902	0.4985
Exp 2		0.5588	0.5548	0.2941	0.2991
0.2800	0.2800	0.2147	0.2132	**Exp 5**	
0.1400	0.1400	0.2353	0.2336	0.7843	0.7976
0.1720	0.1720	0.4676	0.4643	0.3063	0.3081
0.2400	0.2400	0.2647	0.2628	0.7207	0.7249
0.4000	0.4000	0.2824	0.2803	0.3784	0.3806
0.4800	0.4800			0.6126	0.6162
0.3200	0.3200			0.6486	0.6524
0.5200	0.5200			0.6847	0.6887
0.1680	0.1680			0.7748	0.7793
0.2000	0.2000			0.5946	0.5980
0.2400	0.2400			0.6126	0.6162
0.2160	0.2160			0.5405	0.5437
0.2800	0.2800			0.4505	0.4531
0.1920	0.1920			0.9009	0.9061
				0.6306	0.6343
n =		44	44	27	27
Mean		0.2791	0.2799	0.6196	0.6268
Std Dev.		0.1189	0.1174	0.2420	0.2457

Steady-State Cs/Co - Raw data
Microspheres

	Observed Cs/Co	Velocity Corrected Cs/Co		Cs/Co	Velocity Corrected Cs/Co
Exp 6	0.0469	0.0465	Exp 8	0.0102	0.0104
	0.0480	0.0476		0.0101	0.0102
	0.0481	0.0478		0.0102	0.0103
	0.0448	0.0445		0.0106	0.0107
	0.0420	0.0417		0.0116	0.0118
	0.0454	0.0451		0.0109	0.0111
	0.0431	0.0429		0.0115	0.0117
	0.0407	0.0405		0.0117	0.0119
	0.0435	0.0432		0.0119	0.0121
	0.0374	0.0371		0.0121	0.0123
	0.0535	0.0531		0.0118	0.0120
	0.0498	0.0495		0.0116	0.0118
	0.0504	0.0500		0.0110	0.0111
	0.0498	0.0495		0.0119	0.0121
Exp 7	0.0811	0.0805		0.0118	0.0120
	0.0852	0.0846	Exp 9	0.0026	0.0027
	0.0881	0.0875		0.0026	0.0027
	0.0870	0.0864		0.0029	0.0029
	0.0869	0.0862		0.0031	0.0032
	0.0887	0.0881		0.0031	0.0032
	0.0896	0.0890		0.0033	0.0033
	0.0843	0.0837		0.0032	0.0033
	0.0907	0.0901		0.0036	0.0037
	0.1039	0.1032		0.0039	0.0040
	0.1193	0.1184		0.0037	0.0038
	0.1020	0.1013		0.0043	0.0044
	0.1048	0.1041		0.0045	0.0046
				0.0046	0.0047
				0.0062	0.0064
n =	27	27		29	29
Mean	0.0687	0.0682		0.0076	0.0077
Std Dev.	0.0254	0.0252		0.0039	0.0040

WILCOXON RANK-SUM NONPARAMETRIC TEST

Ho: m1 = m2 *1=Experiments 4 & 5* n1 = 18
H1: m1 =/= m2 **2=Experiments 1, 2, & 3** n2 = 26
alpha=0.025 (one-side)
Critical Region: u < 148 (Table A17, p 732) *(Walpole and Meyer* ,1989)

Rank	C/Co	Rank	C/Co
1	*1.10*	23	*0.29*
2	*0.83*	25.5	**0.28**
3	*0.78*	25.5	**0.28**
4	*0.77*	25.5	*0.28*
5	*0.68*	25.5	**0.28**
6	*0.65*	28	**0.27**
7	*0.61*	29.5	**0.26**
8	*0.59*	29.5	**0.26**
9	*0.58*	31.5	**0.24**
10	*0.55*	31.5	**0.24**
11	*0.54*	34.5	*0.23*
12.5	*0.49*	34.5	*0.23*
12.5	*0.49*	34.5	**0.23**
14	**0.47**	34.5	**0.23**
15	**0.44**	37	**0.22**
16	**0.42**	38	**0.21**
17	**0.41**	38.5	**0.21**
18	**0.39**	40.5	**0.20**
19.5	**0.35**	40.5	**0.20**
19.5	**0.35**	42	**0.18**
21	**0.33**	43	**0.17**
22	*0.30*	44	**0.10**

w1 = 230.5

w2 = 759.5

u1 = 59.5

u2 = 408.5

Ho is rejected, u < 148
Sample means are not equal

w1=sum ranks of small sample
w2=(n1+n2)(n1+n2+1)/2 - w1
, or sum ranks of large sample
u1 =w1 - [n1(n1+1)]/2
u2 =w2 - [n2(n2+1)]/2

WILCOXON RANK-SUM NONPARAMETRIC TEST

Ho: m1 = m2 **1=Experiments 6 & 7** n1 = 27
H1: m1 =/= m2 *2=Experiments 8 & 9* n2 = 29
alpha=0.025 (one-side)
Critical Region: u < 148 (Table A17, p 732) *(Walpole and Meyer* ,1989)

Rank	C/Co	Rank	C/Co		
1	**0.119**	31.5	*0.012*	w1 =	378
2	**0.105**	31.5	*0.012*		
3	**0.104**	31.5	*0.012*	w2 =	1218
4	**0.102**	31.5	*0.012*		
5	**0.091**	31.5	*0.012*	u1 =	0
6	**0.090**	31.5	*0.012*		
7	**0.089**	31.5	*0.012*	u2 =	783
8	**0.088**	37.5	*0.011*		
9.5	**0.087**	37.5	*0.011*		
9.5	**0.087**	37.5	*0.011*		
11	**0.085**	37.5	*0.011*	**Ho is rejected, u < 200**	
12	**0.084**	41	*0.010*	**Sample means are not equal**	
13	**0.081**	41	*0.010*		
14	**0.054**	41	*0.010*		
16	**0.050**	43	*0.006*	w1=sum ranks of small sample	
16	**0.050**	44	*0.005*	w2=(n1+n2)(n1+n2+1)/2 - w1	
16	**0.050**	47	*0.004*	, or sum ranks of large sample	
18.5	**0.048**	47	*0.004*	u1 =w1 - [n1(n1+1)]/2	
18.5	**0.048**	47	*0.004*	u2 =w2 - [n2(n2+1)]/2	
20	**0.047**	47	*0.004*		
21.5	**0.045**	47	*0.004*		
21.5	**0.045**	53	*0.003*		
23	**0.044**	53	*0.003*		
24	**0.043**	53	*0.003*		
25	**0.042**	53	*0.003*		
26	**0.041**	53	*0.003*		
27	**0.037**	53	*0.003*		
31.5	*0.012*	53	*0.003*		

Chi-Squared Test of Normal Distribution

Ho = a normal distribution adequately discribes the sample

Cs/Co **Exp1**
0.2000
0.2200
0.2067
0.2000
0.1933
0.2167
0.1333
0.1000
0.1867
0.2667
0.3333
0.2733
Exp2
0.2800
0.1400
0.1720
0.2400
0.4000
0.4800
0.3200
0.5200
0.1480
0.2000
0.2400
0.2160
0.2800
0.1920

Cs/Co **Exp3**
0.3235
0.0882
0.3235
0.2059
0.2059
0.2471
0.5294
0.2971
0.5294
0.4235
0.3235
0.3824
0.5588
0.2147
0.2353
0.4676
0.2647
0.2824

Class	Observation Number	e	(e-o) ^ 2/e
0.1	5	6.16	0.22
0.2	18	11.57	3.57
0.3	12	14.17	0.33
0.4	9	8.8	0.00
Total	44		4.13

n =	44	v = 3
Mean =	0.2791	
Std. Dev	0.1189	

Critical Region	X ^ 2 > 7.8
Level of Significance	0.05

Accept Ho as 4.13 < 7.8

Chi-Squared Test of Normal Distribution

Ho = a normal distribution adequately discribes the sample

Cs/Co **Exp 4**	Cs/Co **Exp 5**
0.637255	0.306306
0.833333	0.720721
0.882353	0.378378
0.294118	0.612613
0.303922	0.648649
1.176471	0.684685
0.784314	0.774775
0.284314	0.594595
0.490196	0.612613
1.127451	0.540541
0.490196	0.45045
0.490196	0.900901
0.294118	0.630631
0.784314	

Class	Observation Number	e	(e-o) ^ 2/e
0.3	6	2.52	4.81
0.5	6	5.9	0.00
0.7	10	8.58	0.24
0.9	5	6.69	0.43
Total	27		5.47

n =	27	v =	3
Mean =	0.6196		
Std. Dev	0.242		
Critical Region		X ^ 2 > 7.8	
Level of Significance		0.05	

Accept Ho as 5.47 < 7.8

Chi-Squared Test of Normal Distribution

Ho = a normal distribution adequately discribes the sample

Cs/Co **Exp 6**	Cs/Co **Exp 7**
0.119	0.054
0.105	0.050
0.104	0.050
0.102	0.050
0.091	0.048
0.090	0.048
0.089	0.047
0.088	0.045
0.087	0.045
0.087	0.044
0.085	0.043
0.084	0.042
0.081	0.041
	0.037

Class	Observation Number	e	(e-o) ^ 2/e
0.04	10	6.2	2.33
0.06	4	7.84	1.88
0.08	13	12.96	0.00
Total	27		4.21

n = 27 v = 2

Mean = 0.0687

Std. Dev 0.0254

Critical Region X ^ 2 > 6.0

Level of Significance 0.05

Accept Ho as 4.21 < 6.0

Chi-Squared Test of Normal Distribution

Ho = a normal distribution adequately discribes the sample

Cs/Co **Exp 8**	Cs/Co **Exp 9**
0.012	0.006
0.012	0.005
0.012	0.004
0.012	0.004
0.012	0.004
0.012	0.004
0.012	0.004
0.012	0.003
0.011	0.003
0.011	0.003
0.011	0.003
0.011	0.003
0.010	0.003
0.010	0.003
0.010	

Class	Observation Number	e	(e-o) ^ 2/e
0.004	13	9.63	1.18
0.008	4	11.3	4.72
0.012	12	8.05	1.94
Total	29		7.83

n =	29	v =	2
Mean =	0.0077		
Std. Dev	0.0039		
Critical Region		X ^ 2 > 6.0	
Level of Significance		0.05	

Reject Ho 7.83 > 6.0

Class 2 is less than 5

t-test comparison of two sample means

Sample 1 is the combined steady-state values of C_s/C_o for each individual plate count in the A0500-4°C experiments. Sample 2 is the combined steady-state values of C_s/C_o for each individual plate count in the A0500-18°C experiments. Both data sets (C_s/C_o) were corrected to a common velocity.

H_o: $\mu_1-\mu_2 = 0$

H_1: $\mu_1-\mu_2 < 0$

$\alpha = 0.025$ (one-sided)

Critical region $t < -1.96$; $\nu = n_1 + n_2 - 2 = 69$

$$t = \frac{(\bar{x}_1 - \bar{x}_2) - d_o}{S_p\sqrt{1/n_1 + 1/n_2}} \qquad S_p = \sqrt{\frac{s_1^2(n_1 - 1) + s_2^2(n_2 - 1)}{n_1 + n_2 - 2}}$$

$$\bar{x}_1 = 0.2799 \qquad s_1 = 0.1174 \qquad n_1 = 44$$
$$\bar{x}_2 = 0.6268 \qquad s_2 = 0.2457 \qquad n_2 = 27$$

$$S_p = 0.1770 \qquad t = -8.0176$$

$$P = P(T > 1.96) = 1.8 \times 10^{-11}$$

$$95\%\ confidence\ limit \Rightarrow \bar{x}_i \pm t_{0.025}\frac{s_i}{\sqrt{n_i}} \; ; \; \nu = n_i - 1$$

Reject H_o , the means are not equal. The mean of sample 2 (18°C) is larger than the mean of sample 1 (4°C) using the 0.025 level of significance.

t-test comparison of two sample means

Sample 1 is the combined steady-state values of C_s/C_o for each 20-field microscope count in the Microsphere - 4°C experiments. Sample 2 is the combined steady-state values of C_s/C_o for each 20-field microscope count in the Microsphere -18°C experiments. Both data sets (C_s/C_o) were corrected to a common velocity.

H_o: $\mu_1 - \mu_2 = 0$

H_1: $\mu_1 - \mu_2 > 0$

$\alpha = 0.025$ (one-sided)

Critical region $t > 1.96$; $\nu = n_1 + n_2 - 2 = 54$

$$t = \frac{(\bar{x}_1 - \bar{x}_2) - d_o}{S_p \sqrt{1/n_1 + 1/n_2}} \qquad S_p = \sqrt{\frac{s_1^2 (n_1 - 1) + s_2^2 (n_2 - 1)}{n_1 + n_2 - 2}}$$

$$\bar{x}_1 = 0.0682 \qquad s_1 = 0.0252 \qquad n_1 = 27$$
$$\bar{x}_2 = 0.0077 \qquad s_2 = 0.0040 \qquad n_2 = 29$$

$$S_p = 0.0177 \qquad t = 12.77$$

$$P = P(T < 1.96) = 2.2 \times 10^{-16}$$

$$95\%\ confidence\ limit \Rightarrow \bar{x}_i \pm t_{0.025} \frac{s_i}{\sqrt{n_i}} \ ; \ \nu = n_i - 1$$

Reject H_o , the means are not equal. The mean of sample 2 (18°C) is smaller than the mean of sample 1 (4°C) using the 0.025 level of significance.

t-test comparison of two sample means

Sample 1 is the combined steady-state values of C_s/C_o as estimated by the effects of temperature on the filtration model . Sample 2 is the combined observed steady-state values of C_s/C_o for each 20-field microscope count in the Microsphere -18°C experiments.

H_o: $\mu_1-\mu_2 = 0$

H_1: $\mu_1-\mu_2 > 0$

$\alpha = 0.025$ (one-sided)

Critical region $t > 1.96$; $\nu = n_1 + n_2 - 2 = 54$

$$t = \frac{(\bar{x}_1 - \bar{x}_2) - d_o}{S_p\sqrt{1/n_1 + 1/n_2}} \qquad S_p = \sqrt{\frac{s_1^2 (n_1 - 1) + s_2^2 (n_2 - 1)}{n_1 + n_2 - 2}}$$

$\bar{x}_1 = 0.034$ $\quad s_1 = 0.016$ $\quad n_1 = 27$

$\bar{x}_2 = 0.0077$ $\quad s_2 = 0.0040$ $\quad n_2 = 29$

$$S_p = 0.0115 \qquad t = 8.69$$

$$P = P(T < 1.96) = 7.8 \times 10^{-12}$$

$$95\%\ confidence\ limit \Rightarrow \bar{x}_i \pm t_{0.025}\frac{s_i}{\sqrt{n_i}} \ ; \ \nu = n_i - 1$$

Reject H_o , the means are not equal. The mean of observed sample 2 (18°C) is smaller than the mean of estimated sample 1 (18°C) using the 0.025 level of significance.

Temperature Effects on Filtration Model Prediction of Fraction Penetration, Assuming Constant Alpha

Microspheres

- Observations are at steady-state from (2) 4 C experiments, or (2) 18 C experiments
- Calculated Eta from 4 C column parameters and Alpha from 4 C Cs/Co
- Estimated Eta at 18 C by changing temperature, density, and viscosity of water in the filtration model
- Estimated Cs/Co at 18 C with Eta-18 and holding Alpha constant
- Assuming no change in sticking coefficient (chemical properties) due to increase in temperature
- **Model predicts 50 %lower Cs/Co at 18 C, observed an order of magnitude lower Cs/Co at 18 C**

	4 C Exp's Observed Cs/Co	Calculated 4 C Eta	Calculated 4 C Alpha	Estimated 18 C Eta (+27%)	Estimated 18 C Cs/Co	18 C Exp's Observed Cs/Co
	0.119	0.0144	0.117	0.0183	0.067	0.012
	0.105	0.0144	0.124	0.0183	0.057	0.012
	0.104	0.0144	0.124	0.0183	0.056	0.012
	0.102	0.0144	0.125	0.0183	0.055	0.012
	0.091	0.0144	0.132	0.0183	0.048	0.012
	0.090	0.0144	0.132	0.0183	0.047	0.012
	0.089	0.0144	0.133	0.0183	0.046	0.012
	0.088	0.0144	0.134	0.0183	0.046	0.012
	0.087	0.0144	0.134	0.0183	0.045	0.011
	0.087	0.0144	0.134	0.0183	0.045	0.011
	0.085	0.0144	0.136	0.0183	0.044	0.011
	0.084	0.0144	0.136	0.0183	0.043	0.011
	0.081	0.0144	0.138	0.0183	0.041	0.010
	0.054	0.0143	0.162	0.0182	0.025	0.010
	0.050	0.0143	0.166	0.0182	0.022	0.010
	0.050	0.0143	0.166	0.0182	0.022	0.006
	0.050	0.0143	0.166	0.0182	0.022	0.005
	0.048	0.0143	0.168	0.0182	0.021	0.004
	0.048	0.0143	0.168	0.0182	0.021	0.004
	0.047	0.0143	0.169	0.0182	0.021	0.004
	0.045	0.0143	0.172	0.0182	0.019	0.004
	0.045	0.0143	0.172	0.0182	0.019	0.004
	0.044	0.0143	0.173	0.0182	0.019	0.003
	0.043	0.0143	0.174	0.0182	0.018	0.003
	0.042	0.0143	0.175	0.0182	0.018	0.003
	0.041	0.0143	0.177	0.0182	0.017	0.003
	0.037	0.0143	0.183	0.0182	0.015	0.003
						0.003
						0.003
n =	27	27	27	27	27	29
Mean =	0.069	0.014	0.151	0.018	0.034	0.008
Std Dev =	0.025	0.000	0.021	0.000	0.016	0.004

APPENDIX C

Breakthrough Curves with Two-Site Transport Model Fits

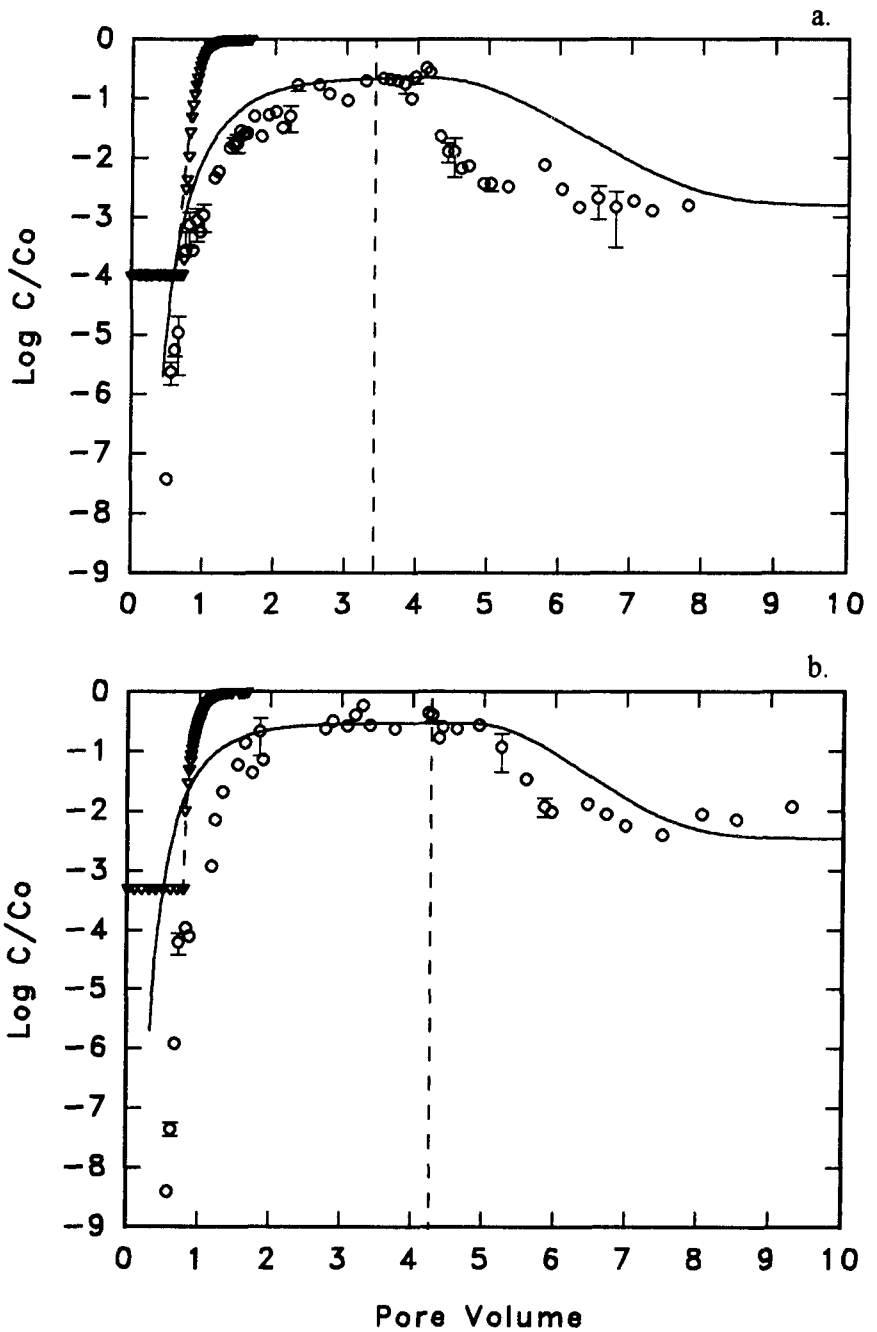

Breakthrough curves of *A0500* bacteria (○) and NaCl tracer (▽) at 4° C with the best fit line of the two-site transport model. a.) Experiment 1 b.) Experiment 2.

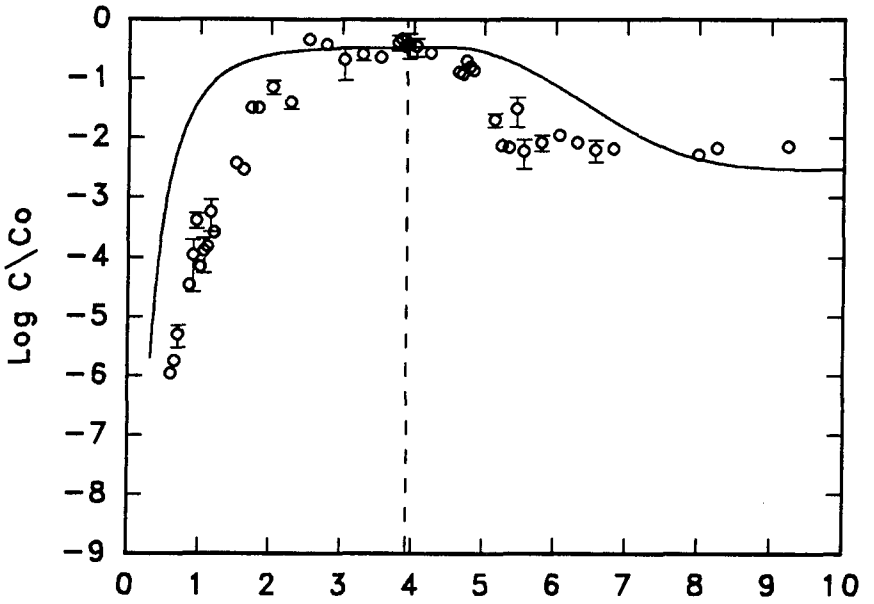

Experiment 3 breakthrough curve of *A0500* bacteria (o) at 4°C with the best fit line of the two-site transport model.

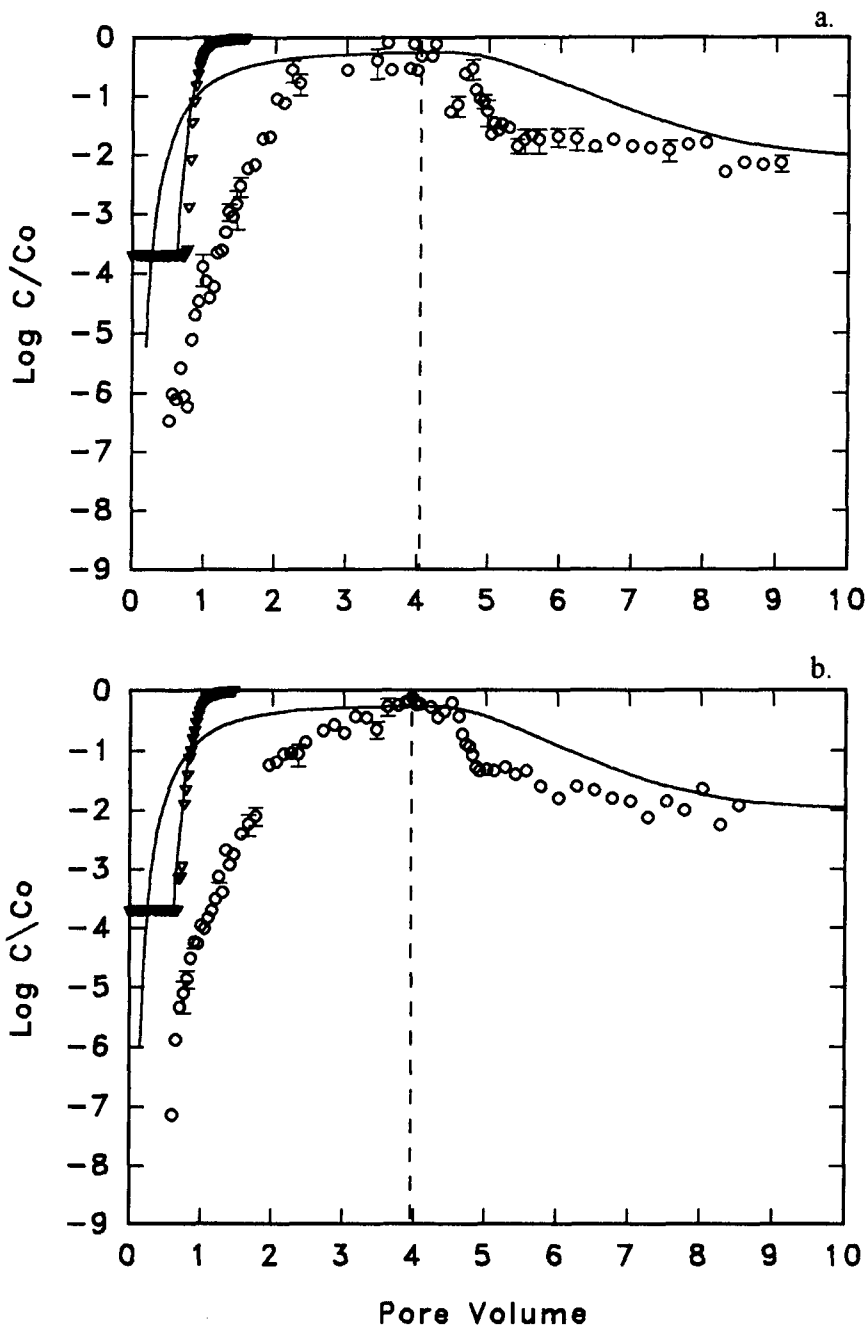

Breakthrough curves of *A0500* bacteria (○) and NaCl tracer (▽) at 18° C with the best fit line of the two-site transport model. a.) Experiment 4 b.) Experiment 5.

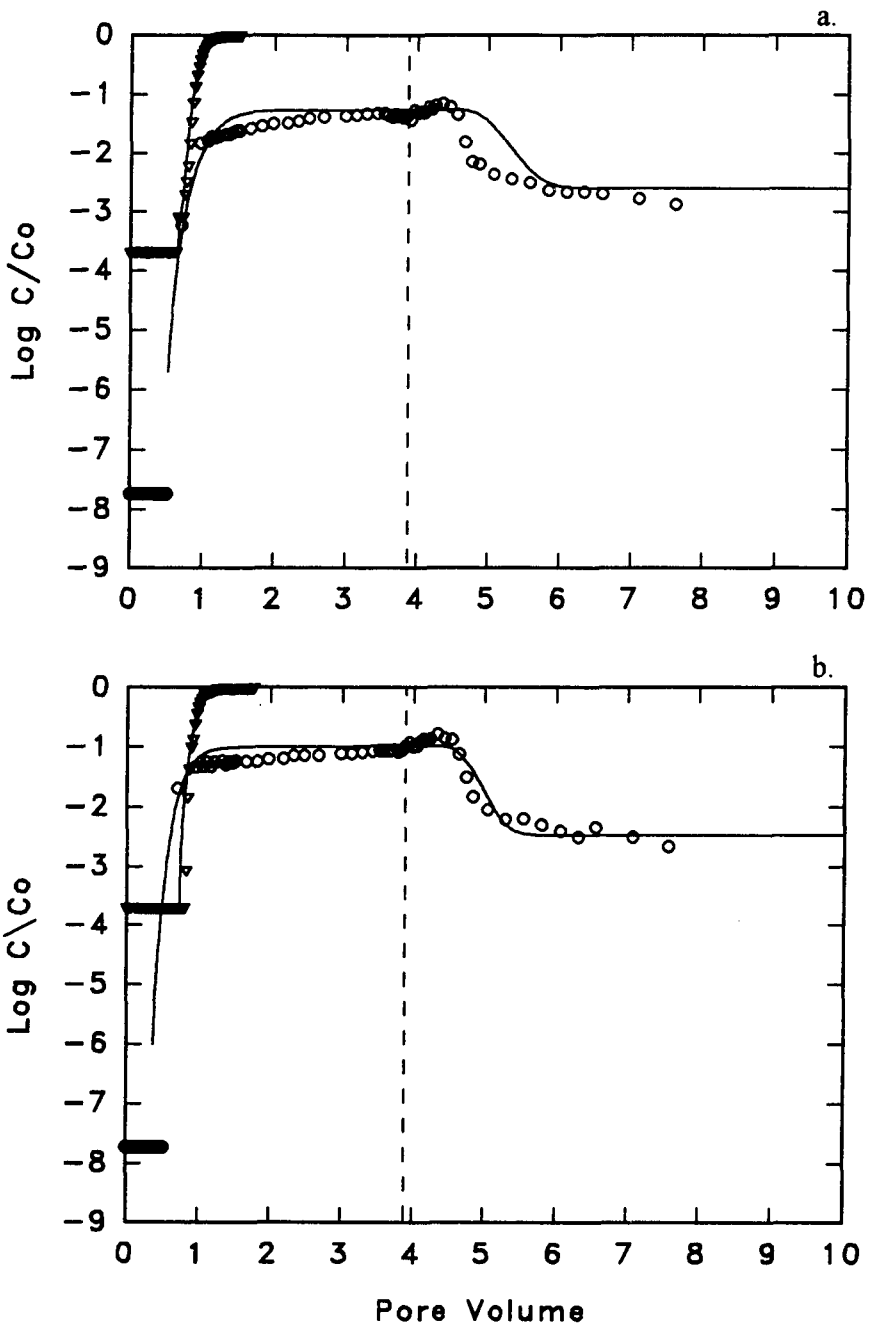

Breakthrough curves of microspheres (o) and NaCl tracer (▽) at 4° C with the best fit line of the two-site transport model. a.) Experiment 6 b.) Experiment 7.

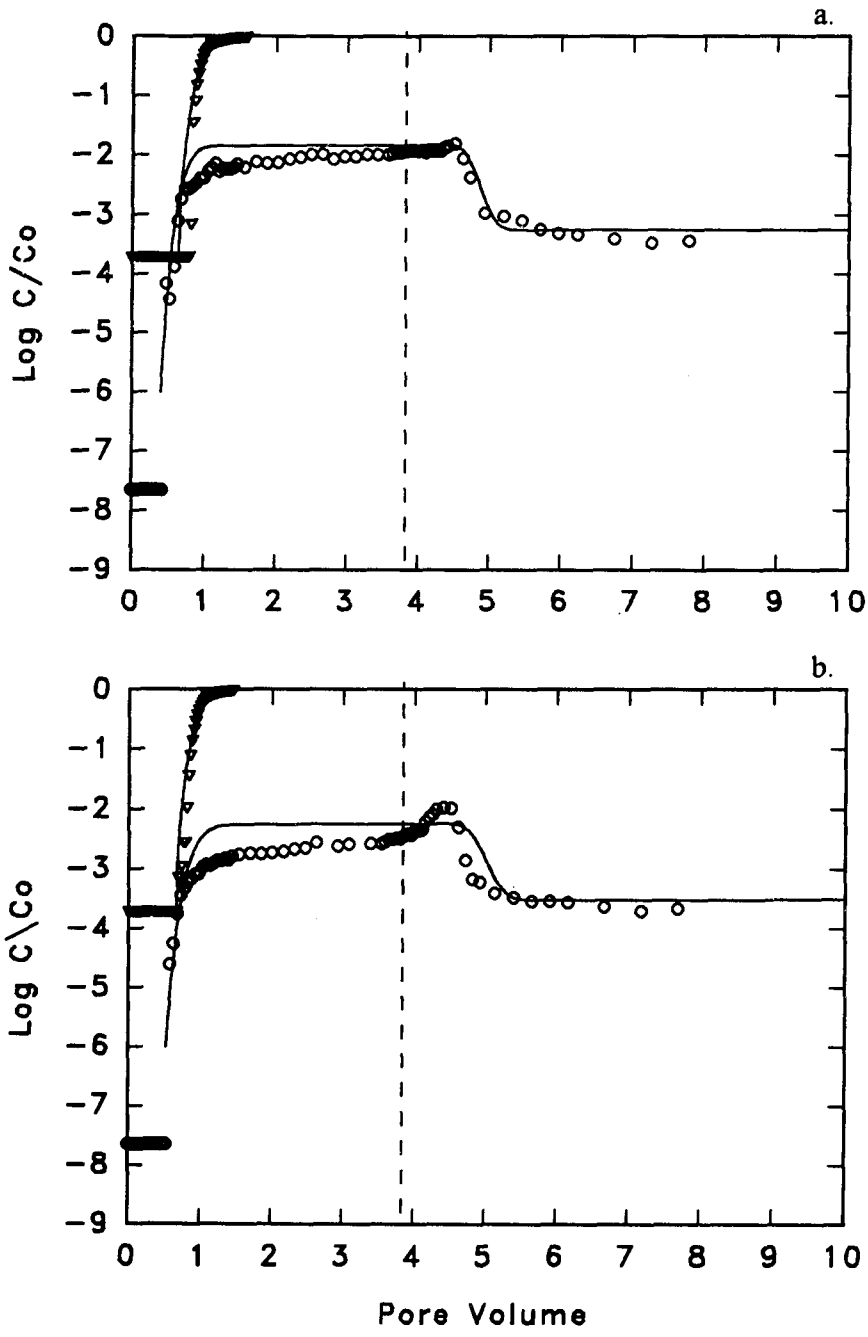

Breakthrough curves of microspheres (○) and NaCl tracer (▽) at 18° C with the best fit line of the two-site transport model. a.) Experiment 8 b.) Experiment 9.

APPENDIX D

Results of Bacteria Column Experiments with Georgetown Sediment

Sediment from Georgetown, South Carolina were used to estimate the transport parameters of *A0500*. The sediment was acquired from the DOE Subsurface Science Program's field site (John McCarthy, Oak Ridge National Laboratories). The sediment came from the most permeable layer at a depth of 2.7 m, where saturated conditions were anoxic and contained large quantities of reduced iron [*Mas-Pla et al., 1992*].

The sediment was delivered to our laboratory saturated and had been oxidized by air in the plastic bags. The surface was orange and 1 cm below the surface was brownish green. Sieve analysis of the Georgetown sediment indicates it was a medium sand with a weighted average grain diameter of 387.7 μm, and had a dry bulk density (ρ_b) of 2.43 g cm^{-3}. Sieve analysis results do not show the large quantity of clay in the sediment. Large, hard clumps of dried sediment led to a larger grain size average because the size of clumps was a function of force used to brake them up. A large portion of the clay was believed to have remained coated to particles because clay was easily rinsed off of the sand particles. Desert Analytics determined the fraction organic carbon to be 0.03 on a dry weight basis using the elemental pyrolysis method. Indigenous microorganisms, 1.8×10^5 organisms g^{-1} wet sediment, were washed from sediment using sterile groundwater.

The first sediment column, experiment 11, was packed with saturated sediment while continuously pumping water from the column. The column was kept saturated by adding sterile groundwater during the packing procedure. Large quantities of orange colloids were mobilized through the 500-μm frits during the packing procedure. Although there was no investigation of the orange colloids, they were most likely ferric hydroxide. After several pore volumes of sterile groundwater were pumped through the column the effluent became clear of colloids. Any movement of the packed column mobilized the orange colloids. I believe that colloids were mobilized from the sediment surface by pH 8 groundwater and became temporally trapped. The second column, experiment 12, was

dry packed similarly to the Ringold columns. Further oxidation occurred when sediments were allowed to air dry for packing. Mobilization of orange colloids was observed during the flushing of the column 12 with sterile groundwater..

The results of the elution experiment show that most of the mobile bacteria were eluted in the first pore volume of effluent (Fig. 16a). A constant pH drop across the sediment column in all the experiments suggest that iron surfaces were oxidizing during the transport experiments (Fig. 16b).

Two *A0500* bacteria transport experiments were run at 4°C (Fig. 17). The first experiment, Fig. 17a, shows an immediate rise to a steady-state C/C_o with large variation in the plate counts. The breakthrough curve suggests a short-circuiting of the sediment column. There were preferential flow paths or macropores that allowed bacteria to travel the length of the column more directly than the usually tortuous pathway through porous media. Therefore, further analysis of the bacteria breakthrough curve was not useful. The packing method used in experiment 12 (Fig. 17b) probably eliminated the short-circuiting problems of experiment 11. The breakthrough of bacteria in experiment 12 shows a slower rising limb with large variations in plate counts between data points. Bacteria solution was injected for almost 4 pore volumes. There were no breakthrough data after 2 pore volumes even though the lower detection limit was about $C/C_o = 10^{-5}$. This suggests that bacteria were retained in the column in much larger numbers than expected. Injected bacteria concentrations were reduced by more than 5 orders of magnitude.

In conclusion, *A0500* bacteria transport through the Georgetown sediment was extremely attenuated. Further investigations need to address the difficulties associated with pumping oxidizing water through anoxic sediments. A more realistic approach would be to use water with the same chemical composition as the field site.

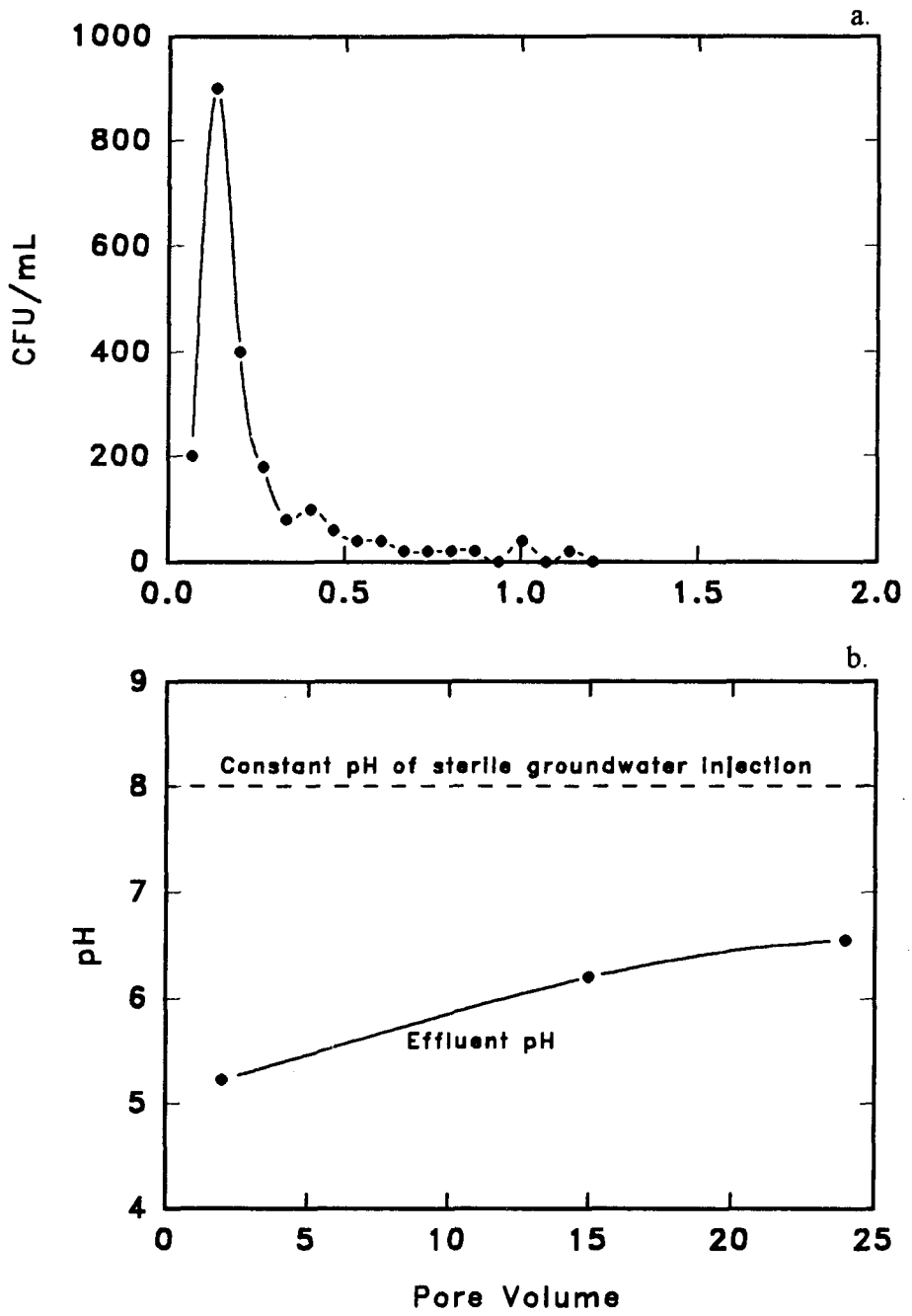

Figure 16. a). Results of flushing Georgetown sediment column with sterile groundwater. Most of the viable bacteria were eluted during first pore volume of flushing water. b.) Effluent pH of flushing groundwater.

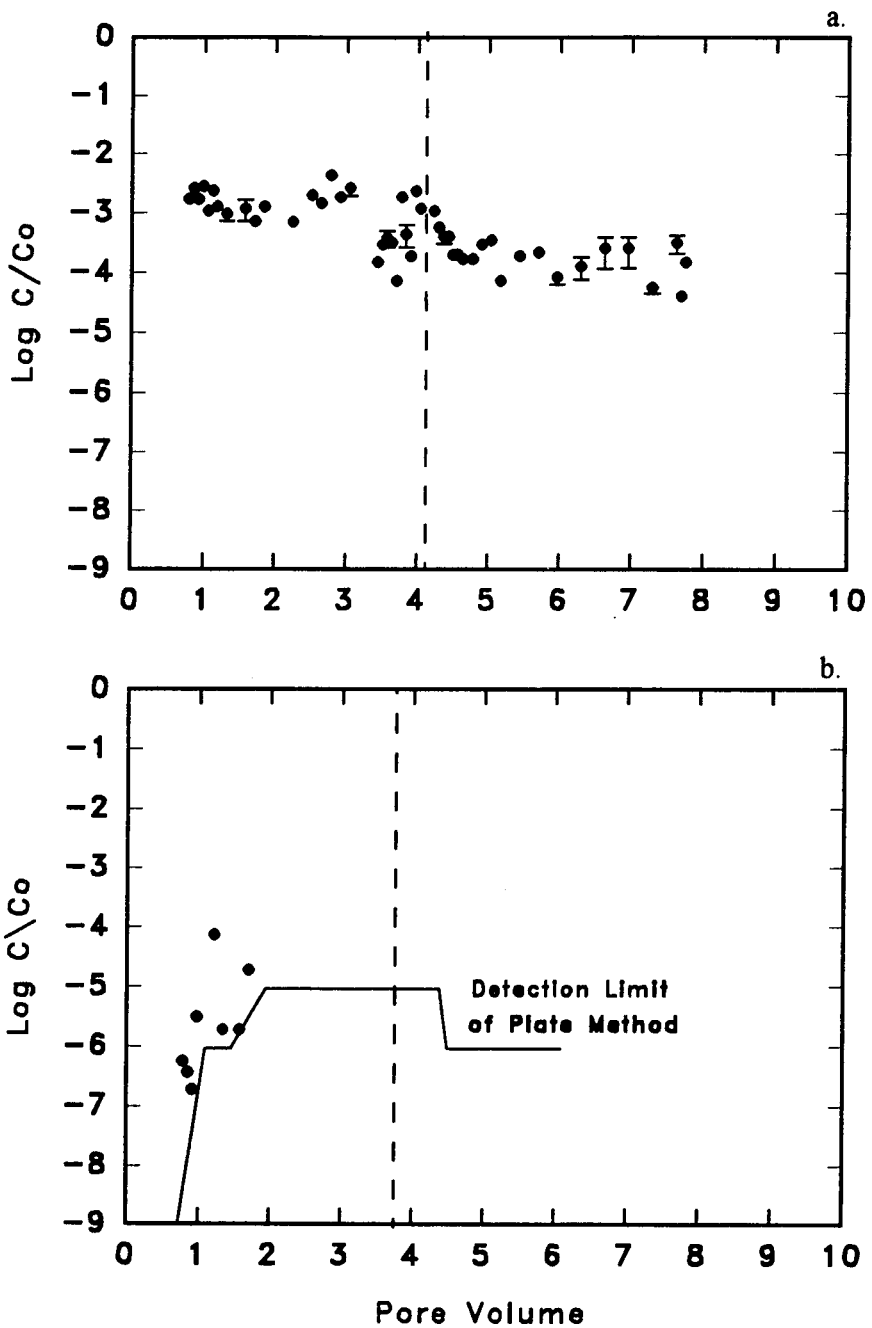

Figure 17. Breakthrough curves of *A0500* bacteria at 4° C. a.) Experiment 11. b.) Experiment 12 with lower detection limit of plating method shown. Breakthrough of *A0500* bacteria was not detected after two pore volumes because data points were below the detection limit.

Experiment 11

A0500
Temperature = 4 C
Georgetown sediment
Column Length = 30.4 cm
Avg. Interstital Velocity = 8.53 E-3 cm/s
Flow rate = 0.755 mL/min.
Pore Vol. = 44.8 mL

Porosity = 0.293
Hydraulic Detention = 59.3 min.
Bacteria solution pH = 7.9
Final effluent pH = 6.55
Co = 1.08E+09 CFU/mL
Pulse = 4.11

Sample	Effluent Volume (mL)	Pore Volume	C/Co (low)	C/Co (high)	C/Co (avg)	STD. DEV
0	0.00	0.000	9.3E-10	9.3E-10	9.3E-10	0
1	2.97	0.066	9.3E-10	9.3E-10	9.3E-10	0
2	5.94	0.133	9.3E-10	9.3E-10	9.3E-10	0
3	8.91	0.199	9.3E-10	9.3E-10	9.3E-10	0
4	11.88	0.265	9.3E-10	9.3E-10	9.3E-10	0
5	14.85	0.331	9.3E-10	9.3E-10	9.3E-10	0
6	17.82	0.398	9.3E-10	9.3E-10	9.3E-10	0
7	20.79	0.464	9.3E-10	9.3E-10	9.3E-10	0
8	23.76	0.530	9.3E-10	9.3E-10	9.3E-10	0
9	26.73	0.597	9.3E-10	9.3E-10	9.3E-10	0
10	29.70	0.663	9.3E-10	9.3E-10	9.3E-10	0
11	32.67	0.729	9.3E-10	9.3E-10	9.3E-10	0
12	35.64	0.796	1.7E-03	1.7E-03	1.7E-03	0
13	38.61	0.862	2.6E-03	2.6E-03	2.6E-03	0
14	41.58	0.928	1.7E-03	1.7E-03	1.7E-03	0
15	44.55	0.994	2.8E-03	2.8E-03	2.8E-03	0
16	47.52	1.061	1.1E-03	1.1E-03	1.1E-03	0
17	50.49	1.127	2.4E-03	2.4E-03	2.4E-03	0
18	53.46	1.193	1.3E-03	1.3E-03	1.3E-03	0
20	59.40	1.326	6.3E-04	1.3E-03	9.7E-04	0.000236
24	71.28	1.591	5.6E-04	1.9E-03	1.2E-03	0.00046
26	77.22	1.724	5.6E-04	9.3E-04	7.4E-04	0.000131
28	83.16	1.856	1.3E-03	1.3E-03	1.3E-03	0
34	100.98	2.254	7.1E-04	7.4E-04	7.2E-04	1.31E-05
38	112.86	2.519	2.0E-03	2.0E-03	2.0E-03	0
40	118.80	2.652	1.5E-03	1.5E-03	1.5E-03	0

42	124.74	2.784	3.7E-03	5.0E-03	4.4E-03	0.00046
44	130.68	2.917	1.9E-03	1.9E-03	1.9E-03	0
46	136.62	3.050	3.7E-03	1.7E-03	2.7E-03	0.000722
52	154.44	3.447	1.5E-04	1.5E-04	1.5E-04	0
53	157.41	3.514	3.0E-04	3.0E-04	3.0E-04	0
54	160.38	3.580	2.1E-04	5.6E-04	3.9E-04	0.000121
55	163.35	3.646	3.2E-04	3.2E-04	3.2E-04	0
56	166.32	3.713	7.4E-05	7.4E-05	7.4E-05	0
57	169.29	3.779	1.9E-03	2.0E-03	1.9E-03	6.57E-05
58	172.26	3.845	1.9E-04	7.1E-04	4.5E-04	0.000184
59	175.23	3.911	1.9E-04	1.9E-04	1.9E-04	0
60	178.20	3.978	2.4E-03	2.4E-03	2.4E-03	0
61	181.17	4.044	9.3E-04	1.5E-03	1.2E-03	0.000197
64	190.08	4.243	1.0E-03	1.1E-03	1.1E-03	3.28E-05
65	193.05	4.309	5.8E-04	5.8E-04	5.8E-04	0
66	196.02	4.375	2.6E-04	5.6E-04	4.1E-04	0.000105
67	198.99	4.442	4.1E-04	4.1E-04	4.1E-04	0
68	201.96	4.508	2.0E-04	2.0E-04	2.0E-04	0
69	204.93	4.574	2.0E-04	2.0E-04	2.0E-04	0
70	207.90	4.641	1.7E-04	1.7E-04	1.7E-04	0
72	213.84	4.773	1.7E-04	1.7E-04	1.7E-04	0
74	219.78	4.906	3.0E-04	3.0E-04	3.0E-04	0
76	225.72	5.038	3.5E-04	3.5E-04	3.5E-04	0
78	231.66	5.171	7.4E-05	7.4E-05	7.4E-05	0
82	243.54	5.436	1.9E-04	1.9E-04	1.9E-04	0
86	255.42	5.701	2.2E-04	2.2E-04	2.2E-04	0
90	267.30	5.967	5.6E-05	1.1E-04	8.4E-05	1.97E-05
95	282.15	6.298	5.2E-05	2.0E-04	1.3E-04	5.38E-05
100	297.00	6.629	5.6E-05	4.6E-04	2.6E-04	0.000144
105	311.85	6.961	5.6E-05	4.5E-04	2.6E-04	0.000141
110	326.70	7.292	3.9E-05	7.4E-05	5.7E-05	1.25E-05
115	341.55	7.624	1.7E-04	4.7E-04	3.2E-04	0.000108
116	344.52	7.690	4.1E-05	4.1E-05	4.1E-05	0
117	347.49	7.756	1.5E-04	1.5E-04	1.5E-04	0

Experiment 12

A0500
Georgetown sediment
Temperature = 4 C
Column Length = 30.4 cm
Avg.Interstital Velocity = 7.62 E-3 cm/s
Pore Vol. = 48.8 mL
Flow rate = 0.735 mL/min.

Porosity = 0.319
Hydraulic Detention = 66.5 min.
Input pH = 8.0
Output pH = 6.55
Co = 1.08E+09 CFU/mL
Pulse = 3.77

Sample	Effluent Volume (mL)	Pore Volume	C/Co (low)	C/Co (high)	C/Co (avg)	STD. DEV
0	0.00	0.000	9.3E-10	9.3E-10	9.3E-10	0
1	2.97	0.061	9.3E-10	9.3E-10	9.3E-10	0
2	5.94	0.122	9.3E-10	9.3E-10	9.3E-10	0
3	8.91	0.183	9.3E-10	9.3E-10	9.3E-10	0
4	11.88	0.243	9.3E-10	9.3E-10	9.3E-10	0
5	14.85	0.304	9.3E-10	9.3E-10	9.3E-10	0
6	17.82	0.365	9.3E-10	9.3E-10	9.3E-10	0
7	20.79	0.426	9.3E-10	9.3E-10	9.3E-10	0
8	23.76	0.487	9.3E-10	9.3E-10	9.3E-10	0
9	26.73	0.548	9.3E-10	9.3E-10	9.3E-10	0
10	29.70	0.609	9.3E-10	9.3E-10	9.3E-10	0
11	32.67	0.669	9.3E-10	9.3E-10	9.3E-10	0
12	35.64	0.730	9.3E-10	9.3E-10	9.3E-10	0
13	38.61	0.791	5.6E-07	5.6E-07	5.6E-07	0
14	41.58	0.852	3.7E-07	3.7E-07	3.7E-07	0
15	44.55	0.913	1.9E-07	1.9E-07	1.9E-07	0
16	47.52	0.974	3.1E-06	3.1E-06	3.1E-06	0
18	53.46	1.095	9.3E-07	9.3E-07	9.3E-07	0
20	59.40	1.217	7.4E-05	7.4E-05	7.4E-05	0
22	65.34	1.339	1.9E-06	1.9E-06	1.9E-06	0
24	71.28	1.461	9.3E-07	9.3E-07	9.3E-07	0
26	77.22	1.582	1.9E-06	1.9E-06	1.9E-06	0
28	83.16	1.704	1.9E-05	1.9E-05	1.9E-05	0
30	89.10	1.826	7.0E-04	7.0E-04	7.0E-04	0
32	95.04	1.948	9.3E-06	9.3E-06	9.3E-06	0
34	100.98	2.069	9.3E-06	9.3E-06	9.3E-06	0

36	106.92	2.191	9.3E-06	9.3E-06	9.3E-06	0
38	112.86	2.313	9.3E-06	9.3E-06	9.3E-06	0
40	118.80	2.434	9.3E-06	9.3E-06	9.3E-06	0
42	124.74	2.556	9.3E-06	9.3E-06	9.3E-06	0
44	130.68	2.678	9.3E-06	9.3E-06	9.3E-06	0
46	136.62	2.800	9.3E-06	9.3E-06	9.3E-06	0
48	142.56	2.921	9.3E-06	9.3E-06	9.3E-06	0
50	148.50	3.043	9.3E-06	9.3E-06	9.3E-06	0
52	154.44	3.165	9.3E-06	9.3E-06	9.3E-06	0
54	160.38	3.286	9.3E-06	9.3E-06	9.3E-06	0
56	166.32	3.408	9.3E-06	9.3E-06	9.3E-06	0
58	172.26	3.530	9.3E-06	9.3E-06	9.3E-06	0
59	175.23	3.591	9.3E-06	9.3E-06	9.3E-06	0
60	178.20	3.652	9.3E-06	9.3E-06	9.3E-06	0
61	181.17	3.713	9.3E-06	9.3E-06	9.3E-06	0
62	184.14	3.773	9.3E-06	9.3E-06	9.3E-06	0
63	187.11	3.834	9.3E-06	9.3E-06	9.3E-06	0
64	190.08	3.895	9.3E-06	9.3E-06	9.3E-06	0
65	193.05	3.956	9.3E-06	9.3E-06	9.3E-06	0
66	196.02	4.017	9.3E-06	9.3E-06	9.3E-06	0
67	198.99	4.078	9.3E-06	9.3E-06	9.3E-06	0
68	201.96	4.139	9.3E-06	9.3E-06	9.3E-06	0
69	204.93	4.199	9.3E-06	9.3E-06	9.3E-06	0
70	207.90	4.260	9.3E-06	9.3E-06	9.3E-06	0
71	210.87	4.321	9.3E-06	9.3E-06	9.3E-06	0
72	213.84	4.382	9.3E-06	9.3E-06	9.3E-06	0
74	219.78	4.504	9.3E-07	9.3E-07	9.3E-07	0
76	225.72	4.625	9.3E-07	9.3E-07	9.3E-07	0
78	231.66	4.747	9.3E-07	9.3E-07	9.3E-07	0
80	237.60	4.869	9.3E-07	9.3E-07	9.3E-07	0
85	252.45	5.173	9.3E-07	9.3E-07	9.3E-07	0
90	267.30	5.477	9.3E-07	9.3E-07	9.3E-07	0
95	282.15	5.782	9.3E-07	9.3E-07	9.3E-07	0
100	297.00	6.086	9.3E-07	9.3E-07	9.3E-07	0

LITERATURE CITED

Standard Methods for the Examination of Water and Wastewater, (1992) American Public Health Association, 18th edition

Absolom, D. R., F. V. Lamberti, Z. Zingg, C. J. van Oss, and A. W. Neumann, (1983) Surface thermodynamics of bacterial adhesion, *Applied and Environmental Microbiology*, **46**, 90-97

Amirthalajah, A., (1988) Some theoretical and conceptual views of filtration, *Journal of AWWA*, (December 1988), 39-46

Bahr. J., and J. Rubin, (1987) Direct comparison of kinetic and local equilibrium formulations for solute transport affected by surface reactions, *Water Resource Research*, **25**, 438-452

Bales, R.C.,(1984) W. M. Keck Laboratories of Environmental Engineering Science report. *Surface-chemical and physical behavior of chrysotile asbestos in natural waters and water treatment*, California Institute of Technology, Pasadena Ca.

Bales, R.C., S. R. Hinkle, T. W. Kroeger, and K. Stocking, (1991) Bacteriophage adsorption during transport through porous media: chemical perturbations and reversibility, *Environmental Science and Technology*, **25**, 2088-2095

Bales R.C., S. Li, K. Maguire, M. Yahya, and C. P. Gerba, (1992) MS-2 phage and Poliovirus transport through porous media: sorbent hydrophobicity and chemical perturbations, *Submitted for Publication.*

Balkwill, D. L., J. K. Fredrickson, and J. M. Thomas, (1989a) Vertical and horizontal variations in the physiological diversity of the aerobic chemoheterotrophic bacterial microflora in deep southeast coastal plain subsurface sediments. *Appied and Environmental Microbiology*, **55**, 1058-1065

Balkwill, D. L., (1989b) Numbers, diversity, and morphological characteristics of aerobic, chemoheterotrophic bacteria in deep subsurface sediments from a site in South Carolina, *Journal of Geomicrobiology*, 7, 33-52

Bouwer, E. J., and B. E. Rittmann, (1992) Comment on use of colliod filtration theory in modeling movement of bacteria through a contaminated sandy aquifer. *Environmental Science and Technology*, **26**, 400-401

Brockman, F. J., T. L. Kieft, J. K. Fredrickson, B. N. Bjordstad, W. L. Shu-mei, W. Spangenburg, P. E. Long, (1992) Microbiology of vadose zone paleosols in south-central Washington state, *Microbial Ecology*, **23**, 279-301

Cameron, D., and A. Klute, (1977) Convective-Dispersive solute transport with combined equilibrium and kinetic adsorption model, *Water Resource Research* **13**, 183-188

Craun, G. F., (1984) Health aspects of groundwater pollution, p. 135-195, *In* G. Bitton and C. P. Gerba (ed.), Groundwater polution Microbiology. John Wiley & Sons Inc., New York.

Fletcher, M., (1977) The effects of culture concentration and age, time, and temperature on bacterial attachment to polystyrene, *Canadian Journal of Microbiology*, **23**, 1-6

Fontes, D. E., A. L Mills, G. M. Hornberger, J. S. and Herman, (1991) Physical and chemical factors influencing transport of microorganisms through porous media. *Applied Environmental Microbiology*, **57**, 2473-2481.

Fredrickson,J.K., T. R. Garland, R. J. Hicks, J. M. Thomas, S. W. Li, K. M. McFadden, (1989) Lithotrophic and heterotrophic bacteria in deep subsurface sediments and their relation to sediment properties, *Journal of Geomicrobiology*, **7**, 53-66

Gannon, J. T., V. B. Manilal, and M. Alexander, (1991) Relationship between cell surface properties and transport of bacteria through soil, *Applied Environmental Microbiology*, **57**, 190-193

Gross, M. J., R. G. Arnold, B. E. Logan, R. C. Bales, O. Albinger, and D. G. Jewett, (1993) Development of a mini-column/radiolabel method for screening transport characteristics. *In preparation*

Harvey, R. W. and S. P. Garabedian, (1991) Use of colliod filtration theory in modeling movement of bacterial through a contaminated sandy aquifer. *Environmental Science and Technology*, **25**, 178-185.

Harvey, R. W., L. H. George, R. L. Smith, and D. R. LeBlanc, (1989) Transport of microspheres and indigenous bacteria through a sandy aquifer: results of natural and forced-gradient tracer experiments, *Environmental Science and Technology*, **23** ,51-56

Harvey, R. W., (1991) Parameters involved in modeling movement of bacteria in groundwater, *In*: Modeling the environmental fate of microorganisms (ed.) C. J. Hurst, American Society for Microbiology, Washington, D. C.

Hazen, T.C., (1989) Deep subsurface bacteria responses to contaminants, *In*: Proceeding of 1st international symposium on microbiology of the subsurface, January 15-19, Orlando, FL, WRSC Information Services, Aiken, SC.

Hendricks, D. W., F. J. Post, D. R. Khairnar, (1979) Adsorption of bacteria on soils, *Water, air, soil pollution*, **12**, 219-232

Hornberger, G. M., A. L. Mills, and J. S. Herman, (1992) Bacterial transport in porous,media: evaluation of a model using laboratory observations. *Water Resource Research*, **28**, 915-938

Horvath, C., H. Lin, (1976) Movement and spreading of unsorbed solutes in liquid chromotography, *Journal of Chromatography*, **126**, 401-420

Jang, L.-K., P. W. Chang, J. E. Findley, and T. F. Yen, (1983) Selection of bacteria with favorable transport properties through porous rock for the application of microbial-enhanced oil recovery, *Applied Environmental Microbiology*, **46**, 1066-1072

Jenneman, G. E., M. J. McInerney, and R. M. Knapp, (1985) Microbial penetration through nutrient-saturated Berea sandstone, *Applied Environmental Microbiology*, **50**, 383-391

Jones R. E., R. E. Beeman, S. Liy, J. M. Suflita, (1989) Anaerobic metabolic potential in the deep terrestrial subsurface, *In*: Proceeding of 1st international symposium on microbiology of the subsurface, January 15-19, Orlando, FL, WRSC Information Services, Aiken, SC.

Keswick, B. H., (1984) Sources of groundwater pollution, p. 135-195, *In* G. Bitton and C. P. Gerba (ed.), Groundwater polution Microbiology. John Wiley & Sons Inc., New York.

Kinosita, T., R. C. Bales, M. Yahya, and C. P. Gerba, (1992) Bacteria Transport in Porous Media: Retention of Bacillus and Pseudomonas on Silica Surfaces *Submitted for Publication*

Lovley, D. R., F. H. Chapelle, (1989) Rates of microbial metabolism in deep subsurface environments, *In*: Proceeding of 1st international symposium on microbiology of the subsurface, January 15-19, Orlando, FL, WRSC Information Services, Aiken, SC.

Kjelleberg, S., B. A. Humphrey, and K. C. Marshall, (1983) Initial phases of starvation and activity of bacteria at surfaces, *Applied Environmental Microbiology,* **46**, 978-984

Marshall, K.C., R. Stout, R. Mitchell (1971) Mechanisms in the initial events in the sorption of marine bacteria to surfaces, *Journal of General Microbiology*, **68**, 337-348

Martin, R. E., L. M. Hanna, and E. J. Bouwer, (1991) Determination of bacterial collision efficiencies in a rotating disk system, *Environmental Science and Technology,* **25**, 2075-2082

Mas-Pla, J., T. -C. J. Yeh, J. F. McCarthy, and T. M. Williams, (1992) A forced gradient tracer experiment in a coastal-sandy aquifer, Georgetown site, South Carolina, *Ground Water*, **30**, 6, 958-964

McCaulou, D. R., R. C. Bales, J. F. McCarthy, (1993) Use of short-pulse experiments to study bacteria transport through porous media, *Submitted for Publication*

O'Melia, C. R., (1980) Aquasols: the behavior of small particles in aquatic systems. *Environmental Science and Technology,* **14**, 1052-1060

O'Melia, C. R., (1985) Particles, pretreatment, and performance in water filtration. *Journal of Environmental Engineering,* **111**, 874-890

Pertoft, H., (1980) Purification of Herpes simplex virus using Percoll. *Separation News 3*, Pharmacia

Rao, P. S., J. Davidson, R. Jessup, and H. Selim, (1979) Evaluation of conceptual models for describing nonequilibrium adsorption-desorption of pesticides during steady flow in soils, *Journal of Soil Science Society of America,* **43**, 22-28

Reynolds, P. J., P. Sharma, G. E. Jenneman, and M. J. McInerney, (1989) Mechanisms of microbial movement in subsurface materials, *Applied Environmental Microbiology*, **55**, 2280-2286

Rouse, H. (1946) Elementary Mechanics of Fluids, Willey and Sons, New York

Sargent, K. A., C. B. Fliermans, (1989) Geology and hydrology of the deep subsurface microbiology sampling sites at the Savannah river plant, South Carolina, *Journal of Geomicrobiology*, 7, 3-13

Scholl, M. A., A. L.Mills, J. S. Herman, and G. M. Hornberger, (1990) The influence of mineralogy and solution chemistry on the attachment of bacteria to representative aquifer materials. *Journal of Contaminant Hydrology*, **6**, 321-336

Scholl, M. A., R. W. Harvey, (1992) Laboratory investigations on the role of sediment surface and groundwater chamistry in transport of bacteria through a contaminated sandy aquifer, *Environmental Science and Technology* **26**, 1410-1417

Sharma, M. M., Y. I. Yang, T. F. Yen, (1985) Reversible and irreversible surface charge modification of bacteria for facilitationg transport theough porous media *Colloids and Surfaces*, **16**, 193-206

Shaw, D. J., (1976) Introduction to colloid and surface chemistry, 2nd ed. Butterworth Inc., Boston.

Sinclair, J. L., W. C. Ghiorse, (1989) Distribution of aerobic bacteria, protozoa, algae, and fungi in deep subsurface sediments, *Journal of Geomicrobiology*, 7, 15-31

Smith, M.S., Thomas, G.W., and White, R.E. (1985) Transport of Escherichia coli through intact and disturbed soil columns. *Journal of Environmental Quality* 7, 487-494

Stumm W., J. J. Morgan, (1981) Aquatic Chemistry (2nd Ed.) Wiley and Sons, 603-667

Valocchi, A. (1985) Validity of the local equilibrium assumption for modeling solute transport through homogeneous soils, *Water Resource Research*, **21**, 808-820

van Genuchten, M. Th., (1981) Non-equilibrium transport parameters from miscible displacement experiments, *Research Report 119*, 88 pp., U. S. Salinity Lab, Riverside, CA.

van Loosdrecht, M. C. M., Lyklema, J., Norde, W., Schraa, G., and Zehnder, A. J., (1987a) The role of bacterial cell wall hydrophobicity in adhesion, *Applied and Environmental Microbiology*, **53**, 1893-1897

van Loosdrecht, M. C. M., Lyklema, J., Norde, W., Schraa, G., and Zehnder, A. J., (1987b) Electrophorectic Mobility and Hydrophobicity as a measure to predict initial steps of Bacterial Adhesion. *Applied and Environmental Microbiology*, **53**, 1898-1901

van Loosdrecht. M. C. M., Lyklema, J., Norde, W., Schraa, G., and Zehnder, A. J., (1989) Bacterial adhesion: A physicochemical approach *Microbial Ecology*, **17**, 1-15

Wollum II, A. G., and Cassel, D. K., (1978) Transport of microorganisms in sand columns. *Soil Sc. Am. J.*, **42**, 72-76

Yao, K. M., M. T. Habibian, and C. R. O'Melia, (1971) Water and Wastewater filtration: concepts and applications, *Environmental Science and Technology*, **11**, 1105-1112